Université de Neuchâtel
Institut de Physique

Aspects of physics beyond the standard model

Thèse

présentée à la Faculté des Sciences
pour obtenir le titre de Docteur ès sciences
par

Peter Bamert

Neuchâtel, Juin 1995

IMPRIMATUR POUR LA THÈSE

Aspects of Physics beyond the Standard Model

de M. Peter Bamert

UNIVERSITÉ DE NEUCHÂTEL

FACULTÉ DES SCIENCES

La Faculté des sciences de l'Université de Neuchâtel sur le rapport des membres du jury,

Messieurs J.-P. Derendinger, J.-L. Vuilleumier, Z. Kunszt (EPF-Zurich), et C.P. Burgess (Montréal)

autorise l'impression de la présente thèse.

Neuchâtel, le 11 juillet 1995

Le doyen:

H.-H. Nägeli

To my parents

Contents

Preface

My research interests are mainly in the general area of the phenomenology of elementary particle physics. When speaking of this field the first thing to notice is that the so-called standard model of elementary particle physics (SM) has celebrated an enormous success during the past few years. On the other hand many theoretical models and ideas imply that this success (hopefully) cannot prevail forever. If there is new physics lurking around the corner, it is of utmost importance and interest to investigate where and how it may show up in present day experiments.

In the past few years I have therefore concentrated on phenomenological implications of new physics beyond the standard model. I have worked mainly in two areas, namely the wide field of neutrino physics and the area of electroweak precision measurements.

The present thesis draws upon work that has been done in both areas and I have found it therefore difficult to invent a title for it. A title should be reasonably short and draw attention to a specific topic. Since the two research areas mentioned above are (almost) completely unrelated it appears impossible to conceive a title that satisfies both requirements and I finally wound up applying a short, simple and necessarily more general one.

For most of the work presented here I have benefitted from fabulous collaborations with Cliff Burgess and Rabi Mohapatra.

The thesis is split into three chapters. Each chapter is preceded by a short abstract intended for insiders and summarizing the most important results.

This abstract is then followed by a more general introduction to the subject presented later on.

Chapter 1 contains the part on electroweak precision measurements and is mainly based on publication [1]. We focus in this chapter on a specific type of new physics, called 'oblique', which affects the values of the various observables measured in high-energy precision experiments through nonstandard contributions to the gauge boson self energies. This new physics can be conveniently parametrized in terms of the Peskin-Takeuchi parameters S and T (and U). We investigate how different types of new physics contribute to these parameters. This is facilitated by two basic observations: First the contributions of new particle types to S and T are entirely determined by their electroweak quantum numbers and by their masses, and second, different such new types of particles contribute additively to the Peskin-Takeuchi parameters so that simple cases can easily be generalized to more complicated new physics scenarios. In our analysis we also generalize the definition of S and T to include light new physics *i.e.* physics with masses of the order of the Z-boson mass.

Chapter two is on neutrinoless double beta decay and is mainly based on publications [2] and [3].

The question whether neutrinos are massive has been addressed experimentally, among others, in searches for lepton number violation. One important class of such experiments looks for neutrinoless double beta decay ($\beta\beta_{0\nu}$) of heavy elements. It is generally believed that observation of such rare events would imply an electron neutrino mass in the eV range. We have provided a counterexample in terms of a model in which $\beta\beta_{0\nu}$ proceeds entirely through heavy sterile states, with masses in the GeV region, that mix with the (massless) electron neutrino, and examined this model in the light of experimental and astrophysical bounds [2].

The problem of the origin of neutrino mass has led to models which

produce an electron neutrino mass via Yukawa interactions. The new scalars that appear in these so-called Majoron models can also be emitted in double beta decay. However high-energy measurements at LEP have excluded many of the original models of this type. In the light of this experimental fact, the various different types of majoron models that are in principle possible have been classified. In publication [3] we have provided explicit examples of models belonging to certain subclasses of this classification that have not been looked at before and discuss their phenomenology.

In an attempt to present the contributions to this field in the right context, old, well-known results have been convoluted with newer ones in the overview given in sections 2.2 and 2.3. These two sections represent therefore some kind of 'extended' introduction that also contains new results. The 'essence' of publications [2] and [3] is therefore concentrated in (sub-)sections 2.3.4, 2.3.6 - 2.3.8 and 2.4 - 2.6.

Chapter 3 finally, based on publication [4], addresses the following issue: In the field of neutrino physics, it is specifically the apparent clash of observations such as the observed solar and atmospheric neutrino fluxes with the minimal SM that has stimulated active research recently. Neutrinos are also of astrophysical importance as a possible candidate for hot dark matter. All these discrepancies can be resolved if the three known neutrinos are almost degenerate in mass. We have given an existence proof of such a kind of mass pattern by providing a minimal extension of the SM which solves simultaneously the solar and the atmospheric neutrino problem and at the same time accounts for the cosmologically preferred amount of hot dark matter.

1

Light oblique new physics on the Z^0-pole

This chapter is about implications on new physics of high precision tests of the standard model (SM), as undertaken at LEP [5] and SLC [6]. It focuses thereby on a subclass of new physics called *oblique* [7]. The original motivation for the work displayed here was a statistical hint for a deviation of these precision data from the standard model, hence a hint for oblique new physics. Specifically the Peskin-Takeuchi parameter S [8] appeared to be negative and about two standard deviations from zero, its SM value. This has led us to investigate how different types of oblique new physics affect the Peskin-Takeuchi parameters [1]. Meanwhile the experimental situation has changed and there is no longer this hint for a negative S.

1.1 Introduction

As present day experiments enter new hitherto unprobed domains of physics and render more and more precise results, they not only test the SM of electroweak interactions to new orders of magnitude but they also provide an efficient basis for searches for new physics. This is because there has been no direct evidence for physics beyond the SM as yet and its possible presence can only manifest itself indirectly.

Such indirect effects on observables can in principle be computed directly in terms of any given model (such as *e.g.* the minimal supersymmetric standard model (MSSM)). However this is an awkward procedure in general and the effort is justified only in very few cases (such as the MSSM). As a consequence it seems highly desirable to parametrize these effects in a model independent way. Once a parametrization is given, bounds on the various parameters can be inferred from experimental data. In order to see whether a model of new physics is phenomenologically viable or not, one then only has to compute its contributions to these parameters[1].

To see how such a parametrization can be found, the first thing to notice is that almost all precisely measured observables can be described in terms of light fermion scattering. This is because present day experiments involve usually either scattering of light leptons or quarks, or they investigate the decay of a light fermion to three fermions. New physics can affect light fermion scattering in three different ways, as illustrated in fig. 1.1, namely by giving non standard contributions to gauge boson propagation, 3-point fermion-boson couplings and 4-point fermion-fermion interactions.

1.1.1 Oblique new physics

Significant simplification can be achieved by requiring new physics to be subject to the following constraints:

[1]For a general review of the use of such parametrizations see *e.g.* [9].

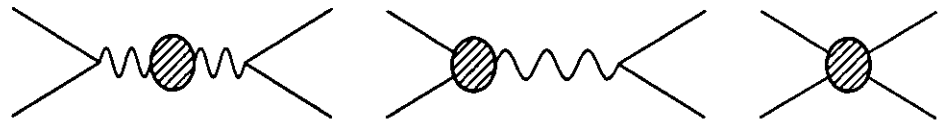

Figure 1.1: Indirect new physics contributions to fermion scattering. (*a*) Gauge boson propagation, (*b*) 3-point fermion-boson couplings and (*c*) 4-point fermion-fermion couplings. *Oblique* new physics only affects gauge boson propagation (*a*).

- (1) The electroweak gauge group $SU(2)_L \otimes U(1)_Y$ remains unchanged and there are no new gauge bosons.
- (2) The new physics couples dominantly to the SM gauge bosons and its couplings to the light fermions are suppressed.
- (3) The intrinsic mass scale of new physics is much heavier than the electroweak scale (*i.e.* $M_{NP} \gg M_Z$).

The first two items in this list ensure that the only relevant contribution to observables is via modification of gauge boson propagation, *i.e.* contributions of type (*a*) in fig. 1.1. This kind of new physics is called *oblique* [7].

Actually condition (2) above can be relaxed if contributions to fermion-boson and fermion-fermion couplings (type (*b*) and (*c*) in fig. 1.1) appear only as linear combinations of SM currents. In this case one can redefine fields in such a way that any dependence of these couplings on new physics is removed and reappears in gauge boson propagation terms.

The advantage of selection criteria (1) and (2) (*i.e.* oblique new physics) is that they contain a large class of well motivated models allowing at the same time for a parametrization in terms of only very few parameters. By fitting those parameters to electroweak precision data one can simultaneously constrain all these models in an efficient way.

Notice also that this kind of new physics acts in a universal way, *i.e.* a way that depends only on the fermion quantum numbers, couplings and masses, but not on the family number. This is again because it can be phrased entirely in terms of self-energy contributions to gauge boson propagation.

The fact that only few parameters are needed to parametrize oblique new physics can most easily be seen when condition (3), which is not a necessity for the qualification *oblique*, of the above list also applies. In this case things are simplified even further and the new physics can be parametrized in terms of a simple effective lagrangian. Now the effective lagrangian approach is very general and can be applied to virtually all sorts of new physics as soon as it is heavy enough (*i.e.* $M_{NP} \gtrsim 1$ TeV) to be integrated out[2]. However this approach is particularly simple in the oblique case and it seems appropriate to sketch the way it works (this goes very much along the lines of [10]).

Effective lagrangian approach

The heavy oblique new physics will, once integrated out, change the gauge boson part of the lagrangian. Since it is heavy it will dominantly contribute to lower dimensional (*i.e.* dimension 4 or lower) operators because any operators with dimension 5 or higher will be suppressed by at least 1 power of the heavy scale[3]. In other words it will change gauge boson kinetic and mass terms and it could possibly contribute to new anomalous gauge boson self interactions. However, we do not consider the latter here since they cannot yet be probed at tree level, which makes them interesting in their own right. So the SM lagrangian is changed to:

$$\begin{aligned} \mathcal{L}_{\text{eff}} &= \mathcal{L}_{\text{SM}}(\tilde{e}_i, \tilde{m}_i) + \mathcal{L}_{\text{new}} \\ \mathcal{L}_{\text{new}} &= -\frac{A}{4}\hat{F}_{\mu\nu}\hat{F}^{\mu\nu} - \frac{B}{2}\hat{W}^{\dagger}_{\mu\nu}\hat{W}^{\mu\nu} - \frac{C}{4}\hat{Z}_{\mu\nu}\hat{Z}^{\mu\nu} - \frac{G}{2}\hat{F}_{\mu\nu}\hat{Z}^{\mu\nu} \\ &\quad -w\tilde{m}_W^2\hat{W}^{\dagger}_{\mu}\hat{W}^{\mu} - \frac{z}{2}\tilde{m}_Z^2\hat{Z}_{\mu}\hat{Z}^{\mu} \end{aligned} \tag{1.1}$$

[2] See *e.g.* Ref. [10] for a general treatment including operators up to dimension 5.

[3] This is discussed in greater detail in [10].

Here $F_{\mu\nu}$ and $Z_{\mu\nu}$ are the usual abelian field strengths whereas $W_{\mu\nu}$ is electromagnetically gauge covariant.

The tilde on coupling constants ($\tilde{e}_i$) and masses ($\tilde{m}_i$) denote parameters as they appear in the SM part of the effective lagrangian. Their values differ from those inferred from measurements in that the latter are altered by the presence of the new physics.

The first thing to notice about lagrangian eq.(1.1) is that there are 6 parameters (A, B, C, G, w and z) which would be zero in the absence of oblique new physics and thus serve to parametrize its effects. Only three independent combinations of those ever appear in physical observables however. This is because there is a three parameter family of field redefinitions which do not alter the form of the SM lagrangian in eq.(1.1). These consist of rescalings of the electroweak gauge fields W_μ, Z_μ and the higgs field Φ.

The second point about lagrangian eq.(1.1) is that due to the new physics terms the electroweak gauge fields are no longer canonically normalized, which is indicated by the caret on the fields.

Now suppose for a moment that there is no new physics, then the theoretical expressions for the electroweak observables are given in terms of the coupling constants and masses as they appear in the SM lagrangian. In other words they are given in terms of $\tilde{s}_w$, $\tilde{m}_Z$, $\tilde{e}$, the CKM mixing elements $\tilde{V}_{ij}$ and the fermion and higgs masses $\tilde{m}_i$.

To see now how parameters A through z enter into observables one first uses the freedom to perform field redefinitions one has to canonically normalize and diagonalize the gauge fields. Upon having done this the gauge boson part of the effective lagrangian takes the form

$$\begin{aligned} - & \frac{1}{4}F_{\mu\nu}F^{\mu\nu} - \frac{1}{2}\hat{W}^\dagger_{\mu\nu}\hat{W}^{\mu\nu} - \frac{1}{4}Z_{\mu\nu}Z^{\mu\nu} \\ - & (1+w-B)\tilde{m}_W^2\hat{W}^\dagger_\mu\hat{W}^\mu - \frac{1}{2}(1+z-C)\tilde{m}_Z^2 Z_\mu Z^\mu. \end{aligned} \tag{1.2}$$

Also the currents, *i.e.* the fermion-gauge boson interaction terms, are

altered. The electromagnetic current *e.g.* becomes:

$$\mathcal{L}_{\text{em}} = -\tilde{e}\left(1 - \frac{A}{2}\right)\sum_i \bar{f}_i \gamma_\mu Q_i f_i A_\mu \tag{1.3}$$

where the Q_i denote the fermion charges.

This allows one to reexpress three of the 'pure' SM parameters, namely $\tilde{s}_w$, $\tilde{m}_Z$ and $\tilde{e}$, in terms of the new physics contributions and the 'real' three parameters s_w, m_Z, e as inferred from the three best measured observables, which at present are M_Z, α and G_F. For example $\tilde{m}_Z$ can be expressed as

$$\tilde{m}_Z^2 = m_Z^2(1 - z + C). \tag{1.4}$$

In other words 3 degrees of freedom out of the original set of six parameters (A through z) have been used to reexpress $\tilde{s}_w, \tilde{m}_Z$ and $\tilde{e}$ in terms of s_w, m_Z and e. Observables can now be computed using the 'real' parameters s_w, m_Z, e and three independent combinations of parameters A through z [4]. These three combinations are conventionally given by the three Peskin-Takeuchi parameters S, T and U [8].

One now sees the power of the method: The possible indirect effects of a large class of unknown heavy new physics have been parametrized in a model independent way in terms of only three parameters.

This approach, as beautiful as it appears, is however only valid in the limit where the new physics is heavy and can be integrated out so that only operators of dimension 4 or lower play a role. To implement lighter new physics the following approach seems to be more appropriate.

1.1.2 Light oblique new physics

Vacuum polarization approach

This approach [11] parametrizes oblique new physics directly in terms of its contributions to the gauge boson vacuum polarizations. This has the

[4] What has been said above becomes now clear from another point of view namely that three degrees of freedom are used up in the renormalizations of the input parameters.

advantage that one can also consider new physics that is comparatively light (*i.e.* of the order of the weak scale M_Z or even lighter) in a convenient way.

To do so one splits up the gauge boson self-energies

$$\Pi_{ab}^{\mu\nu}(q^2) = \Pi_{ab}(q^2)g^{\mu\nu} + (q^\mu q^\nu \text{ terms}) \tag{1.5}$$

in a SM and a new physics part[5]

$$\Pi_{ab}(q^2) = \Pi_{ab}^{\text{SM}}(q^2) + \delta\Pi_{ab}(q^2) \tag{1.6}$$

where indices a and b stand for the gauge bosons and take on values W, Z and γ.

All new physics dependences are now residing in the $\delta\Pi_{ab}(q^2)$, whereas the $\Pi_{ab}^{\text{SM}}(q^2)$ contain all the desired SM radiative corrections.

The link to the case of heavy new physics discussed before can be made by Taylor expanding $\delta\Pi_{ab}(q^2)$ around $q^2 = 0$ and truncating this series after the second term

$$\delta\Pi_{ab}(q^2) = A_{ab} + B_{ab}\, q^2. \tag{1.7}$$

All other terms can be neglected because they are suppressed by at least one power of $\left(\frac{q^2}{M_{NP}^2}\right)$ where M_{NP} is the heavy mass scale.

Upon first inspection of this equation one might think that there are 8 new physics degrees of freedom, namely $A_{WW}, A_{ZZ}, A_{\gamma\gamma}, A_{Z\gamma}, B_{WW}, B_{ZZ}, B_{\gamma\gamma}$ and $B_{Z\gamma}$. However $\delta\Pi_{\gamma\gamma}(0)$ and $\delta\Pi_{Z\gamma}(0)$ (and hence $A_{\gamma\gamma}$ and $A_{Z\gamma}$) vanish due to gauge invariance and one is left with only six degrees of freedom as before[6].

Here, on the other hand, we do not assume any specific form $\delta\Pi_{ab}(q^2)$ might take. Instead we make now use of the fact that precisely measured observables have presently only been probed at two energy scales, namely at $q^2 \approx 0$ and at $q^2 = M_Z^2(M_W^2)$.

[5]Notice that the $q^\mu q^\nu$ terms in eq.(1.5) are not relevant within the framework of light fermion scattering since the electroweak currents are approximately conserved.

[6]At this level the effective lagrangian approach presented before and the method displayed here are actually equivalent.

In other words, a small number of new physics degrees of freedom is realized here not by assuming a specific analytic structure of the self-energies but rather by simply referring to the fact that the available experimental data does not facilitate a more complex parametrization.

The counting of degrees of freedom now proceeds as follows: Essentially all anomalous self energies can contribute at low and high energy. As mentioned before however $\delta\Pi_{\gamma\gamma}(0) = \delta\Pi_{Z\gamma}(0) = 0$ due to gauge invariance. It is therefore convenient to define the quantities

$$\delta\hat{\Pi}_{ab}(q^2) \equiv \frac{\delta\Pi_{ab}(q^2)}{q^2} \tag{1.8}$$

which in the $\gamma\gamma$ and $Z\gamma$ cases are well defined at $q^2 = 0$. So the self-energies $\delta\hat{\Pi}_{\gamma\gamma}(0, M_Z^2)$, $\delta\hat{\Pi}_{Z\gamma}(0, M_Z^2)$, $\delta\Pi_{WW}(0, M_W^2)$ and $\delta\Pi_{ZZ}(0, M_Z^2)$ represent independent degrees of freedom. In addition to those, two more are probed by $W^\pm$ and Z^o decays. This is because the decay amplitudes of these gauge bosons are proportional to their wave function renormalizations. Consequently we have to add $\delta\Pi'_{WW}(M_W^2)$ and $\delta\Pi'_{ZZ}(M_Z^2)$ to our list[7]. Here the prime ($'$) denotes the derivative with respect to q^2.

Out of these 10 degrees of freedom one, namely $\delta\hat{\Pi}_{\gamma\gamma}(M_Z^2)$ corresponds to a new physics contribution to the photon propagator on the Z-peak. Since photon exchange on the Z-pole is already $\sim O(\Gamma_Z/M_Z)$ suppressed compared to Z exchange, $\delta\hat{\Pi}_{\gamma\gamma}(M_Z^2)$ constitutes a correction to a correction and can be ignored. Three of the remaining 9 degrees of freedom enter into the renormalizations of the input parameters leaving us with a net number of six oblique new physics parameters that appear in the expressions for the observables.

1.1.3 Extended oblique parameters

What follows can be derived in a rigorous way using an effective lagrangian that involves also higher dimensional operators [12]. This is done essen-

[7] The anomalous wavefunction renormalizations are *e.g.* $\mathcal{Z}_W = 1 + \delta\Pi'_{WW}(M_W^2)$.

tially by including the anomalous self-energies directly in the effective lagrangian through an 'oblique' operator $\frac{1}{2}G_\mu \delta\Pi_{GG}(-\Box)G^\mu$, where G_μ denotes a gauge boson and $\delta\Pi_{GG}$ is the anomalous contribution to its self-energy. This 'oblique' operator can be recast into a sum of operators of arbitrarily high dimensions, corresponding to the Taylor series of $\delta\Pi_{GG}$. One then uses the equation of motion of the gauge field G_μ to transform the effective lagrangian into a more convenient form which allows one to read off easily the oblique contributions to masses and vertices[8]. The use of the lowest order equations of motion to simplify the effective lagrangian is justified because it can be shown to correspond to a set of field redefinitions and so has no physical meaning.

Let us turn our attention first to the input observables. As mentioned before we have those chosen to be the three currently best measured ones, namely

- α as determined from low energy electron scattering ($q^2 \approx 0$)
- G_F Fermi constant as inferred from muon decay ($q^2 \approx 0$)
- M_Z The pole mass as measured at LEP ($q^2 = M_Z^2$).

In the absence of new physics they are linked to the SM lagrangian parameters e, s_w and m_Z through

$$\begin{aligned} 4\pi\alpha(e) &= e^2(1+O(e^2)) \\ G_F(e,s_w,m_Z) &= \frac{e^2}{4\sqrt{2}s_w^2c_w^2m_Z^2}(1+O(e^2)) \\ M_Z^2(e,s_w,m_Z) &= m_Z^2(1+O(e^2)) \end{aligned} \tag{1.9}$$

where $O(e^2)$ denote the renormalization scheme dependent radiative corrections. As soon as new physics is present however, parameters e, s_w and m_Z as defined above are no longer the 'pure' SM lagrangian parameters $\tilde{e}$, $\tilde{s}_w$

[8]This whole procedure has been presented in a pedagogical way in [12].

and $\tilde{m}_Z$ as in eq.(1.1), because they have been derived from α, G_F and M_Z *assuming* only SM physics.

SM expressions of general observables on the other hand are given in terms of $\tilde{e}$, $\tilde{s}_w$, $\tilde{m}_Z$[9] which cannot directly be obtained from the measured values of α, G_F and M_Z. In the presence of new physics observables would thus have to be computed as a sum of their 'pure' SM part and the total new physics contribution:

$$\mathcal{O} = \mathcal{O}_{\rm SM}(\tilde{e}, \tilde{s}_w, \tilde{m}_Z) + \delta\mathcal{O}^{\rm tot}_{\rm NP} \tag{1.10}$$

It is clear that a much more convenient way would be to first compute the shift SM parameters experience due to new physics, *i.e.* to reexpress the 'pure' parameters $\tilde{e}$, $\tilde{s}_w$, $\tilde{m}_Z$ in terms of e, s_w and m_Z and then to compute observables as

$$\mathcal{O} = \mathcal{O}_{\rm SM}(e, s_w, m_Z) + \delta\mathcal{O}^{\rm net}_{\rm NP} \tag{1.11}$$

i.e. as the sum of the value the observable would have when inferred from measurements *assuming* only SM physics and the net new physics contribution.

To compute this shift we now write the input parameters also in the way of eq.(1.10)[10]:

$$\begin{aligned} 4\pi\alpha(e) &= \tilde{e}^2(1+O(\tilde{e}^2))\left[1+\delta\hat{\Pi}_{\gamma\gamma}(0)\right] \\ G_F(e,s_w,m_Z) &= \frac{\tilde{e}^2}{4\sqrt{2}\tilde{s}_w^2\tilde{c}_w^2\tilde{m}_Z^2}(1+O(\tilde{e}^2))\left[1-\frac{\delta\Pi_{WW}(0)}{M_W^2}\right] \\ M_Z^2(e,s_w,m_Z) &= \tilde{m}_Z^2(1+O(\tilde{e}^2))\left[1+\delta\hat{\Pi}_{ZZ}(M_Z^2)\right] \end{aligned} \tag{1.12}$$

Upon comparison with eq.(1.9) we can extract $\tilde{e}$, $\tilde{s}_w$ and $\tilde{m}_Z$. Since we work only in lowest order of the new physics contributions the radiative corrections

[9] All other SM parameters, such as Yukawa couplings and CKM mixing elements, are not affected by oblique new physics and do not concern us here.

[10] Notice that eq.(1.9) corresponds to eq.(1.11) in the case of the input parameters.

drop out of the equations and we end up with

$$\begin{aligned}
\tilde{e} &= e\left[1-\frac{1}{2}\delta\hat{\Pi}_{\gamma\gamma}(0)\right] \\
\tilde{s}_w^2 &= s_w^2\left[1-\frac{c_w^2}{c_w^2-s_w^2}\left(\delta\hat{\Pi}_{\gamma\gamma}(0)-\delta\hat{\Pi}_{ZZ}(M_Z^2)+\frac{\delta\Pi_{WW}(0)}{M_W^2}\right)\right] \\
\tilde{m}_Z^2 &= m_Z^2\left[1-\delta\hat{\Pi}_{ZZ}(M_Z^2)\right]
\end{aligned} \tag{1.13}$$

The absence of SM radiative corrections in these equations means that this way of parametrizing new physics is independent of the renormalization scheme.

So once this has been done we can write observables in the form of eq.(1.11) where the net contribution $\delta\mathcal{O}_{\rm NP}^{\rm net}$ of new physics can be expressed in terms of the remaining 6 degrees of freedom which we parameterize as S,T,U,V,W and X [11, 13, 12]:

$$\begin{aligned}
\frac{\alpha S}{4s_w^2c_w^2} &= \left[\delta\hat{\Pi}_{ZZ}(M_Z^2)-\frac{\delta\Pi_{ZZ}(0)}{M_Z^2}\right]-\frac{(c_w^2-s_w^2)}{s_wc_w}\delta\hat{\Pi}_{Z\gamma}(0)-\delta\hat{\Pi}_{\gamma\gamma}(0) \\
\alpha T &= \frac{\delta\Pi_{WW}(0)}{M_W^2}-\frac{\delta\Pi_{ZZ}(0)}{M_Z^2} \\
\frac{\alpha U}{4s_w^2} &= \left[\delta\hat{\Pi}_{WW}(M_W^2)-\frac{\delta\Pi_{WW}(0)}{M_W^2}\right]-s_w^2\delta\hat{\Pi}_{\gamma\gamma}(0) \\
&\quad -c_w^2\left[\delta\hat{\Pi}_{ZZ}(M_Z^2)-\frac{\delta\Pi_{ZZ}(0)}{M_Z^2}\right]-2s_wc_w\delta\hat{\Pi}_{Z\gamma}(0) \\
\alpha V &= \delta\Pi'_{ZZ}(M_Z^2)-\left[\delta\hat{\Pi}_{ZZ}(M_Z^2)-\frac{\delta\Pi_{ZZ}(0)}{M_Z^2}\right] \\
\alpha W &= \delta\Pi'_{WW}(M_W^2)-\left[\delta\hat{\Pi}_{WW}(M_W^2)-\frac{\delta\Pi_{WW}(0)}{M_W^2}\right] \\
\alpha X &= -s_wc_w\left[\delta\hat{\Pi}_{Z\gamma}(M_Z^2)-\delta\hat{\Pi}_{Z\gamma}(0)\right]
\end{aligned} \tag{1.14}$$

The first important remark about eq.(1.14) is that V,W and X vanish in the limit of heavy new physics when anomalous vacuum polarizations are written as quadratic functions in q^2 (see eq.(1.7)). In this case we are left with the three conventional Peskin-Takeuchi parameters S,T and U.

Also, as long as only low energy observables are considered, V, W and X do not play a role since compared to $q^2 \approx 0$ all new physics is heavy.

1.1.4 Some observables

The W-mass

As a simple example we first compute the W-mass. At lowest order it receives a renormalization contribution from the new physics vacuum polarization $\delta\hat{\Pi}_{WW}(M_W^2)$ so that we can write it in the form of eq.(1.10) as

$$M_W^2 = M_W^2(\tilde{s}_w, \tilde{m}_Z)(1 + \delta\hat{\Pi}_{WW}(M_W^2)) = \tilde{m}_Z^2\tilde{c}_w^2(1 + \delta\hat{\Pi}_{WW}(M_W^2)) \quad (1.15)$$

upon taking into account the shifts of the SM parameters eq.(1.13) *i.e.* reexpressing $\tilde{m}_Z, \tilde{c}_w$ in terms of m_Z and c_w one obtains (as in eq.(1.11)

$$\begin{aligned} M_W^2 = \; & M_W^2(s_w, m_Z)\left[1 - \frac{c_w^2}{c_w^2 - s_w^2}\delta\hat{\Pi}_{ZZ}(M_Z^2)\right. \\ & \left. + \frac{s_w^2}{c_w^2 - s_w^2}\left(\delta\hat{\Pi}_{\gamma\gamma}(0) + \frac{\delta\Pi_{WW}(0)}{M_W^2}\right) + \delta\hat{\Pi}_{WW}(M_W^2)\right] \end{aligned} \quad (1.16)$$

which is, reexpressed in the basis eq.(1.14)

$$M_W^2 = M_W^2(s_w, m_Z)\left[1 - \frac{\alpha S}{2(c_w^2 - s_w^2)} + \frac{c_w^2\alpha T}{c_w^2 - s_w^2} + \frac{\alpha U}{4s_w^2}\right] \quad (1.17)$$

The invisible width

In a similar way one proceeds to compute $\Gamma(Z \to \nu\bar{\nu}) \equiv \Gamma_{\text{inv}}$ the invisible Z-width. Here the tree-level SM expression receives a contribution from an anomalous wave function renormalization term $\mathcal{Z}_Z = (1 + \delta\Pi'_{ZZ}(M_Z^2))$, so that

$$\Gamma_{\text{inv}} = \frac{\tilde{e}M_Z}{32\pi\tilde{s}_w^2\tilde{c}_w^2}\left(1 + \delta\Pi'_{ZZ}(M_Z^2)\right). \quad (1.18)$$

Here M_Z rather than $\tilde{m}_Z$ has been used since it enters the expression through a phase space factor. With the help of eq.(1.13) and the use of

$$\frac{s_w^2 c_w^2}{\tilde{s}_w^2 \tilde{c}_w^2} = 1 - \delta\hat{\Pi}_{\gamma\gamma}(0) + \delta\hat{\Pi}_{ZZ}(M_Z^2) - \frac{\delta\Pi_{WW}(0)}{M_W^2} \tag{1.19}$$

this can be rewritten as

$$\begin{aligned} \Gamma_{\text{inv}} &= \Gamma_{\text{inv}}(e, s_w, M_Z)\left(1 - \delta\hat{\Pi}_{ZZ}(M_Z^2) + \frac{\delta\Pi_{WW}(0)}{M_W^2} + \delta\Pi'_{ZZ}(M_Z^2)\right) \\ &= \Gamma_{\text{inv}}(e, s_w, M_Z)\,(1 + \alpha T + \alpha V) \end{aligned} \tag{1.20}$$

Clearly V enters only because the wave function renormalization factor $\mathcal{Z}_Z$ has been used. Similarly the oblique parameter W enters into the expression for the total decay width of the W boson. Actually among all of the relevant precisely measured observables the parameters U and W enter only into the expressions for the W-mass and -width.

The effective weak mixing angle

Finally we derive the expression for the effective weak mixing angle as observed in parity violation measurements like the left-right (A_{LR}) and forward-backward (A_{FB}) asymmetries in electron-electron scattering. Since these observables are essentially proportional to the vectorlike coupling g_V (as well as the axial coupling g_A) they receive, beyond SM tree level, a contribution from $Z-\gamma$ mixing terms. For the effective weak mixing angle extracted from those observables this means, in the presence of new physics, that

$$s_{w\,\text{eff}}^2(q^2) = \tilde{s}_w^2 - s_w c_w \delta\hat{\Pi}_{Z\gamma}(q^2). \tag{1.21}$$

Upon applying eq.(1.13) again this can be written as

$$s_{w\,\text{eff}}^2(q^2) = s_w^2\left[1 + \left(\frac{\alpha S}{4 s_w^2(c_w^2 - s_w^2)} - \frac{c_w^2 \alpha T}{c_w^2 - s_w^2}\right) - \frac{c_w}{s_w}\left(\delta\hat{\Pi}_{Z\gamma}(q^2) - \delta\hat{\Pi}_{Z\gamma}(0)\right)\right] \tag{1.22}$$

where the last term vanishes for $q^2 = 0$ so that $s^2_{w\text{eff}}$ only depends on S and T as it should. For $q^2 = M_Z^2$ the last term above is proportional to X and $s^2_{w\text{eff}}$ can be expressed as

$$s^2_{w\text{eff}}(M_Z^2) = s_w^2 \left(1 + \frac{\alpha S}{4s_w^2(c_w^2 - s_w^2)} - \frac{c_w^2 \alpha T}{c_w^2 - s_w^2} + \frac{\alpha X}{s_w^2}\right). \tag{1.23}$$

1.2 Oblique new physics on the Z^o-pole

1.2.1 Using only high energy data

High energy measurements, most notably those at LEP and SLC, have now reached a level of precision that justifies analysing high energy data all on its own.

When doing so, all low energy observables, except for the input parameters α and G_F, are being neglected and consequently one can no longer independently constrain the 6 oblique parameters eq.(1.14). To see how many parameters still can be constrained we count the remaining degrees of freedom: Out of the original 9 degrees of freedom (remember that $\delta\widehat{\Pi}_{\gamma\gamma}(M_Z^2)$ was neglected) the four low-energy contributions drop out. These four contained the two degrees of freedom that renormalized the low energy input parameters α and G_F. One more is used up by the third input parameter M_Z. This leaves us with a total of four degrees of freedom. Finally in what follows we do not consider measurements of the W width and so the oblique parameter W, which only appears in this observable, no longer concerns us. Therefore we are ultimately left with three degrees of freedom, which in the limit of heavy new physics are precisely the conventional Peskin-Takeuchi parameters S, T and U as can be seen from eqs.(1.17-1.23).

If light new physics is present however they also receive contributions from V and X. It therefore seems appropriate to define a 'high energy' set of oblique parameters.

The primed parameters

This 'high energy' set of parameters should be defined in a way such that the various analyses of high energy data, that have been undertaken using only the conventional Peskin-Takeuchi parameters, can conveniently be applied to this modified set and so to the more general case of light new physics. This is achieved by letting the main observables that are measured in those experiments, namely the W-mass M_W eq.(1.17), the overall normalization of the weak neutral current as measured in $\Gamma_{\rm inv}$ eq.(1.20) and the effective weak mixing angle as determined by parity asymmetry measurements eq.(1.23), having the same analytical dependence on the new parameters, which we take to be S', T' and U', as they would have on the conventional S, T and U in the limit of heavy new physics. In other words we define S', T' and U' through

$$\begin{aligned} \Gamma_{\rm inv} &= \Gamma_{\rm inv}(e, s_w, M_Z)\,(1+\alpha T') \\ s^2_{w\rm eff}(M_Z^2) &= s_w^2\left(1+\frac{\alpha S'}{4s_w^2(c_w^2-s_w^2)}-\frac{c_w^2\alpha T'}{c_w^2-s_w^2}\right) \\ M_W^2 &= M_W^2(s_w, m_Z)\left(1-\frac{\alpha S'}{2(c_w^2-s_w^2)}+\frac{c_w^2\alpha T'}{c_w^2-s_w^2}+\frac{\alpha U'}{4s_w^2}\right). \end{aligned} \tag{1.24}$$

This assures that *e.g.* fits of S and T to high energy data can be directly read as fits to the primed parameters S' and T'. The original parameters S and T are themselves only constrained independently from S' and T' by additional data at $q^2 \sim 0$.

Notice that the primed parameters are closely related to the epsilon parameters of [14]. This relation has been described in detail in [12, 15, 9].

Comparison of eq.(1.24) with eqs.(1.17-1.23) then yields the primed parameters in terms of the extended oblique parameters eq.(1.14):

$$\begin{aligned} S' &= S + 4s_w^2c_w^2V + 4(c_w^2-s_w^2)X \\ T' &= T + V \\ U' &= U - 4s_w^2c_w^2V + 8s_w^2X \end{aligned} \tag{1.25}$$

Notice that S', T' and U' as defined above are indeed identical to the conventional parameters S, T and U in the limit of heavy new physics when V and X vanish.

1.2.2 Using only Z^o-pole data

A further simplification is achieved by restricting oneself to using only Z-pole data and neglecting measurements of the W-mass. The influence of oblique new physics on the remaining observables can then be parametrized using only the 2 parameters S' and T'.

1.2.3 The experimental situation

Z-pole measurements of various observables are currently done at the four experiments of CERN's Large Electron Positron ring (LEP). They are supplemented by a single, very accurate measurement of the left-right asymmetry A_{LR} at the Stanford Linear Collider (SLC). A_{LR}, probing essentially the same quantity as the τ-polarization asymmetry $A_e(P_\tau)$ at LEP, differs from the latter by about 2.5σ [5, 6]. This discrepancy alone is hard to account for by means of new physics because the two quantities measure in principle the same thing[11]. Keeping this in mind one can, and should, still include A_{LR} in fits to the data. For the case of oblique new physics this means that the SLD result tends to push S' and T' towards negative values, away from their SM numbers $S' = T' = 0$.

About a year ago this tendency for negative S' (about 2σ) was significant enough to provoke the work described here. Upon analyzing more recent data one notices however that the discrepancy has since diminished. A recent fit yields $S' = -0.18 \pm 0.19$ and $T' = -0.09 \pm 0.18$ with a correlation of 0.85

[11] This essentially means that all fits (to new physics and/or to SM parameters (m_t, m_H, α_S)) that are done using simultaneously LEP and SLC data are much worse than 'LEP only' fits, hinting at the possibility of an experimental problem.

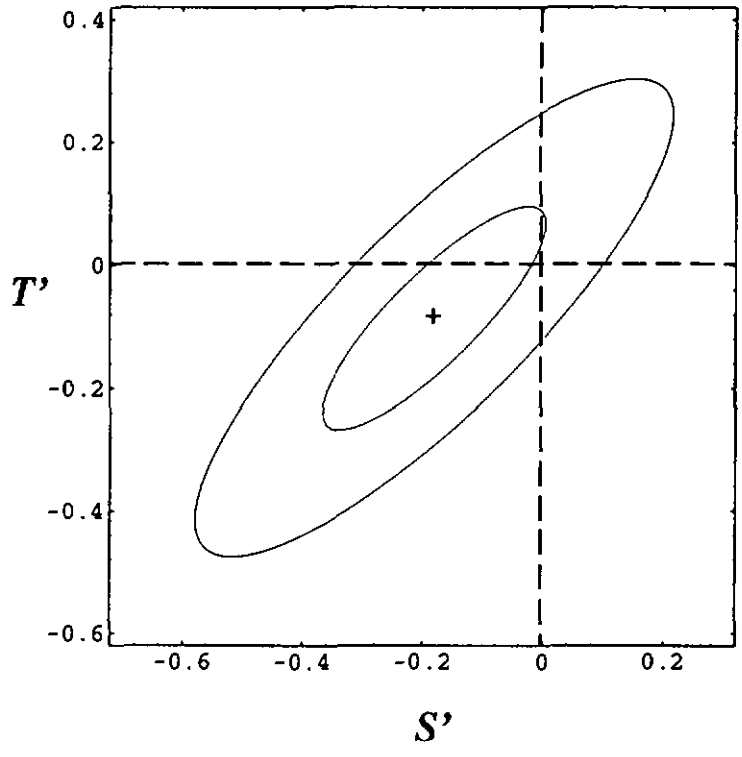

Figure 1.2: A fit of the oblique parameters S' and T' to the combined data from LEP and SLC (A_{LR}). The data has been taken from the second ref. in [5] and the following fiducial values have been used for the top mass m_t, the Higgs mass m_H and the strong coupling constant α_s: $m_t = 179$ GeV, $m_H = 300$ GeV and $\alpha_s = 0.125$. The inner curve denotes the $1-\sigma$ error ellipsoid, whereas the outer curve (corresponding to a $2.15-\sigma$ error ellipsoid) bounds an area within which the true values of both S and T lie *simultaneously* with a probability of 90% (90% CL ellipsoid). Clearly the data is consistent with the SM ($S = T = 0$) in the oblique new physics case.

between the two parameters and is displayed in fig.1.2. So one sees that the oblique parameters as inferred from high energy measurements are now clearly consistent with zero, *i.e.* with no new physics. However the results of our analysis are still valid and can be immediately taken at hand should there be once again a hint for new physics in the oblique sector.

1.3 Contributions of different types of oblique new physics to S' and T'

In this section we construct several types of models which contribute to precision electroweak observables dominantly (or, for some models, exclusively) through oblique corrections. As we will see many of them actually can give significant negative contributions to S' (and also to T'), and therefore point in the direction suggested (albeit only marginally) by the data.

Notice that the difference between the primed eq.(1.25) and unprimed parameters discussed before is not merely an academic point. We find in our search for models that it frequently happens that S' and T' take their most negative values when the new physics is light enough to permit positive, or slightly negative, values for S and T to be compensated in S' and T' by negative contributions to V and X. Since the models to which we are led therefore typically involve comparatively light particles, they can be expected to have more direct experimental implications in experiments in the comparatively near future.

Finding new physics that contributes negatively to S is particularly interesting when contrasted with technicolor models. This is because an additional strongly interacting technifamily generally yields large positive contributions to S [16]. Due to the nonperturbative nature of the involved calculations it is however reasonably difficult to obtain reliable estimates for the oblique parameters. The best predictions have been obtained assuming a custodial isospin symmetry. Extrapolations away from the isospin preserv-

ing limit point to a possible loophole where technicolor models could be in agreement with experiments provided there are light technifermions in the model [17]. Below we will examine the case of a weakly interacting 4^{th} family which also exhibits these features.

In order to see how different types of new physics contribute to S' and T' we take a conservative approach and simply supplement the SM by a few additional spin-zero or spin-half particle types, and explore the one-loop oblique parameters they generate as a function of the assumed quantum numbers and masses of the new particles. Of particular interest among our results are some particular cases of new particles, since these arise quite naturally among the low-energy spectrum of more complicated, but theoretically better motivated, models (such as the supersymmetric standard model *etc.*).

1.3.1 Scalars

The first class of models we investigate simply consists of complicating the SM Higgs sector by adding various scalar multiplets to the standard $Y = \frac{1}{2}$ doublet. Since, at one loop, each new multiplet contributes additively to the oblique parameters, we may consider the contributions of such new particles one multiplet at a time.

The contributions of scalar multiplets to parameters S through X have been computed in [18]. This is done in the following way: First one computes the vacuum polarizations $\delta\Pi_{ab}$ according to the diagrams in fig.1.3. Upon doing so one has to regularize (dimensional regularization) and renormalize ($\overline{MS}$) them. The anomalous self-energies then depend on the associated renormalization scale μ : $\delta\Pi_{ab}(\mu^2)$. For the cases considered below all these dependences on μ^2 cancel once one proceeds to compute the scalar contributions to S, T, U, V, W and X through eqs.(1.14) and finally to S' and T' via eqs.(1.25). This is because we choose representations and masses such that the scalar fields do not contribute to S' and T' at tree level and so these parameters do not need to be renormalized.

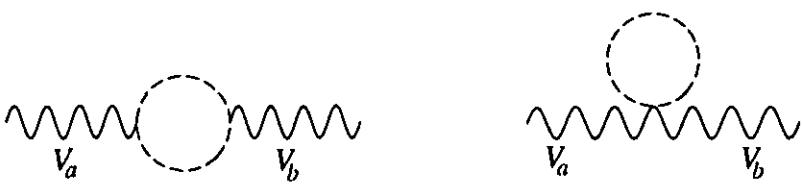

Figure 1.3: The lowest order (1-loop) contributions of new scalar isospin multiplets to gauge boson vacuum polarizations. $V_{a,b}$ stand for the gauge bosons γ, W and Z.

We have surveyed the parameter space of couplings and masses for various scalar multiplets. The results of this survey are summarized in figs. 1.4 through 1.7, which illustrate the dependence of the oblique parameters on scalar masses, by displaying the region of the $S' - T'$ plane which can be reached by varying the scalar masses from 50 to 200 GeV. Scalar masses below 50 GeV have not been considered to avoid bounds coming from direct production at LEP. We were also interested to see how large the contributions of the different scalar representations can be in the general 'negative' direction of the $S' - T'$ plane. To do so we created a table in which we display for which sets of scalar masses the negative contributions to the oblique parameters have been maximized. In order to perform this maximization we subjected the ratio of S'/T' to the constraint $S'/T' = (0.58/0.38)$ the value that was suggested by the contemporary fit results. The idea was merely to get a general 'feeling' as to what one might expect should the experimental trends towards negative values ever be reinforced. This table, table 1.1, also illustrates the difference between the primed and the unprimed parameters in this limit of light new physics.

Specifically we have considered the following types of scalar multiplets:

Isosinglet scalars

The simplest possible scalar multiplet to add is an $SU(2)_L$ singlet. Such particles arise in several interesting theoretical scenarios. They arise: (i) as

scalar partners to the right-handed leptons and quarks in supersymmetric models, (*ii*) in the class of models proposed by Zee [19] some years ago, and (*iii*) in leptoquark models where they can couple leptons to quarks in unorthodox, but baryon- and lepton-number preserving, ways. The contribution of a singlet scalar to S' and T' has been depicted in fig.1.4(b).

Isodoublet scalars

$SU(2)_L$ doublets constitute particularly well explored additions to the minimal standard model, since a second $Y = \frac{1}{2}$ scalar doublet appears naturally in many of its alternatives. Among the models which naturally incorporate doublet scalars are: (*i*) supersymmetric models, for which the extra scalars arise as an additional Higgs doublet (with $Y = \frac{1}{2}$), as well as the scalar superpartners of the left-handed quarks and leptons (having $Y = \frac{1}{6}$ and $\frac{1}{2}$ respectively), and (*ii*) models of (spontaneous or explicit) CP-violation at the electroweak scale, such as might be required for electroweak baryogenesis. The area in the $S' - T'$ plane that can be covered by various isodoublet scalars is displayed in figs.1.4 through 1.6. Fig.1.5 shows the oblique contributions due to light sleptons and squarks. Since the latter ones are subject to stringent CDF bounds [20] they cannot contribute significantly to negative (S', T'), as can be seen from this very figure. For this reason they are omitted from table 1.1.

Isotriplet scalars

Isotriplet scalars arise in many situations, such as in left-right symmetric models. Typically, if these fields are permitted to acquire vacuum expectation values (*vev*'s), they can spell trouble for low-energy weak-interaction measurements, through their tree level contributions to the rho parameter (*i.e.* T). We sidestep these bounds by assuming all *vev*'s to be zero[12]. In

[12]Notice that it is possible to avoid these bounds by artificially imposing a custodial symmetry on the scalar sector that ensures that rho attains its SM value at tree level,

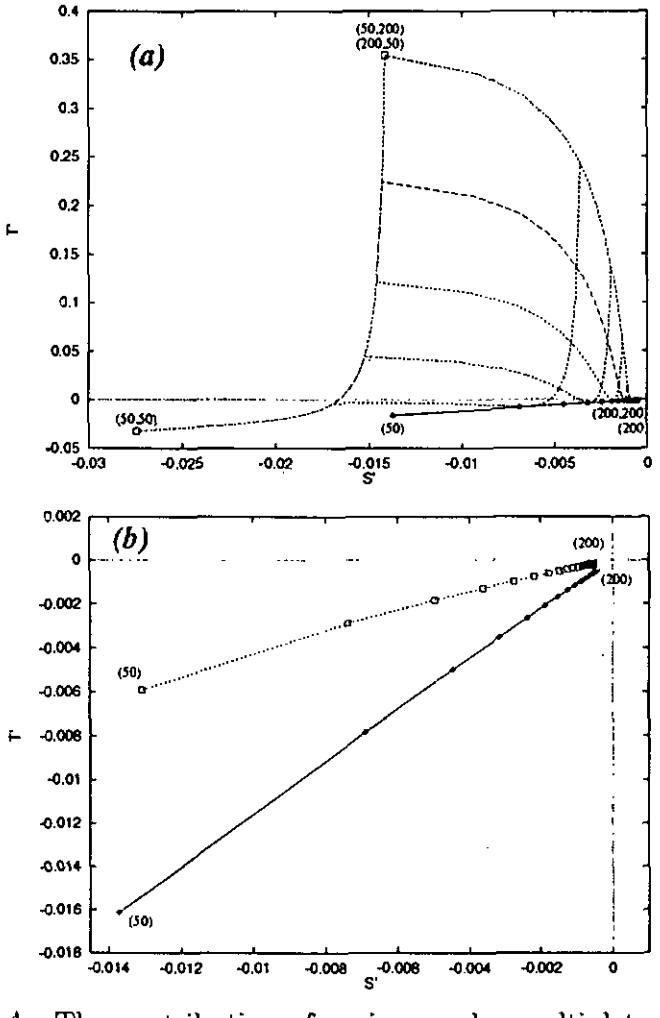

Figure 1.4: The contribution of various scalar multiplets to the oblique electroweak parameters S' and T'. In Figure (a) the dotted line represents a colour-singlet $Y = 0$ doublet with masses $(m_{\frac{1}{2}}, m_{-\frac{1}{2}})$ whereas the solid line depicts a colour-singlet, $Y = 0$ real doublet plotted against its mass, $m_{\frac{1}{2}}$. The grid spacing is 30 (resp. 10) GeV for dotted (resp. solid) plots. Figure (b): Here the lower (solid) line reproduces the colour-singlet, $Y = 0$ real doublet as in Figure $(4a)$, while the upper (dotted) line corresponds to a colour-singlet, $Y = 1$ singlet having mass (m_1). The Grid spacing in both cases is 10 GeV.

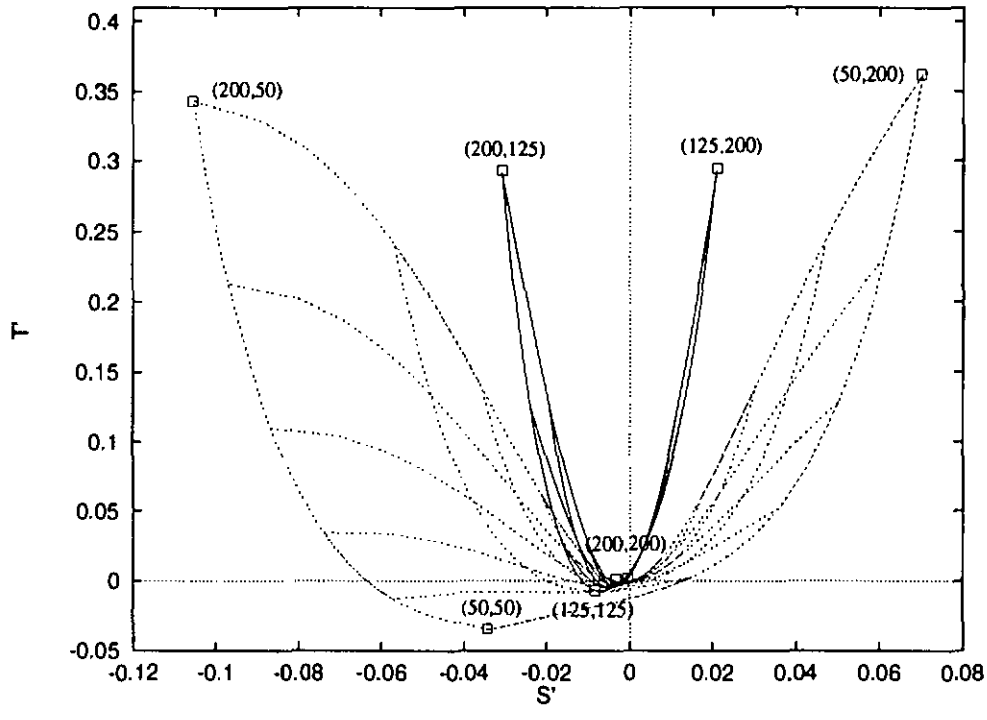

Figure 1.5: More scalar-generated oblique parameters. Solid line: a colour-triplet, $Y = \frac{1}{6}$ doublet (squarks) with masses $(m_{\tilde{u}}, m_{\tilde{d}})$. Dotted line: a colour-singlet, $Y = \frac{1}{2}$ doublet (a new Higgs or slepton *etc.*) with masses (m_1, m_0). The grid indicates steps of 25 (resp. 30) GeV for the solid (resp. dotted) plots.

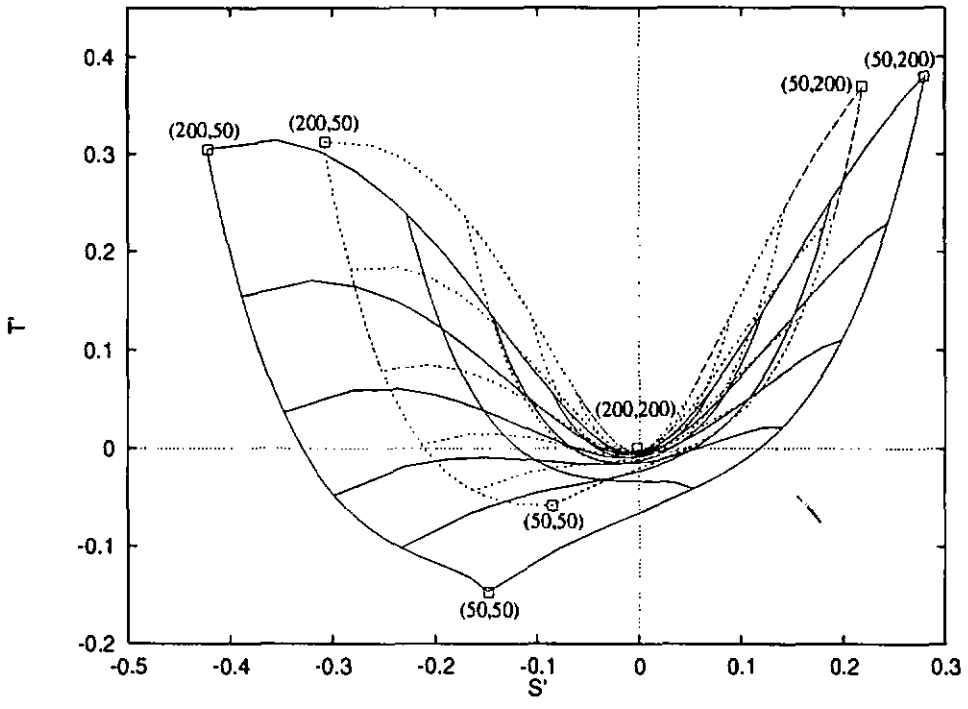

Figure 1.6: More scalar representations that affect the oblique parameters. Solid line: a colour-singlet, $Y = 1$ triplet with masses $(m_2^2, m_1^2, m_0^2) = (a^2, \frac{1}{2}(a^2+b^2), b^2)$, where a and b take the values given in brackets: (a, b). Dotted line: A colour-singlet, $Y = \frac{3}{2}$ doublet with masses (m_2, m_1) as indicated in brackets. The grid in both cases represents steps of 30 GeV.

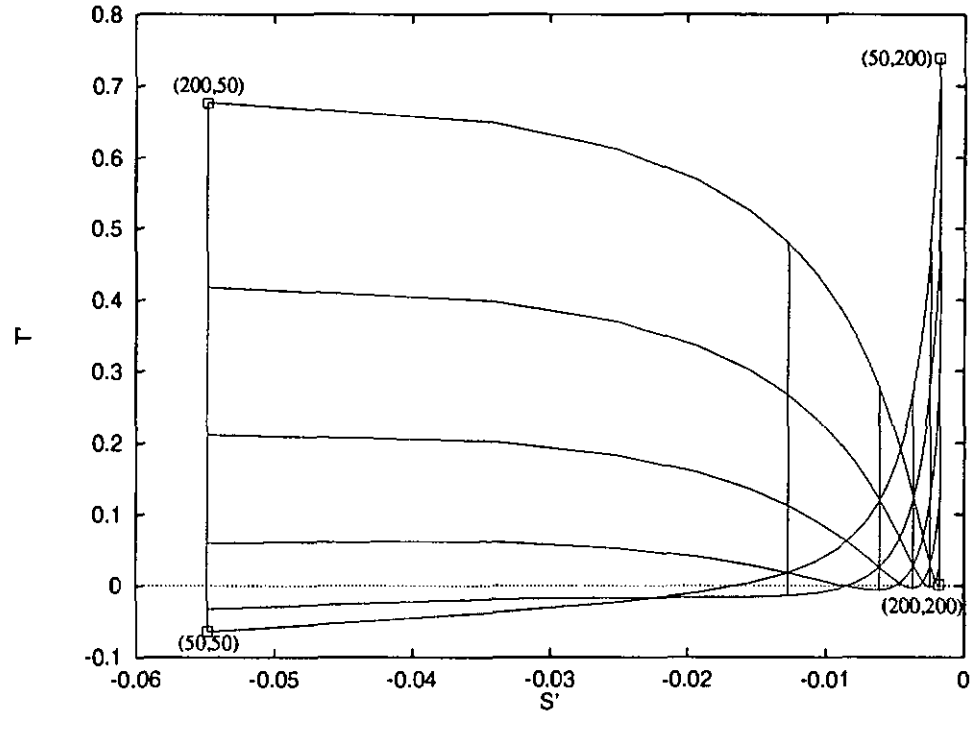

Figure 1.7: The oblique corrections due to a colour-singlet $Y = 0$ real triplet scalar with masses (m_0, m_1) given in brackets. The grid spacing is 30 GeV.

order to do so we have also to make sure that the scalar masses we use do not require such a nonzero *vev*. For the triplet depicted in fig. 1.6 *e.g.* an equal splitting of the squared masses can be obtained using gauge invariant interactions with the SM doublet and require only the SM *vev* to be nonzero. Oblique contributions to various triplet representations can be found in figures 1.6 and 1.7.

even for nonvanishing *vev*'s [21]. However this comes at a price: Keeping rho close to its SM value once radiative corrections are included requires fine-tuning of the scalar self interactions, thus rendering any such model highly unnatural.

Scalar contributions: general points

When inspecting figures 1.4 through 1.7 and table 1.1 one notices several features scalar generated oblique corrections to the SM exhibit.

First of all, all of the allowed regions in these figures include the origin, $S' = T' = 0$, with the corollary that it is always possible to produce negative values for S' and T'. There is a simple explanation why this is always so for scalars, even though, as we shall see, the same is *not* true for fermions. The main point is that all of the oblique electroweak parameters must vanish in the limit that the new physics becomes heavy in an $SU(2)_L \times U(1)_Y$-invariant way. And, unlike for fermions, gauge-invariant masses are *always* possible for scalar multiplets.

Notice also that the largest values of S' and T' generally arise from the smallest values for the scalar masses. As a result, the most important regions of parameter space are precisely those for which the difference between S and S' and T and T' is the most important.

Another point is that their oblique contributions to S' and T' can serve to bound the masses of exotic scalar particles. Those bounds are quite robust, since the 1-loop vacuum polarizations depend solely on the electroweak transformations properties of the involved multiplet (in the absence of significant mixing amongst various electroweak multiplets). The same is generally not true for other bounds, since these can depend on such things as the existence and strength of their Yukawa couplings to fermions, as well as on whether they exhibit nonzero *vev*'s or not. In fact, it is quite simple to arrange for scalars to contribute to experiments predominantly through their oblique corrections, just by forbidding (or suppressing) their non-gauge couplings by a (possibly approximate) symmetry.

Finally there are several points concerning the potential size of such scalar based oblique corrections to the SM. Typically, larger values for S' and T' are possible given larger values for Y, or given a larger $SU(2)_L$ representation. This can be most clearly seen from Table I, for which S' increases both with increasing weak isospin, and with increasing Y for fixed weak isospin. The

Multiplet $(3 \times 2 \times 1)$	Optimal Masses (GeV)	S'	T'	U'	S	T	U
$(\mathbf{1},\mathbf{1},Y=1)$	$m = 50$	-0.01	-0.006	0.002	-0.003	0	0.003
$(\mathbf{1},\mathbf{2},Y=\frac{1}{2})$	$\begin{pmatrix} m_1 \\ m_0 \end{pmatrix} = \begin{pmatrix} 62 \\ 50 \end{pmatrix}$	-0.04	-0.03	0.03	-0.03	0.003	0.003
$(\mathbf{1},\mathbf{2},Y=0)$	$\begin{pmatrix} m_{+\frac{1}{2}} \\ m_{-\frac{1}{2}} \end{pmatrix} = \begin{pmatrix} 50 \\ 72.5 \end{pmatrix}$	-0.02	-0.01	0.02	-0.01	0.009	0.003
$(\mathbf{1},\mathbf{2},Y=\frac{3}{2})$	$\begin{pmatrix} m_2 \\ m_1 \end{pmatrix} = \begin{pmatrix} 51 \\ 50 \end{pmatrix}$	-0.09	-0.06	0.04	-0.03	0.00002	0.01
$(\mathbf{1},\mathbf{3},Y=0)^\dagger$	$\begin{pmatrix} m_1 \\ m_0 \\ m_{-1} \end{pmatrix} = \begin{pmatrix} 50 \\ 78 \\ 50 \end{pmatrix}$	-0.06	-0.04	0.1	-0.03	0.03	0.07
$(\mathbf{1},\mathbf{3},Y=1)$	$\begin{pmatrix} m_2 \\ m_1 \\ m_0 \end{pmatrix} = \begin{pmatrix} 63 \\ 57 \\ 50 \end{pmatrix}$	-0.2	-0.1	0.1	-0.1	0.003	0.01

† Self-conjugate multiplet.

Table 1.1: Exotic Scalars

One-loop oblique electroweak parameters due to exotic scalar multiplets. This table displays the masses which 'optimize' the oblique electroweak parameters in the sense described in the text, together with the resulting optimal values. Masses have not been allowed to be smaller than 50 GeV in order to avoid direct detection at LEP. $(\mathbf{r_1},\mathbf{r_2},Y=y)$ denotes the representation of $SU_C(3) \times SU_L(2) \times U_Y(1)$ in which the scalars transform, and m_q represents the mass of a state having electric charge q.

variation with Y is simplest to see for $SU(2)_L$ singlets, for which all of the oblique parameters are simply proportional to Y^2.

A similar enhancement of the oblique parameters can be achieved by coupling the scalar multiplets to the strong gauge group, $SU(3)_c$. In this case all oblique parameters must be multiplied by the dimension, d_c, of the appropriate $SU(3)_c$ representation. (These factors, together with the factors of hypercharge mentioned earlier, can be quite large. For instance, a colour-sextet $SU(2)_L$-singlet scalar having $Y = \frac{4}{3}$, as would be required for a Yukawa coupling to two right-handed up-type quarks, has $d_c Y^2 = \frac{96}{9} = 10\frac{2}{3}$.) Using colour to amplify the oblique corrections does not come without its price, however, since the masses of colored particles are often subject to more stringent bounds than are those for colour singlets, due to their non-observation in $p - \bar{p}$ [22] and $e - p$ [23] collisions. These bounds can be sensitive to the nature of the new particle's dominant decay mode, however, and so can be more model dependent than are those furnished by LEP.

As we will see in the next section, scalar contributions to oblique parameters are generally smaller than those generated by fermions. To get sizeable scalar contributions away from the SM one therefore often has to invoke several new scalars, all contributing together to produce the desired size effect.

1.3.2 Fermions

We turn now our attention to the addition of exotic fermions of various types to the Standard Model. As we found for scalars, at one loop we may consider separately the contribution to the oblique parameters of each additional multiplet. A calculation of the six oblique parameters as functions of general fermion masses and couplings is given in [11]. Again one proceeds by computing the μ^2 dependent vacuum polarizations according to fig.1.8, and again the μ^2 dependence cancels when S' and T' are extracted from eqs.(1.14) and (1.25). An exception to this is the case of a non-degenerate mirror fermion

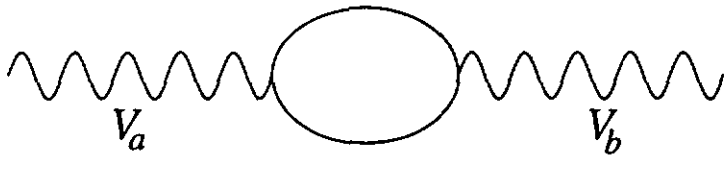

Figure 1.8: One loop contributions of exotic fermions to gauge boson vacuum polarizations. As before $V_{a,b}$ stands for a either γ, Z or W.

multiplet which is discussed in detail later on.

The survey of the parameter space of couplings and masses for the various fermion multiplets is organized in the same way as it was for the exotic scalars: Figs.1.9 and 1.10 plot the dependence of the oblique parameters on the fermion masses, which we take to range from 50 to 200 GeV. Table 1.2 displays the values for these masses which are 'optimal' in the same sense as was used for the scalars. While optimizing we forbid masses which are smaller than 50 GeV, due to the bounds from direct production at LEP.

The following two types of fermions are of particular interest:

Sequential quarks and leptons

These constitute one out of two kinds of isodoublet fermions that have been widely considered in the literature (the other one is described below), and could describe an extra family for example.

Figure 1.9 displays the effect such an extra family could have on oblique parameters. Here as well as in table 1.2 Tevatron bounds [22] to the 4^{th} generation quarks have been applied. Due to the higher energies at this collider these bounds are much stronger than are those from LEP. It is possible though, should the 4^{th} generation quarks not mix with the usual ones, that the Tevatron bounds would be somewhat weaker. For completeness we therefore include the optimized values for an extra quark doublet, subject only to the LEP bounds, in table 1.2.

Other points emerge from an inspection of figure 1.9: First, unlike the scalar case, it is not necessarily true that the origin, $S' = T' = 0$, needs

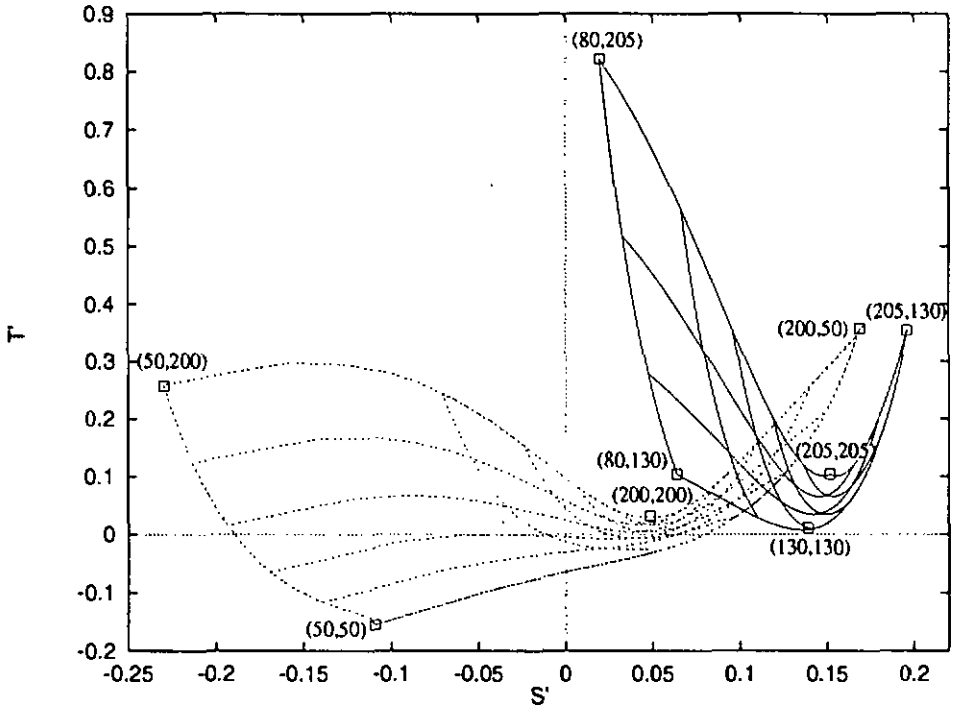

Figure 1.9: The contribution of an extra SM family to the oblique parameters. Solid line: a colour-triplet, $Y = \frac{1}{6}$ quark doublet with masses $(m_{\nu'}, m_{l'})$ as indicated in brackets. Dotted line: a colour-singlet, $Y = \frac{1}{2}$ lepton doublet with masses $(m_{\nu'}, m_{l'})$. The grid spacing represents steps of 25 (resp. 30) GeV for the solid (resp. dotted) plots.

lie in the parameter space of an exotic fermion multiplet, provided that this multiplet lies in a chiral representation of $SU(2)_L \times U(1)_Y$ (as does an additional sequential lepton or quark). A quark multiplet, in particular, definitely favours positive S', making a real trend to negative S' strongly disfavor such particles. (This is essentially the observation which was originally used to disfavor technicolor models [8] and has also been used to argue against an additional very heavy fermion generation [24].) As may also be seen from table 1.2, for a complete additional generation the contribution of extra quarks can be compensated by the additional leptons, but *only* if the additional leptons are reasonably light.

Also we reproduce in figure 1.9 the growth of T, and hence the low-energy rho parameter, in the limit that the mass splitting in a standard multiplet becomes large.

Mirror fermions

Mirror fermions, fermions for which both the left and right-handed parts are multiplets with identical dimension under $SU(2)_L$ and identical hypercharge, are an alternative way of supplementing the SM with additional fermions. Due to their specific chirally symmetric structure they can have an $SU(2)_L \times U(1)_Y$ invariant degenerate mass term. Arbitrary masses are therefore possible for a mirror singlet, the simplest possible way of supplementing the SM with additional fermions. Another possibility is to add a mirror doublet.

Figure 1.10 and table 1.2 display the values for S' and T' that are obtained for a mirror singlet as well as mirror doublets with various hypercharges. Only the case of a degenerate multiplet is shown here because it is only in this case that all of the parameters S through X are independent of the renormalization scale, μ. (This is in contrast with all of the previous examples we consider, which are μ-independent for any choices for the masses.) For a non-degenerate mirror fermion multiplet the parameter T develops a μ-dependence which is proportional to the square of the mass splittings within

Multiplet $(3 \times 2 \times 1)$	Optimal Masses (GeV)	S'	T'	U'	S	T	U
$(\mathbf{1},\mathbf{2},Y=-\frac{1}{2})^*$	$\begin{pmatrix} m_{\nu'} \\ m_{e'} \end{pmatrix} = \begin{pmatrix} 50 \\ 92 \end{pmatrix}$	-0.2	-0.1	0.1	-0.06	0.03	0.04
$(\mathbf{3},\mathbf{2},Y=\frac{1}{6})^*$	$\begin{pmatrix} m_{t'} \\ m_{b'} \end{pmatrix} = \begin{pmatrix} 104 \\ 50 \end{pmatrix}$	-0.1	-0.08	0.3	-0.01	0.2	0.1
(extra SM family)	$\begin{pmatrix} m_{\nu'} \\ m_{e'} \\ m_{t'} \\ m_{b'} \end{pmatrix} = \begin{pmatrix} 50 \\ 100 \\ 130 \\ 95 \end{pmatrix}$	-0.06	-0.04	0.2	0.04	0.1	0.05
$(\mathbf{1},\mathbf{1},Y=1)^\dagger$	$m = 50$	-0.2	-0.09	0.03	-0.03	0	0.03
$(\mathbf{1},\mathbf{2},Y=0)^\dagger$	$m = 50$	-0.4	-0.5	0.4	-0.2	0	0.009
$(\mathbf{1},\mathbf{2},Y=\frac{1}{2})^\dagger$	$m = 50$	-0.5	-0.5	0.4	-0.2	0	0.005

† Plus a mirror multiplet with conjugate quantum numbers.
* Plus right-handed isosinglets with identical electric charges.

Table 1.2: Exotic Fermions

One-loop oblique electroweak parameters due to exotic fermions. This table displays the masses which 'optimize' the oblique electroweak parameters in the sense described in the text, together with the resulting optimal values. $(\mathbf{r_1},\mathbf{r_2},Y=y)$ denotes the transformation properties of the left-handed fermions. The second line displays the values obtained for a 4^{th} generation quark doublet subject only to LEP bounds and so represents a 'most optimistic' case as explained in the text.

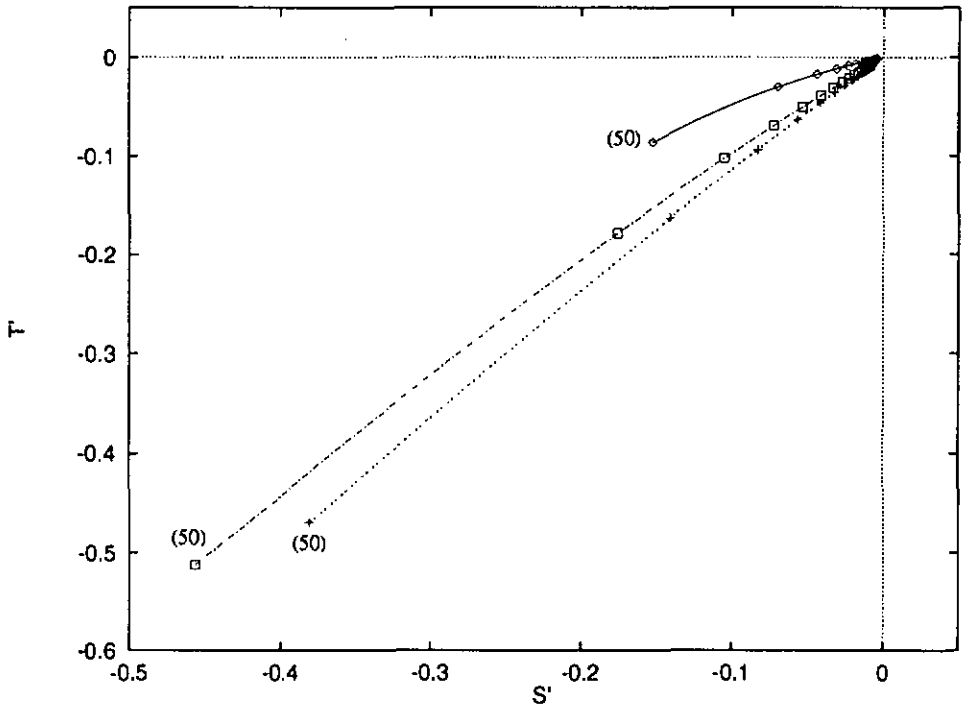

Figure 1.10: Oblique parameters due to colour-singlet mirror fermions. Solid line: a $Y = 1$ mirror singlet with mass (m_1). Dotted line: a $Y = 0$ mirror doublet with (degenerate) mass $(m_{\frac{1}{2}})$. Dash-dotted line: a, $Y = \frac{1}{2}$ mirror doublet with (degenerate) mass $m_1 = m_0$. The grid spacing represents steps of 10 GeV for all three plots.

the multiplet.

There is a simple reason for the appearance of the μ dependence for a non-degenerate multiplet. The main point is that although a mirror doublet can acquire a common degenerate mass in an gauge invariant way, renormalizable interactions can split the masses within a multiplet only if new, non-doublet, scalars are introduced and acquire a *vev*. As a result these scalars contribute to the parameter T at the tree level, and so this parameter must be renormalized — thereby developing a dependence on μ — just as must any other classical parameter[13].

Fermionic contributions: general points

Not much remains to be said. As already observed for the scalar case the largest values for S' and T' arise from the smallest values for the fermion masses, again emphasizing the difference between the primed and unprimed parameters. And again, as in the scalar case, the magnitude of the oblique parameters grows with the hypercharge and the size of the color representation of the multiplet concerned. Notice, however, that the overall contribution of a given fermion representation is significantly larger than that of additional scalars which transform in the same representation.

1.3.3 Conclusions

In conclusion of this section and of this chapter I would like to emphasize a few important points.

First we have explored in a systematic way the kinds of oblique new physics which can produce sizeable deviations from the SM predictions for Z^o-pole physics. We have thereby found that the presence of light oblique new physics, *i.e.* exotic particles with masses not much above their threshold

[13]The same happens for scalars if the desired mass pattern requires such vacuum expectation values.

of direct detection ($M_Z/2$ for most cases), can significantly alter conventional analyses in terms of the original three Peskin-Takeuchi parameters S, T and U. This is so because light new physics can give non-zero contributions to the extended oblique parameters V and X [11, 13], which would be approximately zero in the presence of heavy new physics ($M_{\rm NP} \gtrsim 1$ TeV), and which in turn alter the values of S', T' and U'. We emphasize the necessity for interpreting the data on the Z^o-pole (and the W mass) in terms of the variables S', T' and U', which are linear combinations of the usual variables, S, T, U with the new ones, V and X.

Also we were interested in obtaining negative contributions to the oblique parameters S' and T', since this is the direction preferred by the data, and found that for some models it is possible to obtain a correction which predicts S' and T' as large as -0.1 to -0.6. New fermions are preferable to new scalars in this regard, since they generate vacuum polarizations which are systematically larger than the scalars, given similar couplings and masses. In all cases we find that requiring relatively large contributions to the oblique parameters points to new particles whose masses are *not* very large compared to m_W or m_Z. Should the tendency of the data towards negative values of S' ever become statistically significant this preference for comparatively light particles should have happy consequences since they stand a good chance of being seen in other experiments once higher energies become directly observable. In particular, since it is the coupling of these particles to the W and the Z which is responsible for their contributions to the oblique vacuum polarizations, they should be directly pair-produced at LEP-200 if they are light enough for this to be kinematically allowed.

Interestingly our analysis tends to disfavor an additional SM family of fermions, provided that it mixes with the usual three families, and that the lepton masses (especially the neutrino mass) are not too close to their present LEP lower limits $\simeq M_Z/2$. This reasoning goes along the same lines as those used to disfavor technicolor models [8].

At last it should be emphasized that the present experimental situation

does not allow to distinguish between different models. The intention has merely been to classify the effects oblique new physics can have on Z^o-pole observables, hence facilitating a basis for more detailed investigations should there once again be a hint for new physics in the oblique sector.

2

Neutrinoless double beta decay

This chapter is mainly based on publications [2, 3] and addresses the following two issues:

First we investigate the possibility of producing observable neutrinoless double beta decay ($\beta\beta_{0\nu}$) *without* having an electron neutrino with a mass in the vicinity of 1 eV. The basic idea behind this is that the electron neutrino could mix with a much heavier ($m \gtrsim 1$ GeV) sterile neutrino, which in turn dominantly contributes to the $\beta\beta_{0\nu}$ decay rate.

Second two new Majoron emitting modes for neutrinoless double beta decay are presented. These new modes have electron spectra which differ from the decays that are usually considered. One of them even predicts an electron spectrum which is softer than the usual two-neutrino spectrum of the standard model and has not been considered before.

Finally we construct illustrative models in both cases to show how other phenomenological bounds can be accommodated. In the first case this leads us to a simple model which satisfies all existing laboratory, astrophysical and cosmological information. For the case of models for Majoron emission it is exactly this phenomenological viability that constrains the rates to be at best large enough to be detectable in current experiments.

2.1 Introduction

The aim of this introduction is not to give a lesson in the basics of neutrino physics, which to my eyes is made obsolete by the rich existing literature on the subject, but rather to give a short overview and some motivation of the work presented later on in this chapter.

Out of the large number of reviews on neutrino physics and double beta decay there are many that could be recommended. To keep things simple however the reader is referred to an excellent and recent general review by Gelmini and Roulet [25]. Among summarizing some general issues related to double beta decay and neutrino oscillations in a concise way, this review also gives a very good introductory account on the subject of spinors as they appear in neutrino physics. Specifically it explains the differences between Weyl, Dirac and Majorana spinors and some subtleties of their definitions some people might be unaware of.

Why double beta decay? There have been several indications for deviations from the SM in the neutrino sector in recent years. Those have mainly been direct or indirect hints for neutrino mass. Since neutrinos, as described by the minimal version of the standard model (SM), have no mass, any such experimental observation necessitates physics beyond the SM. From the theoretical point of view on the other hand there are many well motivated models that incorporate nonzero neutrino masses in a natural way. For instance, it is by now well known that if neutrinos have a mass, the smallness of this mass is easily understood if there is an additional heavy, isosinglet Majorana neutrino which mixes with the known ones *via* the so-called see-saw mechanism [26].

The three main signatures for neutrino mass are

- (1) Mixing (high energy experiments, universality, lepton and meson decays) and oscillation (reactor-, accelerator-, atmospheric neutrino- and solar neutrino experiments, *c.f.* chapter 3)

- (2) Kinematic detection in β decays (Tritium, lepton and meson decays)

- (3) Neutrinoless double beta decay $\beta\beta_{0\nu}$ (Germanium, Xenon and Tellurium decays)

Each of these signatures is able to provide different information on neutrino masses. Experiments that are sensitive to flavor oscillations (1) only constrain mass-squared differences and/or mixing angles and are thus in general not able to give explicit values or upper bounds on single mass eigenvalues. Kinematic analyses of beta decay spectra (2) on the other hand yield upper bounds of the total Dirac and/or Majorana mass of the electron neutrino. $\beta\beta_{0\nu}$ (3) finally is sensitive to the effective Majorana mass of the electron neutrino.

This unique capability of $\beta\beta_{0\nu}$ to measure directly the amount of involved electron-number (L_e) violation has stimulated experimental research. Also there are several other types of non-standard decay modes to which these experiments are sensitive, such as the decay ($\beta\beta_{\varphi}$) into two electrons plus a neutral scalar, φ, which has been predicted by a number of plausible alternatives to the SM, starting with the simple Gelmini-Roncadelli (GR) model of spontaneous lepton-number breaking [27, 28]. In other words $\beta\beta$ decay experiments are very sensitive to physics beyond the SM.

On the other hand, these very same experiments have provided a new confirmation of the SM in the recent years with the unambiguous observation of the SM two-neutrino double beta decay $\beta\beta_{2\nu}$[1]. This decay, which occurs at the second order in electroweak charged-current interactions, emits two antineutrinos in addition to the two electrons due to the conservation of lepton-number.

Over the years there has been a large variety of non-standard $\beta\beta$ decay modes proposed in the literature. This '$\beta\beta$-decay zoo' often leads to a considerable amount of confusion and it seems therefore reasonable to devote the

[1] The experimental situation has recently been thoroughly reviewed in [29] and [30].

next section to a classification of the different possible non-standard double beta decays.

2.2 Classification of double beta decays

The aim of this section is to give a comprehensive and clear overview of the different classes of neutrinoless double beta decay modes that have been considered in the literature. It therefore necessarily mixes old results that have been obtained elsewhere (see e.g. [31] - [36]) with new ones [3].

To do so we use a simple classification in terms of available experimental signatures that has first been proposed in [31] and is summarized in table 2.1. This classification is then supplemented, in the following section, with a list of the decay rates for most of these classes. The expressions for these rates are obtained via some very general model of the underlying interactions.

More specific models are then needed to see how other phenomenological bounds can be accommodated and whether an observable $\beta\beta_{0\nu}$ decay rate is feasible or not. This is done in sections 2.4 and 2.5 where new hitherto unconsidered decay modes [2, 3] are examined in detail.

2.2.1 Naive classification

A straightforward naive classification of different $\beta\beta$ decays is given in terms of the involved decay products. Although it is of no practical value it serves to fix the notation:

$$\beta\beta_{0\nu} \quad \begin{cases} \beta\beta_{2\nu} & : \; N \to N' + 2e^- + 2\overline{\nu_e} \\ \beta\beta_{0\nu}^{\text{pure}} & : \; N \to N' + 2e^- \\ \beta\beta_{\varphi} & : \; N \to N' + 2e^- + \varphi \\ \beta\beta_{\varphi\varphi} & : \; N \to N' + 2e^- + 2\varphi \end{cases} \tag{2.1}$$

here $N(Z,A)$ and $N'(Z+2,A)$ denote the parent and the daughter nucleus respectively. The first line in equation (2.1) is the normal two neutrino double beta decay as it occurs in the SM. The other three lines represent decays which do not have neutrinos among their decay products and which I therefore commonly call $\beta\beta_{0\nu}$ in what follows. To distinguish the symbol $\beta\beta_{0\nu}$ from the 'pure' neutrinoless double beta decay, where neither neutrinos nor Majorons are emitted, the latter has been called $\beta\beta_{0\nu}^{\mathrm{pure}}$. Decays where one scalar is emitted ($\beta\beta_{\varphi}$) comprise most of the early models (including GR) as well as some newer models [33]. Two Majoron emission ($\beta\beta_{\varphi\varphi}$) finally is a more recent notion ([3, 34]) and will be discussed in detail in sections 2.3.6, 2.3.8 and 2.5. In these decays two Majorons rather than one are emitted because the one Majoron mode is either strongly suppressed or completely forbidden by the approximate or exact conservation of an additive quantum number (e.g. L_e).

The classification presented above is however not very practical. This is because decays of the same type (e.g. $\beta\beta_{\varphi}$) can have very different experimental signatures according to the underlying model and similarly different modes (e.g. $\beta\beta_{\varphi}$ and $\beta\beta_{\varphi\varphi}$) can turn out to be almost indistinguishable experimentally.

A more practical classification in terms of available experimental signatures is asked for. Such a classification has first been presented in [31] and is largely reproduced here.

2.2.2 Classification in terms of experimental signatures

The theoretical evolution [32, 33, 34, 35, 36, 3] that has ultimately led to this classification has been stimulated by two recent experimental observations:

First of all several of the original models for Majoron emission in $\beta\beta$ decays, such as the Gelmini-Roncadelli model, have been excluded by electroweak precision measurements on the Z-pole [5]. And second there have

been some indications for an excess numbers of electrons in the decay spectra of $\beta\beta$ decay which could be explained - if taken seriously - by means of non-standard (*i*.e. Majoron emitting) $\beta\beta$ decays [37]. Although these statistical hints have since diminished (see *e.g.* [29]) the conclusions of the theoretical investigations still stand: Models that can produce observable $\beta\beta$ decay rates and satisfy all phenomenological bounds at the same time are possible, the new physics they describe, however, typically has properties that are rather different from what one would expect based on experience with the older models (GR *etc.*).

One of these differences is based on the simple observation that many of the bounds coming from LEP can be avoided if the scalars emitted in $\beta\beta_{0\nu}$ are $SU(2)_L \times U(1)_Y$ singlets, contrary to *e.g.* the GR model where the Majoron was part of a $SU(2)_L$ triplet representation. In fact many of the new models that so have been proposed are actually variations of the old singlet Majoron model [38]. Another difference is due to $\beta\beta$ experiments themselves, which, through the non-observation of $\beta\beta_{0\nu}^{\text{pure}}$, continuously lowered the upper limit on electron-number violation. Whereas older models, in which lepton-number was broken (GR), were sensitive to this bound, many of the newer theories were devised such that they conserve L_e.

One of the main experimental signatures to discriminate different models of $\beta\beta$ decay is therefore the observation of $\beta\beta_{0\nu}^{\text{pure}}$ and hence of L_e violation. In $\beta\beta_{0\nu}^{\text{pure}}$ the total energy of the outgoing electrons $\epsilon = \epsilon_1 + \epsilon_2$ is equal to the energy $Q = M - M'$ liberated in the decay. Here ϵ_1 and ϵ_2 denote the two electron energies and M (M') are the masses of the parent (daughter) nucleus respectively.

As soon as other relativistic decay products are present however ($\beta\beta_{2\nu}$, $\beta\beta_{\varphi}$, $\beta\beta_{\varphi\varphi}$), events are distributed over the whole range of the total electron energy $2m_e \leq \epsilon \leq Q$ and it is the shape of this distribution *i.e.* the rate as a function of the electron energies that provides the second important signature. Luckily it turns out that this rate has, quite generally, a very

simple form:

$$\frac{d\Gamma}{d\epsilon_1 d\epsilon_2} \propto (Q - (\epsilon_1 + \epsilon_2))^n p_1\epsilon_1 F(\epsilon_1) p_2\epsilon_2 F(\epsilon_2) \tag{2.2}$$

where 'n', the so-called spectral index, is an integer (typically $n = 1, 3, 5, 7$), p_i are the absolute values of the three momenta of the electrons and the $F(\epsilon_i)$ are the Fermi functions (see next subsection).

It is ultimately the small size of the energy, $Q \sim 2$ MeV, in comparison with the typical momenta, $p_F \sim 60$ MeV, of the nucleons in the decaying nucleus that ensures that the electron spectrum takes such a simple form - *i.e.* one that is characterized simply by the integer n. This is because the small ratio of these two scales justifies, for the precision required here, keeping only the lowest term in an expansion of the decay rate in powers of the momenta of the decay products $(e^-, \varphi, \overline{\nu_e})$. The index, n, that is appropriate for any particular kind of decay is determined by the leading term in this expansion of the relevant decay rate.

Models can now be distinguished from one another by the value they predict for n. This value is determined first by the phase space element of the invisible decay products and second by the scalar-fermion couplings. For instance the phase space contribution of the two neutrinos in the SM decay $\beta\beta_{2\nu}$ implies a spectral index of $n = 5$. The phase space volume element of the single scalar in a model of class IIB of table 2.1 on the other hand yields $n = 1$. If the scalar is a Goldstone boson as *e.g.* in class IID it couples derivatively to the neutrinos and one more power of the scalar momentum can enter into the amplitude leading to an index $n = 3$. The shape of the different electron spectra is shown in figure 2.1 and the classification of different models for $\beta\beta_{0\nu}$ decay is summarized in table 2.1.

Upon inspecting table 2.1 one notices that the models have been divided into two types (I and II) according to whether electron-number is broken or not. Any type II models that predict the emission of scalars necessarily incorporate Majorons that carry lepton-number (*i.e.* IIB-IIE). They have therefore also been called 'charged Majoron models' [32]. A further experi-

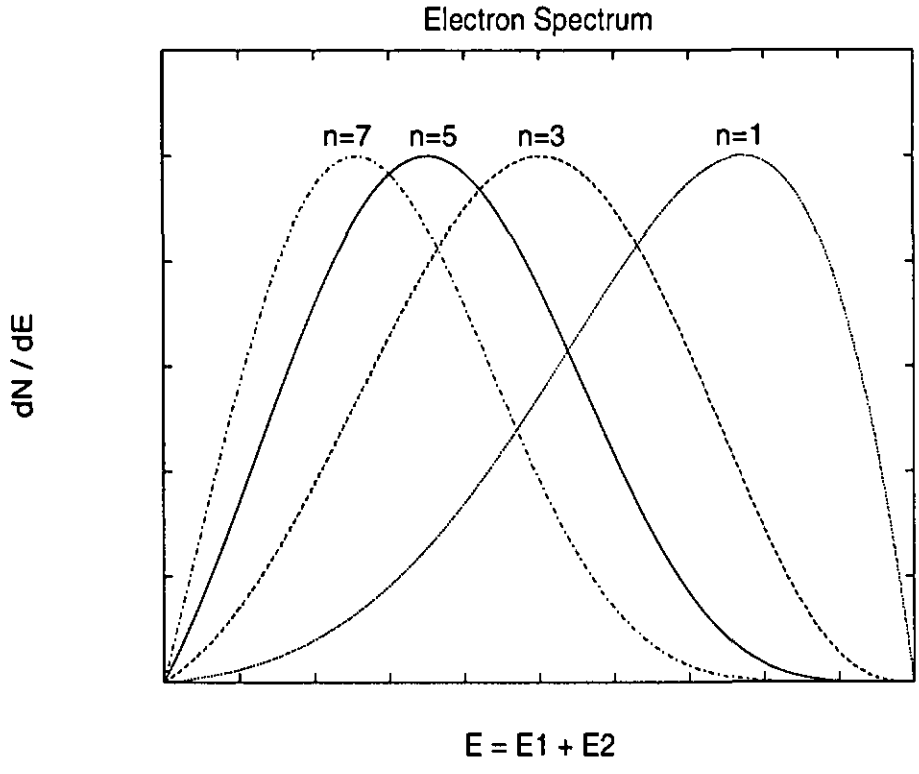

Figure 2.1: The $\beta\beta$ spectrum as a function of the two electrons' total kinetic energy for various choices of the 'spectral index' n. $n = 1$ (GR) corresponds to the dotted line, $n = 3$ is the dashed line, $n = 5$ ($\beta\beta_{2\nu}$) is the solid line and $n = 7$ is the dash-dotted line. All four curves have been arbitrarily assigned the same maximal value for purposes of comparison.

	L_e	A New Scalar:	$\beta\beta_{0\nu}^{\text{pure}}$	Dominant Scalar Decay	Spectral Index
IA	Broken	Does Not Exist	Yes	None	N.A.
IB	Broken	Is Not a Goldstone Boson	Yes	$\beta\beta_{\varphi}$	$n=1$
IC	Broken	Is a Goldstone Boson	Yes	$\beta\beta_{\varphi}$	$n=1$
ID	Broken	Is Not a Goldstone Boson	Yes	$\beta\beta_{\varphi\varphi}$	$n=3$
IE	Broken	Is a Goldstone Boson	Yes	$\beta\beta_{\varphi\varphi}$	$n=3$
IIA	Unbroken	Does Not Exist	No	None	N.A.
IIB	Unbroken	Is Not a Goldstone Boson ($L_e=-2$)	No	$\beta\beta_{\varphi}$	$n=1$
IIC	Unbroken	Is Not a Goldstone Boson ($L_e=-1$)	No	$\beta\beta_{\varphi\varphi}$	$n=3$
IID	Unbroken	Is a Goldstone Boson ($L_e=-2$)	No	$\beta\beta_{\varphi}$	$n=3$
IIE	Unbroken	Is a Goldstone Boson ($L_e=-1$)	No	$\beta\beta_{\varphi\varphi}$	$n=7$

Table 2.1: Classification of $\beta\beta_{0\nu}$ decay modes

Alternatives for modelling double beta decay are classified in this table based on whether they break electron-number (type I) or not (type II), the spectral index 'n' they predict and on whether the emitted boson is a Goldstone boson or not.

mental distinction is then facilitated by the spectral index n given in the last column. Models which are of the same type and which have the same spectral index only differ in the nature of the emitted boson(s). A massive boson will be experimentally distinguishable from a Nambu-Goldstone boson only when its mass is large enough to alter the shape of the electron spectrum in an observable way[2]. Given that it's practically impossible to see the effects of a very light Majoron, the models (IB&IC), (ID&IE) and (IIC& IID) can often not be told from one another.

We are therefore left with the following seven basic categories of double beta decay:

- IIA: This class contains the SM and represents the 'boring' case when no new physics is seen in $\beta\beta$ decay experiments.

- IA: Any model of an effective Majorana mass for the electron neutrino and no scalar emission belongs to this class (*i.e.* any model that predicts $\beta\beta^{\text{pure}}_{0\nu}$ as the only exotic decay mode, such as the basic See-Saw scenario). A variant model of this type [2] will be discussed in detail in section 2.4.

- IB,IC: Most of the older models (including GR) as well as many of the newer proposals fall into this category. It is at first sight surprising to see that the spectral index predicted by the GR model (1C) is $n = 1$ since one would naively expect a softer ($n = 3$) spectrum due to the derivative coupling of the Goldstone scalar. The reason for this is that since the GR model does not conserve lepton-number the Goldstone boson also develops a nonzero coupling to electrons, once the interactions are written in the derivative form. It can then be emitted as bremsstrahlung from the outgoing electron line. As the scalar momentum q goes to zero the intermediate electron propagator diverges and compensates for the factor of q coming from the vertex.

[2]Take *e.g.* the case when a boson of mass m is emitted. Then the factor $(Q-(\epsilon_1+\epsilon_2))$ of eq.(2.2) should be replaced by $((Q-(\epsilon_1+\epsilon_2))^2-m^2)^{1/2}$.

- IIB: A new type of $\beta\beta_{0\nu}$ which has been discovered and studied in [33].

- ID,IE: These two classes predict an electron spectrum which is intermediate to the GR and the SM ones. Class IE contains a supersymmetric model [34] which unfortunately has been ruled out by LEP.

- IIC,IID: Similar to the category above only this time lepton-number is conserved. Ref.[33] considers the case of a Goldstone scalar carrying two units of lepton charge (IID) whereas ref.[3] investigates a model of two scalar emission each carrying one unit of lepton number (IIC). This latter case, as well as category IIE below, will be discussed in greater detail in section 2.5.

- IIE: This is an entirely new class of models which predict, due to the emission of two derivatively coupled Goldstone bosons, an electron spectrum that is softer than the two-neutrino spectrum [3]. If the electron spectrum that is currently observed in $\beta\beta$ decays contained such a component it could have hidden behind the very large background of low-energy electrons and remained undetected. The same background as well as the smallness of the rate due to the soft spectrum will however most likely prevent an observation of this $n = 7$ mode in the foreseeable future.

As long as $\beta\beta_{0\nu}^{\rm pure}$ is not observed it cannot be decided whether a spectrum of index n belongs to type I or to type II models. It is therefore possible that models which have entirely different theoretical features, such as *e.g.* IC in which L_e is broken and the emitted boson is a Nambu-Goldstone boson and IIB which conserves electron-number and in which the emitted boson is not a Goldstone boson, could explain the same exotic component of the electron spectra. In other words as long as the question of L_e violation is not settled models of classes IB,IC and IIB as well as those of ID,IE,IIC and IID remain indistinguishable from the point of view of $\beta\beta$ decay experiments.

2.3 Decay rates

After the classification of different types of new physics in the context of double beta decays presented above we now focus on the decay rates that are predicted by some of the classes in table 2.1. To do so we assume some general underlying model for each class and compute the rate within the context of this model. This then allows us to see how the individual rates depend on the masses and couplings of the underlying theory and also points to possible generic features the rates of different classes could have.

2.3.1 General expression

Double beta decay rates can be cast in the following general form

$$d\Gamma(\beta\beta) = \frac{(G_F \cos\theta_c)^4}{4\pi^3} |\mathcal{A}(\beta\beta)|^2 d\Omega(\beta\beta) \tag{2.3}$$

which separates the kinetic part $d\Omega(\beta\beta)$ from the part which contains the nuclear physics and the details of the underlying theory $\mathcal{A}(\beta\beta)$. The prefactor represents, apart from a normalization, the overall strength of the low-energy charged current weak interaction: G_F is Fermi's constant and θ_c is the Cabbibo mixing angle.

The phase space volume element $d\Omega(\beta\beta)$ describes the distribution of the electron energies and is of the form (*c.f.* eq.(2.2))

$$d\Omega(\beta\beta_{0\nu}^{\text{pure}}) = \frac{1}{64\pi^2}\delta(Q - (\epsilon_1 + \epsilon_2)) \prod_{k=1}^{2} p_k \epsilon_k F(\epsilon_k) d\epsilon_k \tag{2.4}$$

for the case of pure neutrinoless double beta decay, and

$$d\Omega(\beta\beta_i) = \frac{1}{64\pi^2}(Q - (\epsilon_1 + \epsilon_2))^{n_i} \prod_{k=1}^{2} p_k \epsilon_k F(\epsilon_k) d\epsilon_k \tag{2.5}$$

for all the decays which involve also other decay products besides the electrons ($\beta\beta_i = \beta\beta_{2\nu}, \beta\beta_\varphi, \beta\beta_{\varphi\varphi}$). The index n_i is either 1,3,5 or 7 depending on the decay.

The Coulomb field of the nucleus enhances the probability of e^- emission at low electron energies - the electrons get slowed down by the attractive force exerted by the positively charged nucleus. This correction is represented by the Fermi factors $F(\epsilon_i)$ in the above equations. To a good approximation (Primakov-Rosen [39]) they can be written as

$$F(Z,\epsilon) = \left(2\pi\alpha Z\frac{\epsilon}{p}\right)\left[1-\exp\left(-2\pi\alpha Z\frac{\epsilon}{p}\right)\right]^{-1} \tag{2.6}$$

for nonrelativistic electrons (for electron energies much larger than the electron mass the effect of the Coulomb force becomes negligible and the Fermi factors approach unity). Here Z represents the total electric charge of the daughter nucleus in units of the electron charge e and α is the fine structure constant ($\alpha \approx 1/137$). In the limit of vanishing nucleon charge this expression approaches 1.

2.3.2 Nuclear form factors

Before computing the decay amplitudes $\mathcal{A}(\beta\beta)$ for various classes of table 2.1, we briefly pause to discuss the involved nuclear form factors. As long as the decay process proceeds through second order electroweak interactions, and the leptonic part of the diagram couples to the weak charged currents of the nucleus, only a small number of independent form factors can contribute to the amplitude. It is then the following tensor that enters into the computation of the amplitudes [33]:

$$W_{\mu\nu}(P,P',q) \equiv (2\pi)^3\sqrt{\frac{EE'}{MM'}}\int d^4x\,\langle N'|T^*\left[J_\mu(x)J_\nu(0)\right]|N\rangle\, e^{iq\cdot x} \tag{2.7}$$

In this expression P and P' denote the four momenta of the parent (0^+) and the daughter (0^+) nuclei which themselves are denoted by N and N' as before. q_μ is the four momentum exchanged between the two hadronic charged currents which are given by $J_\mu = \overline{u_u}\gamma_\mu(1-\gamma_5)u_d$ and which cause the transition between nucleons. The energy to mass ratios in the prefactor

are needed to ensure that $W_{\mu\nu}$ transforms as a tensor. This is because the nuclear states have not been covariantly normalized - which is a common convention in the literature. The proportionality factor of $(2\pi)^3$ finally is purely conventional.

To see how many independent quantities 'dwell' within $W_{\mu\nu}$ we first observe that the exchanged four-momentum q_μ is typically of the order of the nuclear fermi momentum $p_F \sim 60$ MeV and is therefore large compared to the difference between the initial and final nuclei momenta $(P - P')$ which is around a few MeV. One can therefore neglect $(P - P')$ to a good approximation and replace P and P' by the common four velocity u_μ of the two nuclei. Since $W_{\mu\nu}(u, q)$ now depends only on two four vectors it can be generally expressed as [33]:

$$\begin{aligned} W_{\mu\nu}(u,q) &= w_1\eta_{\mu\nu} + w_2 u_\mu u_\nu + w_3 q_\mu q_\nu + w_4(q_\mu u_\nu + q_\nu u_\mu) \\ &\quad + w_5(q_\mu u_\nu - q_\nu u_\mu) + i w_6 \epsilon_{\mu\nu\sigma\rho} u^\sigma q^\rho \end{aligned} \tag{2.8}$$

The six Lorentz invariant matrix elements $w_1 - w_6$ defined in this equation depend on the two Lorentz invariant combinations that can be formed using u and q so that $w_i = w_i(u \cdot q, q^2)$. The Bose statistics of the weak currents implies that $W_{\mu\nu}(u, q) = W_{\nu\mu}(u, -q)$ so that all of these form factors are even under the transformation $q \to -q$. The sole exception is w_4 which is odd.

As we will see it turns out that many $\beta\beta$ decay rates depend only on the trace $W_\mu{}^\mu$ which is independent of w_5 and w_6:

$$W_\mu{}^\mu = 4w_1 + w_2 + w_3 q^2 + 2w_4(u \cdot q) \tag{2.9}$$

In the rest frame of the decaying nucleus ($u^0 = 1$, $\vec{u} = 0$) these form factors become independent functions of the time (q^0) and spacelike ($\vec{q}$) parts of the 4-momentum q so that $w_i = w_i(q^0, \vec{q}^2)$. In this frame we can link the trace defined above to the better known Fermi w_F and Gamow-Teller w_{GT} nuclear form factors by:

$$w_F \equiv W_{00}(q^0, \vec{q}^2) = w_1 + w_2 + w_3 q_0^2 + 2w_4 q_0$$

$$w_{GT} \equiv \sum_{i=1}^{3} W_{ii}(q^0, \vec{q}^2) = -3w_1 + w_3\vec{q}^2 \tag{2.10}$$

so that

$$W_\mu{}^\mu = w_F - w_{GT}. \tag{2.11}$$

Using the closure and the non-relativistic impulse approximation one can now compute these form factors in a model of independent nucleons inside the nucleus. For w_F and w_{GT} one obtains [32]:

$$\begin{aligned} w_F &= \frac{2i\mu g_V^2}{(q_0^2 - \mu^2 + i\varepsilon)} \langle\langle N' | \sum_{mn} \mathrm{e}^{-i\vec{q}\cdot\vec{r}_{mn}} \tau_m^+ \tau_n^+ | N \rangle\rangle \\ w_{GT} &= \frac{2i\mu g_A^2}{(q_0^2 - \mu^2 + i\varepsilon)} \langle\langle N' | \sum_{mn} \mathrm{e}^{-i\vec{q}\cdot\vec{r}_{mn}} \tau_m^+ \tau_n^+ \vec{\sigma}_m \cdot \vec{\sigma}_n | N \rangle\rangle \end{aligned} \tag{2.12}$$

here the indexes n, m mark the nucleons in the nucleus and $\vec{r}_{mn} = \vec{r}_m - \vec{r}_n$ is the internucleon separation with $\vec{r}_n$ denoting the position of the individual nucleons. Furthermore τ_m^+ and $\vec{\sigma}_m$ are isospin and spin matrices for the mth nucleon, g_V and g_A denote the vector and the axial charged current couplings of the nucleons and μ is the average excitation energy of the intermediate nuclear state. The double bracket means that in these matrix elements the overall centre of mass motion of the nucleus has been separated out so that the positions of the individual nucleons satisfy the constraint $\sum_n \vec{r}_n = 0$. Equation (2.12) provides the connection to the various estimates for the nuclear matrix elements in the context of a specific model of the nucleus that can be found in the literature [40, 41, 42, 43]. It is the estimation of these matrix elements that gives rise to the largest uncertainty in the computation of the decay rates.

Approximating the nuclear matrix elements

In order to obtain rough quantitative estimates of the rates it is useful to approximate the nuclear matrix elements w_F and w_{GT} in a way which allows us to compute the involved integrals analytically. Following ref.[44] we therefore

write w_F and w_{GT} as step functions in energy (q^0) and momentum ($\vec{q}$):

$$w_i(q^0, \vec{q}^2) = w_i^0 \Theta(E_F - q^0)\Theta(p_F - |\vec{q}|) \tag{2.13}$$

where p_F and E_F are the nuclear Fermi momentum and energy respectively and the index i stands for either 'F' or 'GT'. This approximation not only simplifies the computation of the involved integrals, it also allows us to sidestep any explicit model-dependent computation of the nuclear matrix elements by parametrizing its results through the values of w_i^0 and p_F. Furthermore, given the fact that estimates of the nuclear matrix elements involve themselves already large uncertainties, this approximation is sufficiently precise for our purposes. The unknown parameters w_i^0 as well as p_F can now be fixed by comparing the rates obtained with this approximation (see below) to the real calculations. One gets:

$$|w_F^0 - w_{GT}^0| = 4 \text{ MeV}^{-1} ; \quad p_F \approx 60 \text{ MeV} \tag{2.14}$$

Where the value for $|w_F^0 - w_{GT}^0|$ has been obtained by comparing to the observed two neutrino decay rate $\beta\beta_{2\nu}$ (eq.(2.15) below). Current lower limits on the lifetimes for pure neutrinoless double beta decay $\beta\beta_{0\nu}^{\text{pure}}$ (see eq.(2.19) below) fix then p_F to the above value. With $p_F \sim 60$ MeV the Fermi energy then becomes $E_F = p_F^2/2m_N \sim 2$ MeV where m_N is the mass of a nucleon.

2.3.3 The standard model $\beta\beta$ decay

We are now ready to compute the missing element of the rates - the leptonic part of the interaction. We can easily do this by computing the Feynman diagrams of figure 2.2 and expressing the result in terms of the tensor $W_{\mu\nu}$ of eq.(2.7). This way we can explicitly see on which matrix elements (w_1-w_6,w_F and w_{GT}) the individual rates depend. Upon having done this we can then obtain quantitative estimates for the rates by approximating the nuclear matrix elements as described above. Below follow the expressions for the amplitudes $\mathcal{A}(\beta\beta)$, of equation (2.3), that so result for a variety of cases.

If not explicitly mentioned otherwise we consider fermion mediated decays in what follows. Alternatively $\beta\beta$ decays could also be mediated through the exchange of exotic scalars. Such models are however often subject to more stringent experimental bounds and we will therefore only consider one example to demonstrate some nonstandard features one can expect in this case.

We first start with the 'classic' SM two neutrino decay as represented by the Feynman diagram (a) in figure 2.2. The first thing to notice about this diagram is that there is no intermediate fermion line connecting the two nucleon currents. The four momentum q is therefore itself only of the order of magnitude of the total energy released in the decay and can be neglected to a similar approximation that $(P - P')$ was neglected. The nuclear form factors simplify considerably in this case. Also it turns out that the amplitude $\mathcal{A}(\beta\beta_{2\nu})$ is directly proportional to the trace $W_\mu{}^\mu$ so that it can be written in the following simple form:

$$\mathcal{A}(\beta\beta_{2\nu}) \approx \frac{2}{\sqrt{15}\pi} W_\mu{}^\mu(0,0) \tag{2.15}$$

which is, expressed in terms of the Fermi- and Gamow-Teller matrix elements: $\mathcal{A}(\beta\beta_{2\nu}) \approx \frac{2}{\sqrt{15}\pi}(w_F(0,0) - w_{GT}(0,0))$. The spectral index one obtains in this case is $n = 5$ and is purely due to the phase space factor of the two outgoing neutrinos (see eq.(2.5)). Notice that since $q \sim 0$ one can relate the form factors w_1, w_2 to w_F, w_{GT} in a simple way: $w_1 = -w_{GT}/3$ and $w_2 = w_F + w_{GT}/3$.

2.3.4 Pure neutrinoless double beta decay ($\beta\beta^{\text{pure}}_{0\nu}$)

The nextmost well known case is the case of pure neutrinoless double beta decay. As can be seen from figure 2.2 this decay proceeds through the exchange of Majorana neutrinos between the two nucleon currents. The rate then depends on the mass pattern of the neutrinos in the underlying theory. The neutrino mass term can be written in a basis of Majorana neutrinos ν_i

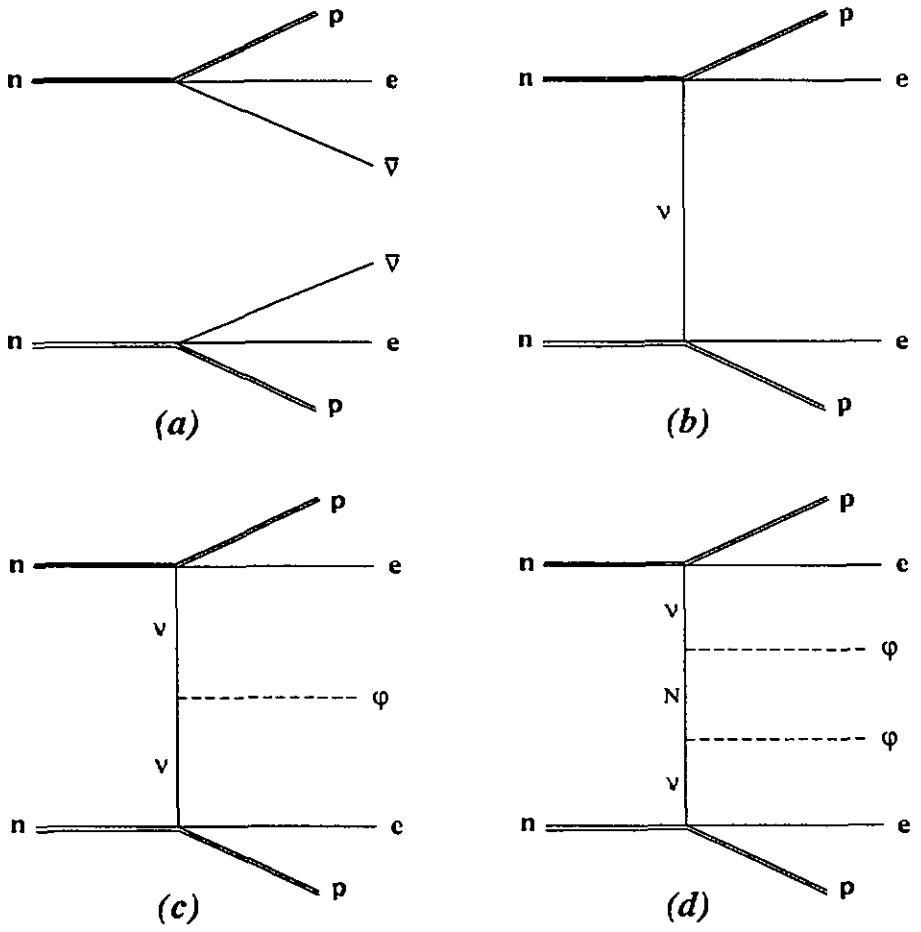

Figure 2.2: The lowest order contributions to various $\beta\beta$ decays. Diagram (a) represents the SM two neutrino double beta decay $\beta\beta_{2\nu}$, (b) is the 'pure' neutrinoless process $\beta\beta_{0\nu}^{\text{pure}}$ a variant of which is investigated in section 2.4, (c) depicts the single Majoron emission mode (GR or type IIB,IID) and diagram (d) corresponds to double Majoron emission (the case of type IIC,IIE is discussed in greater detail in section 2.5). The processes shown here rely on scalar-neutrino interactions as opposed to *e.g.* purely scalar mediated decays. For clarity of presentation the virtual W line has been omitted in all diagrams - which is justified because for the energies involved the effective weak charged current interaction is given by a contact term of the strength of the Fermi coupling constant G_F.

as

$$\mathcal{L}_{\text{mass}} = -\frac{1}{2}\overline{\nu_i} M_{ij} \nu_j \tag{2.16}$$

where M_{ij} the (symmetric) neutrino mass matrix has been taken to be real for simplicity. Notice that our use of Majorana spinors implies that for any Majorana spinor ν the following condition holds: $\overline{\nu} = \nu^T C^{-1}$. Where C is the charge conjugation matrix. The physical masses m_i are then given by the absolute eigenvalues of M. The relative sign of these eigenvalues reflects the different CP assignments the mass eigenstates have. Upon diagonalizing eq.(2.16) one can then express the flavor eigenstates ν_i in terms of the mass eigenstates ν_i' through a CKM type mixing matrix **U**. Relevant for $\beta\beta_{0\nu}^{\text{pure}}$ are the mixings of the electroweak eigenstate of the electron neutrino with the mass eigenstates which are denoted by the corresponding elements of **U**: U_{ei}. With these definitions we can now readily compute the amplitude associated with diagram (b) of figure 2.2:

$$\mathcal{A}(\beta\beta_{0\nu}^{\text{pure}}) = 8\sqrt{2}\pi \sum_i U_{ei}^2 m_i \int \frac{d^4q}{(2\pi)^4} \frac{W_\mu{}^\mu(q)}{(q^2 - m_i^2 + i\varepsilon)} \tag{2.17}$$

Since, by means of energy conservation, the energy of the two outgoing electrons equals exactly the total energy Q released in the decay the electron spectrum is described by eq.(2.4) in this case. Notice that the integral takes on a value which is in general independent of m_i in the limit of light neutrinos. In other words, as soon as the neutrino masses are significantly smaller than any involved energy scale ($m_i \ll E_f, p_F$) the amplitude is directly proportional to the so-called effective electron neutrino mass $m_{\nu_e}^{\text{eff}}$:

$$\mathcal{A}(\beta\beta_{0\nu}^{\text{pure}}) \propto m_{\nu_e}^{\text{eff}} \simeq \sum_i U_{ei}^2 m_i \qquad (m_i \ll \text{MeV}) \tag{2.18}$$

and so the rate goes in this case as $m_{\nu_e}^{\text{eff}\,2}$. Experimentalists often quote their results from $\beta\beta_{0\nu}$ decay experiments in terms of upper bounds on $m_{\nu_e}^{\text{eff}}$. The current state of the art is summarized in ref.[45]. The most stringent upper bounds on $m_{\nu_e}^{\text{eff}}$ come from direct searches for $\beta\beta_{0\nu}^{\text{pure}}$ decay in ^{76}Ge decays

and have recently been lowered to [46]

$$m_{\nu_e}^{\text{eff}} \lesssim 0.68 \text{ eV} \quad (90\%\text{C.L.}) \tag{2.19}$$

This bound uses nuclear matrix elements as computed *e.g.* in [42]. The limit can be relaxed considerably to $m_{\nu_e}^{\text{eff}} \lesssim 1.7$ eV when estimates of other authors are used [43], reflecting the involved theoretical uncertainty. Experiments based on other nuclei yield less stringent bounds, such as *e.g.* ^{136}Xe which leads to an upper limit of $m_{\nu_e}^{\text{eff}} \lesssim 2.3$ eV [45] (same matrix elements as in eq.(2.19)).

Notice that the factor U_{ei}^2 in eq(2.18) is not an absolute square of the mixing elements. This allows for cancellations (if the U_{ei} are complex) as was first remarked by Wolfenstein [47] in 1981 [3]. This cancellation has to be exact in all models that conserve lepton number. As an example take the case of a Dirac spinor that is described by two Majorana spinors of opposite CP eigenvalues in eq.(2.16).

Returning now to the expression for the amplitude (eq.(2.17)) and applying the approximation of the nuclear matrix elements discussed before (eqs. (2.13) and (2.14)) we can obtain the following simplification [2]:

$$\mathcal{A}(\beta\beta_{0\nu}^{\text{pure}}) \simeq C \sum_i U_{ei}^2 m_i \int_0^{E_F} du \left[p_F - \sqrt{u^2 + m_i^2} \tan^{-1} \left(\frac{p_F}{\sqrt{u^2 + m_i^2}} \right) \right] \tag{2.20}$$

where $C = i \frac{2\sqrt{2}}{\pi^2} (w_F^0 - w_{GT}^0)$. When the neutrinos are light ($m_i \ll E_F \ll p_F$) this simplifies to

$$\mathcal{A}(\beta\beta_{0\nu}^{\text{pure}}) \approx C \sum_i U_{ei}^2 m_i \left\{ E_F p_F - \frac{\pi E_F^2}{4} - \frac{\pi m_i^2}{4} \left[\log \left(\frac{2E_F}{m_i} \right) + \frac{1}{2} \right] \right\} + \cdots \tag{2.21}$$

whereas in the other limit ($E_f \ll p_F \ll m_i$) one obtains

$$\mathcal{A}(\beta\beta_{0\nu}^{\text{pure}}) \approx C \sum_i \frac{U_{ei}^2 E_F p_F^3}{3 m_i} + \cdots \tag{2.22}$$

[3] Alternatively one could write eq.(2.18) in the form $m_{\nu_e}^{\text{eff}} = \sum_i c_i |U_{ei}^2| m_i$ where the prefactors c_i represent the CP eigenvalues of the Majorana neutrinos ν_i.

From equation (2.21) we recover the expression for $m_{\nu_e}^{\rm eff}$ in the case of light neutrinos as in eq.(2.18). The amplitude is then $\mathcal{A}(\beta\beta_{0\nu}^{\rm pure}) \simeq CE_F p_F m_{\nu_e}^{\rm eff}$.

As can be seen from eq.(2.22) $\beta\beta_{0\nu}^{\rm pure}$ need however not necessarily proceed through the exchange of light neutrinos, since heavy ($m_\nu \gtrsim 100$ MeV) neutrinos can also give appreciable contributions to $m_{\nu_e}^{\rm eff}$. This idea is pursued more in detail and in the context of an explicit model in section 2.4. Such heavy neutrinos would then yield the following contribution to $m_{\nu_e}^{\rm eff}$:

$$m_{\nu_e}^{\rm eff} \simeq \sum_i U_{ei}^2 \frac{p_F^2}{3m_i} \qquad (m_i \gtrsim 100 \text{ MeV}) \tag{2.23}$$

which depends not only on masses and mixing angles but also on p_F and hence on the type of the involved nucleus. Notice that this equation means that the contribution of neutrinos to $\beta\beta_{0\nu}^{\rm pure}$ decouples like $1/m_i$ as they become heavy.

2.3.5 Single Majoron emission in neutrinoless double beta decay ($\beta\beta_\varphi$)

This is the class that contains the Gelmini-Roncadelli [27] model. Single Majoron emission has recently been closely reexamined in [32, 33] and results obtained there are displayed here mainly for the purpose of completeness.

$n = 1$ single Majoron emission (IB,IC,IIB)

The spectral index of $n = 1$ is obtained in any model of one scalar emission where the emitted scalar is either *not* a Nambu-Goldstone boson or is the Goldstone boson of spontaneously broken lepton number such as in the GR model. To obtain a general expression for the $\beta\beta_\varphi$ rate in such models we assume generic interactions of Majorana neutrinos ν_i with a complex scalar φ:

$$\mathcal{L}_{\rm yuk} = -\frac{1}{2}\overline{\nu_i}(A_{ij}\gamma_L + B_{ij}\gamma_R)\nu_j\varphi^* + \text{h.c.} \tag{2.24}$$

where A_{ij} and B_{ij} are arbitrary Yukawa coupling matrices and γ_L and γ_R denote the usual projections onto left- and right-handed spinors. Upon evaluating diagram (c) in figure 2.2 one obtains the following expression for the rate [33]:

$$\mathcal{A}(\beta\beta_\varphi^{(n=1)}) = 4\sqrt{2}\sum_{ij} U_{ei}U_{ej}\int \frac{d^4q}{(2\pi)^4}\frac{W_\mu{}^\mu(q)(A_{ij}m_im_j + q^2B_{ij})}{(q^2-m_i^2+i\varepsilon)(q^2-m_j^2+i\varepsilon)} \quad (2.25)$$

The case of the GR model is then readily obtained from this expression. One simply has to observe that the scalar emitted in this model is in fact real, so that $B_{ij} = A_{ij}^*$, furthermore there is only one neutrino ν_e in this case so that the effective interaction eq.(2.24) reduces to

$$\mathcal{L}_{\rm GR} = \frac{ig_{\rm eff}}{2}\overline{\nu_e}\gamma_5\nu_e\varphi \quad (2.26)$$

where $B_{\nu_e\nu_e} = ig_{\rm eff}$. Also the only involved neutrino mass, m_{ν_e}, is much lighter than p_F in this model so that the terms quadratic in m_i in the numerator of eq.(2.25) can be neglected. This then leads to

$$\mathcal{A}(GR) = i4\sqrt{2}g_{\rm eff}\int \frac{d^4q}{(2\pi)^4}\frac{W_\mu{}^\mu}{(q^2-i\epsilon)} \quad (2.27)$$

The effective coupling $g_{\rm eff}$ defined above is conventionally used by experimentalists to indicate the bounds on the $n = 1$ decay spectrum obtained in $\beta\beta_{0\nu}$ experiments. The best limit currently comes from ^{136}Xe decay [45, 48]

$$g_{\rm eff} \lesssim 1.4\cdot 10^{-4} \quad (2.28)$$

corresponding to a half-life of $T_{1/2}^{(n=1)} > 1.1\cdot 10^{22} yr$.

$n = 3$ single Goldstone emission (IID)

As soon as the emitted boson is a Nambu-Goldstone boson and lepton number is conserved one obtains a different spectral index. This additional softening of the electron spectrum (from $n = 1$ to $n = 3$) is due to the derivative nature

of the coupling of the Goldstone boson so that the amplitude contains one more factor of the scalar momentum. This is not evident when starting from the generic interaction of eq.(2.24). What happens is that the broken symmetry of which the scalar is the Goldstone boson imposes a specific structure on the coupling matrices A_{ij} and B_{ij}. Once inserted into the amplitude that has been obtained for the $n = 1$ case eq.(2.25) one then finds that this expression vanishes identically [33]. This is because in deriving (2.25) all final momenta of the decay products have been neglected. Once the amplitude is expanded to the next order in the relevant momenta one obtains [33] a spectral index of $n = 3$ and

$$\mathcal{A}(\beta\beta_{\varphi}^{(n=3)}) = 8\sqrt{2}\sum_{ij} U_{ei}U_{ej}B_{ij}\int \frac{d^4q}{(2\pi)^4}\frac{(w_5+w_6)q^2}{(q^2-m_i^2+i\varepsilon)(q^2-m_j^2+i\varepsilon)} \tag{2.29}$$

Notice that one does not obtain such a softening of the electron spectrum in the case of the GR model although the emitted boson is a Nambu-Goldstone boson. This has to do with the fact that Lepton number is broken in these models so that the scalar can couple to the outgoing electron lines. This part of the diagram then dominates over the diagram shown in figure 2.2 (c) for small scalar momenta and causes a harder spectral index of $n = 1$. All this is explained more in detail in ref. [33].

The new electron spectrum of $n = 3$, which is intermediate to the GR and the SM $\beta\beta_{2\nu}$ spectrum, has recently also been looked for in $\beta\beta$ decays. The bound on the lifetime that has been so obtained is for ^{76}Ge [46]:

$$T_{1/2}^{(n=3)} \gtrsim 7.0 \cdot 10^{21}\text{yr} \tag{2.30}$$

Analog analyses for ^{136}Xe yield $T_{1/2}^{(n=3)} \gtrsim 1.5 \cdot 10^{21}$yr [48].

2.3.6 Double Majoron emission in neutrinoless double beta decay ($\beta\beta_{\varphi\varphi}$)

We now focus on a class of models which predict the emission of two Majorons in $\beta\beta_{0\nu}$ rather than one [3, 34]. Two Majorons are emitted in these models because of an exact (or approximate) global symmetry which forbids (or strongly suppresses) the one Majoron emission mode. In the models discussed below (classes IIC and IIE) this global symmetry is electron number which is assumed to be exactly conserved. The emitted scalars then each carry one unit of lepton number. Notice that this is similar to the model of $n = 3$ shown above where L_e is also conserved only that there the emitted boson carries two units of lepton number rather than one. What is presented below closely follows ref. [3].

$n = 3$ two Majoron emission (IIC)

To be as general as possible we we assume a theory of Majorana neutrinos ν_i and N_a which are coupled to a scalar φ in the following generic way:

$$\mathcal{L}_{\text{yuk}} = -\overline{\nu_i}\,(A_{ia}\gamma_L + B_{ia}\gamma_R)\,N_a\phi + \text{h.c.}, \tag{2.31}$$

where the matrices A_{ia} and B_{ia} are again arbitrary Yukawa coupling matrices. Here the scalar ϕ as well as the neutrinos ν_i carry one unit of lepton number whereas the Majorana neutrinos N_a are neutral under this symmetry *i.e.* $L_e(N_a) = 0$. Furthermore one assumes that the neutrinos ν_i and N_a receive masses m_{ν_i} and m_{N_a} in a lepton number invariant way. For the charged neutrinos ν_i this essentially means that they have to pair up with opposite chirality eigenstates to form L_e invariant Dirac masses.

As long as some of the ν_i's participate in the charged-current weak interactions (*i.e.* mix with the electron neutrino), the couplings of eq.(2.31) generically produce $\beta\beta_{\varphi\varphi}$ decay due to the Feynman graph of figure 2.2 (d). The phase space factor of the two emitted scalars leads in this case to the

spectral index $n = 3$ and one obtains the following amplitude:

$$\mathcal{A}(\beta\beta^{(n=3)}_{\varphi\varphi}) = -\left(\frac{2}{3\pi^2}\right)^{\frac{1}{2}} \sum_{ija} \int \frac{d^4q}{(2\pi)^4} \frac{U_{e\nu_i} U_{e\nu_j} \mathcal{N}_{ija} W_\mu{}^\mu}{(q^2 - m^2_{\nu_i} - i\epsilon)(q^2 - m^2_{\nu_j} - i\epsilon)(q^2 - m^2_{N_a} - i\epsilon)} \tag{2.32}$$

where the Kobayashi-Maskawa type matrix elements are as always denoted by the U_{ei}. The factor $\mathcal{N}_{ija}$ in the numerator of this expression is given by

$$\begin{aligned} \mathcal{N}_{ija} \equiv\ & q^2 \left[A_{ia} B_{ja} m_{\nu_i} + A_{ja} B_{ia} m_{\nu_j} + B_{ia} B_{ja} m_{N_a}\right] \\ & + A_{ia} A_{ja} m_{\nu_i} m_{\nu_j} m_{N_a} \end{aligned} \tag{2.33}$$

As we will see in section 2.5 this expression for the amplitude A can usually be simplified considerably given an explicit underlying model.

Notice that since lepton number is conserved in this type of models, so that $\beta\beta^{\text{pure}}_{0\nu}$ is completely forbidden, they are not subject to the more and more stringent bounds on lepton number violation coming from $\beta\beta_{0\nu}$ decay experiments. This was in fact the original motivation that led to the development of L_e conserving models [32]. The scalars emitted in the model described here are however generic scalars which can have arbitrary masses in principle. In order to be emitted in $\beta\beta$ decays they need however to be lighter than ~ 1 MeV. This requirement then forces these models to entertain another hierarchy - the light scalar mass compared to the electroweak scale - which can in general only be realized by a finetuning of the scalar couplings. The most straightforward way to overcome this problem is to assume that the emitted scalars are the Nambu-Goldstone bosons of a broken global theory[4] as in models of type IID and IIE. If lepton number is conserved simultaneously then the broken symmetry has to be another one. This usually leads to scalar sectors that involve several different scalars rather than only one as will become clear from the explicit model described below and in section 2.5.

[4]Another way to accomplish this would be to invoke supersymmetry. However the associated models are more complicated and less straighforward to construct.

$n = 7$ two Goldstone emission (IIE)

The spectral index ($n = 7$) in this type of models is softer than the SM two neutrino spectrum. This is due to the fact that both emitted scalars are Goldstone bosons and so are coupled derivatively. As in the case IID where only one Goldstone is emitted one observes that the amplitude eq.(2.32) vanishes when compute in terms of the interactions (2.31). In fact it turns out that the same amplitude also vanishes to linear order in the external momenta so that the first nonzero contribution to the amplitude is actually quadratic in the scalar momenta. This leads to the softening of the spectral index from $n = 3$ to $n = 7$. The involved calculation in terms of couplings eq.(2.31) is quite cumbersome.

Luckily there is a simpler and more straightforward way of computing the amplitude in this type of models. It consists of performing a change of variables which makes the derivative coupling nature of the Goldstone bosons manifest from the outset. This redefinition of fields proceeds in the following way: use exponential parametrization of the scalar fields that have non-zero *vev* so that the Goldstone field appears in the exponential. Then redefine the fermion fields so that the new fermion field is given by $F' \equiv Fe^{i\varphi/v}$ (in our case F' is a heavy neutral lepton). After this redefinition, the Yukawa interaction becomes completely independent of the Goldstone field, which reappears with a derivative coupling in the fermion kinetic energy terms.

Once this has been done the generic couplings of neutrinos ν_i and N_a to a Goldstone scalar carrying one unit of electron number can be written as:

$$\mathcal{L}_{gb} = -i\overline{\nu_i}\gamma^\mu(X_{ia}\gamma_L + Y_{ia}\gamma_R)N_a\partial_\mu\phi + \text{h.c.} \tag{2.34}$$

Notice that the coupling matrices X_{ia} and Y_{ia} have energy-dimension -1. The contribution of this interaction to $\beta\beta_{\varphi\varphi}$ arises from the same Feynman graph as in the $n = 3$ case before (fig. 2.2 (d)). The resulting expression for the rate is fairly complicated. It simplifies however considerably in the special case of purely left-handed couplings, for which $Y_{ia} = 0$. Since this case is sufficient to analyze the model in section 2.5 we just quote the amplitude

in the limit $Y_{ia} = 0$:

$$\mathcal{A}(\beta\beta^{(n=7)}_{\varphi\varphi}) = -\left(\frac{4}{105\pi^2}\right)^{\frac{1}{2}} \sum_{ija} \int \frac{d^4q}{(2\pi)^4} \frac{U_{e\nu_i} U_{e\nu_j} \tilde{\mathcal{N}}_{ija} W_\mu{}^\mu}{(q^2 - m^2_{\nu_i} - i\epsilon)(q^2 - m^2_{\nu_j} - i\epsilon)(q^2 - m^2_{N_a} - i\epsilon)} \tag{2.35}$$

This expression is very similar to the one obtained in the $n = 3$ case eq.(2.32). Only the normalization and the factor $\tilde{\mathcal{N}}_{ija}$ in the nominator differ. $\tilde{\mathcal{N}}_{ija}$ is given by

$$\tilde{\mathcal{N}}_{ija} \equiv q^2 X_{ia} X_{ja} m_{N_a} \tag{2.36}$$

2.3.7 General features of fermion mediated decays

Nuclear matrix elements

Most of the decays considered above are governed by the same combination of nuclear form factors:

$$W_\mu{}^\mu = w_F - w_{GT}$$

These have been well studied in the literature since they also appear in the rates of the SM two-neutrino decay $\beta\beta_{2\nu}$ as well as in the originally proposed $\beta\beta_{0\nu}$ models ($\beta\beta^{\text{pure}}_{0\nu}$ and GR). The uncertainty involved in estimating exotic decays that depend on this combination is therefore relatively small. The exception to the rule are models of class IID where the rates depend on the nonstandard form factors w_5 and w_6 (*c.f.* eqs.(2.8) and (2.29)).

Angular electron distribution

The differential decay distribution of the outgoing electrons in terms of the angle θ between the two electron momenta is exactly the same in all fermion mediated decays considered above. It does therefore not provide an additional experimental signature to distinguish between different decays of the

same spectral index n. This angular distribution is explicitly given by

$$\frac{1}{\Gamma}\frac{d\Gamma}{d\cos\theta} = \frac{1}{2}(1 - v_1 v_2 \cos\theta) \tag{2.37}$$

where the $v_i = p_i/\varepsilon_i$ denote the speed of the corresponding electrons in the nuclear rest frame.

2.3.8 Scalar mediated double Majoron emission

Double beta decay can also proceed through scalars entirely, without invoking neutrinos at all. This is interesting because it offers the possibility that $\beta\beta_{0\nu}$ is independent of neutrino physics altogether. Various models of such scalar mediated decays have been considered in the literature. However we describe here only one case [3]: class (IIC) of table 2.1. This is mainly because this case suffices to demonstrate some interesting properties such scalar mediated decays can have. Also one should keep in mind that since this type of decay necessitates scalars that are not electroweak singlets it is difficult to obtain observable rates in this type of models. This is because, again, compatibility with current LEP bounds requires these scalars to be very heavy ($\gtrsim M_Z/2$) and the rate will then be suppressed by powers of the heavy masses.

$n = 3$ two Majoron emission (IIC)

Two Majoron emission mediated entirely by scalars asks for a more complicated scalar sector than in the models considered previously. For the sake of generality we therefore supplement the SM with a collection of new scalars, which we classify using their lepton and electric-charge quantum numbers, L_e and Q. Besides the very light $(Q, L_e) = (0, +1)$ particle, φ, which is emitted in the decay, we imagine also adding two other new classes of fields, χ_i and Δ, which respectively have the (Q, L_e) assignments: $(+1, -1)$ and $(-2, +2)$. These quantum numbers permit the following types of L_e-invariant couplings:

$$\mathcal{L}_{\text{tri}} = -\frac{1}{2}\mu^{ij}\chi_i\chi_j\Delta + \text{h.c.}$$

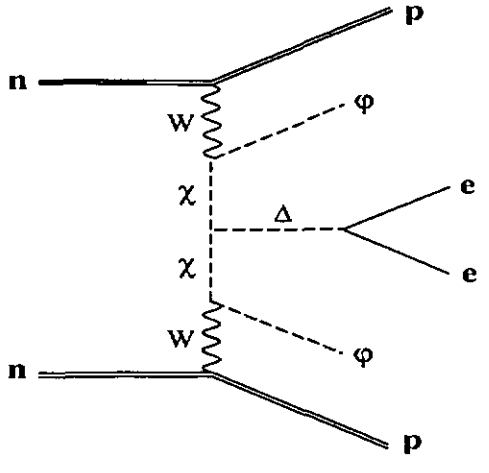

Figure 2.3: The Feynman graph contributing to $\beta\beta_{\varphi\varphi}$ decay purely due to the self-interactions of the Higgs sector.

$$\begin{aligned} \mathcal{L}_{\text{yuk}} &= -\frac{1}{2}\overline{e}(h_L\gamma_L + h_R\gamma_R)e^c\Delta + \text{h.c.} \\ \mathcal{L}_{\text{cc}} &= -i\lambda^i g W^\mu\,(\chi_i\partial_\mu\varphi - \partial_\mu\chi_i\varphi) + \text{h.c.} \end{aligned} \tag{2.38}$$

in addition to the trilinear Higgs self-interaction $\mathcal{L}_{\text{tri}}$ there is the Yukawa coupling $\mathcal{L}_{\text{yuk}}$ that facilitates the emission of the two electrons. In this expression e^c denotes the Dirac conjugate of the electron field. Finally there is the part of the lagrangian which describes the charged-current coupling of the scalars $\mathcal{L}_{\text{cc}}$. The parameter λ_i gives the strength of this interaction relative to the usual $SU(2)_L$ gauge coupling g. In lagrangian (2.38) we have assumed the existence of only one (-2,+2) scalar Δ. Generalization to several scalars Δ_a is straightforward but only unnecessarily complicates the following expressions. We denote the masses of χ_i and Δ by M_i and M_Δ respectively.

The amplitude can then be computed according to the diagram of figure 2.3.

$$\mathcal{A}_s(\beta\beta^{(n=3)}_{\varphi\varphi}) = -\left(\frac{32}{3\pi^2}\right)^{\frac{1}{2}}\frac{hR}{M_\Delta^2}\sum_{ij}\int\frac{d^4q}{(2\pi)^4}\frac{\lambda^i\lambda^j\mu^{ij}[w_F q_0^2 + \frac{1}{3}w_{GT}\vec{q}^2]}{(q^2 - M_i^2 - i\epsilon)(q^2 - M_j^2 - i\epsilon)} \tag{2.39}$$

where $h = \sqrt{|h_L|^2 + |h_R|^2}$, and

$$R = \left(1 + \frac{\xi m_e^2}{(h)^2 \varepsilon_1 \varepsilon_2}\right)^{\frac{1}{2}}, \tag{2.40}$$

with $\xi = 2\mathrm{Re}[h_L h_R^*]$ and m_e denoting the electron mass.

Again one obtains a spectral index of $n = 3$ as was the case for the fermion mediated decay of the same class (IIC) and which is determined by the phase space contribution of the two scalars.

Features of the scalar mediated rate

The amplitude (2.39) depends on the well known Fermi and Gamow-Teller form factors w_F and w_{GT} as do most of the fermion mediated decays discussed before. However this time they enter through a different linear combination than the usual trace $W_\mu{}^\mu$. The situation is entirely different though should the W-boson in fig.2.3 be replaced by yet another scalar which couples directly to the quarks. The nuclear matrix elements that so arise need then not originate form the electroweak quark currents and can thus be totally unrelated to the ones introduced in eq.(2.8).

An interesting new feature of scalar mediated $n = 3$ decays is the non-standard angular distribution of the outgoing electrons:

$$\frac{1}{\Gamma}\frac{d\Gamma}{d\cos\theta} = \frac{1}{2}\left(1 - \frac{v_1 v_2}{R^2}\cos\theta\right) \tag{2.41}$$

The deviation of this decay distribution from that of eq.(2.37) is controlled by the difference between R and unity. Having a nonstandard distribution, $R \neq 1$, then requires that the Δ-electron coupling has a right-handed component $h_R \neq 0$. This provides a new experimental signature which can be used to differentiate between fermion and scalar mediated $n = 3$ decays.

However these points are more or less academical since the main feature of the rate seems to be that the decay is undetectable. This is due to the

strong limits put on the masses of electro-weakly interacting scalars by high-energy experiments. Further details can be found in section 2.5.2 where this is quantified in the context of a simple model.

2.4 Pure neutrinoless double beta decay and heavy sterile neutrinos

2.4.1 Motivation

If pure neutrinoless double beta decay was observed today then the most straightforward and possibly also the simplest explanation would be that it proceeds via the exchange of a light ($m_{\nu_e} \sim 1$ eV) Majorana (electron) neutrino[5]. The aim of this section, which follows largely ref.[2], is to demonstrate that this is not generally the case and that quite simple models exist which contradict this maxim. To do so we provide an existence proof for such models by investigating a simple extension of the SM which has the required properties and is phenomenologically viable. In this model all neutrinos are either much lighter or much heavier than the eV mass region and in fact $\beta\beta_{0\nu}^{\text{pure}}$ proceeds through the exchange of heavy ($m \gtrsim 100$ MeV) Majorana neutrinos which mix with the electron neutrino[6].

Examining the phenomenological bounds this model has to satisfy then not only allows us to reduce the allowed parameter space of the model and thereby to gain indications on the properties of the involved new physics, but also points to other experiments that could further differentiate between the

[5] For an excellent discussion of Majorana neutrinos and their connection to $\beta\beta_{0\nu}$ decay see [49].

[6] Alternative scenarios have also been explored for having $\beta\beta_{0\nu}$ decay without requiring m_{ν_e} to be in the eV range [50]. The approach here is more similar to, and updates, the framework of ref.[51].

different mechanisms for $\beta\beta_{0\nu}^{\text{pure}}$ should it ever be observed.

2.4.2 The model

We restrict ourselves for simplicity to supplementing the SM with sterile (gauge singlet) neutrinos that mix only with the first generation.

Adding only one sterile neutrino (the 'right-handed partner' of the electron neutrino) does not realize the goal mentioned above however[7]. This is because the electron neutrino ν_e gets a see-saw induced mass that contributes to $m_{\nu_e}^{\text{eff}}$ and the heavy mass eigenstate can never be made to dominate the $\beta\beta_{0\nu}^{\text{pure}}$ decay rate in the range allowed by phenomenological bounds. If one tries to reduce the ν_e contribution by letting m_{ν_e} approach zero the sterile neutrino completely decouples and becomes invisible. The situation changes however when more than one sterile neutrino are added since then the electron neutrino can in principle be completely massless and still mix with the heavier mass eigenstates.

In the simplest scenario we therefore add two sterile neutrinos $N_\pm$ to the SM particle content. From here on the subscript ($+, -$ or 0) of Majorana fields will always denote the lepton number of the corresponding left-handed state so that $L_e(\gamma_L N_\pm) = \pm 1$. The interaction lagrangian can then be split into two parts:

$$\mathcal{L} = \mathcal{L}_{\text{cons}} + \mathcal{L}_{\text{break}} \tag{2.42}$$

where $\mathcal{L}_{\text{cons}}$ conserves lepton number

$$\mathcal{L}_{\text{cons}} = -m\overline{N_+}\gamma_R N_- - \lambda_e(\overline{L}\gamma_R N_-)H + \text{h.c.} \tag{2.43}$$

and $\mathcal{L}_{\text{break}}$ breaks it:

$$\mathcal{L}_{\text{break}} = -\frac{\mu_+}{2}\overline{N_+}\gamma_R N_+ - \frac{\mu_-}{2}\overline{N_-}\gamma_R N_- - \tilde{\lambda}_e(\overline{L}\gamma_R N_+)H + \text{h.c.} \tag{2.44}$$

[7]Such a model falls in a sub-class of models that use the see-saw mechanism and have been discussed widely in the literature (see *e.g.* [52, 53]).

Here H is the usual SM Higgs doublet and $L = \binom{\nu_e}{e}$ is the first-generation lepton doublet. For simplicity we assume the prefactors $m, \lambda_e, \tilde{\lambda}_e, \mu_+$ and μ_- to be real. Keep also in mind that for Majorana spinors $\overline{N} = N^T C^{-1}$ where C is the charge conjugation matrix. This lagrangian then leads, after SM gauge symmetry has been broken, to a mass term of the form of eq.(2.16) on page 55 for the fields ν_e, N_+ and N_-:

$$\mathcal{L}_m = -\frac{1}{2} \begin{pmatrix} \overline{\nu_e} \\ \overline{N_+} \\ \overline{N_-} \end{pmatrix}^T \begin{pmatrix} 0 & \tilde{\lambda}_e v & \lambda_e v \\ \tilde{\lambda}_e v & \mu_+ & m \\ \lambda_e v & m & \mu_- \end{pmatrix} \begin{pmatrix} \nu_e \\ N_+ \\ N_- \end{pmatrix} \tag{2.45}$$

where $v \simeq 174$ GeV is the SM Higgs vacuum expectation value (vev).

The mass matrix (2.45), having rank three in general, leads to three nonzero eigenvalues, one of which is the physical electron neutrino ν_e'. Since the direct laboratory limits on the mass of a dominantly electron neutrino are quite low we must ask under what circumstances a massless neutrino can emerge from this mass matrix. There are two possible regimes:

(1) $\tilde{\lambda}_e = \mu_+ = 0$

In this case the rank of the mass matrix reduces to two and we have a zero eigenvalue. The mass eigenstates can then be written as:

$$\begin{pmatrix} \nu_e' \\ N_+' \\ N_-' \end{pmatrix} = \begin{pmatrix} c_1 & -s_1 & 0 \\ s_1 c_2 & c_1 c_2 & -s_2 \\ i s_1 s_2 & i c_1 s_2 & i c_2 \end{pmatrix} \begin{pmatrix} \nu_e \\ N_+ \\ N_- \end{pmatrix} \tag{2.46}$$

where c_i (s_i) denotes $\cos\theta_i$ ($\sin\theta_i$) and the angles θ_i are given by

$$\tan\theta_1 = \frac{\lambda_e v}{m}; \qquad \text{and} \qquad \tan 2\theta_2 = 2\frac{\sqrt{m^2 + \lambda_e^2 v^2}}{\mu_-}. \tag{2.47}$$

Finally, the factors of 'i' in the last row of eq.(2.47) come from the chiral rotation that is required to ensure that all of the entries in the final mass

matrix are positive. This also means that the mass eigenstates N'_+ and N'_- have opposite CP properties. The corresponding masses are:

$$M_{\nu'_e} = 0, \qquad \text{and} \qquad M_{N'_\pm} = \frac{1}{2}\left[\sqrt{\mu_-^2 + 4(m^2 + \lambda_e^2 v^2)} \mp \mu_-\right] \tag{2.48}$$

Notice that in the limit $\mu_- \to 0$, lepton number is exactly conserved, and $N'_\pm$ forms a degenerate Dirac pair. In this case all lepton-number violating processes, such as $\beta\beta^{\text{pure}}_{0\nu}$ decay, are forbidden.

(2) $\lambda_e = \mu_- = 0$
This alternative is identical to case (1) above, but with the two sterile states $N_\pm$ interchanged. The physical implications of this case are therefore identical to case (1), and we need not further pursue this alternative separately. We henceforth exclusively focus on mass-matrix parameters that are in the vicinity of case (1).

For later purposes it is useful to define a dimensionless parameter, ϵ, which measures the strength of the lepton-number violation in the mass matrix:

$$\epsilon = \frac{\mu_-}{\sqrt{m^2 + \lambda_e^2 v^2}} \tag{2.49}$$

The ratio of the nonzero mass eigenvalues has a simple expression in terms of this parameter:

$$\frac{M_{N'_-}}{M_{N'_+}} = \frac{\sqrt{1 + 4/\epsilon^2} + 1}{\sqrt{1 + 4/\epsilon^2} - 1} = \cot^2\theta_2 \tag{2.50}$$

so that N'_- is always heavier than N'_+. In the lepton-number conserving limit, $\epsilon \ll 1$, $M_{N'_-} \simeq M_{N'_+}$ as would be expected for pseudo-Dirac particles. In this case the opposite CP properties of the mass eigenstates, $N'_\pm$, lead to a cancellation of their contributions to $m^{\text{eff}}_{\nu_e}$. For $\epsilon \gg 1$ we instead have $M_{N'_-}/M_{N'_+} \sim \epsilon^2$, so that in this limit N'_- is much heavier than N'_+.

We could now turn on small non-vanishing values for $\tilde{\lambda}_e$ and μ_+, so that the electron neutrino acquires a small nonzero mass. However, we are interested in the situation for which $M_{\nu_e} \ll 1$ eV and yet for which there are nevertheless potentially observable contributions to $\beta\beta_{0\nu}$ decay. We therefore keep $\tilde{\lambda}_e$ and μ_+ negligibly small in what follows, although we return to the naturalness of this choice later on.

To see how this model can contribute to neutrinoless double beta decay we ignore for the moment all other phenomenological bounds and envision the possibility that the two sterile states N'_+ and N'_- can have any masses from below the MeV to the GeV region. From the mixing matrix **U** of eq.(2.46) we extract the mixing angles that are relevant for $\beta\beta_{0\nu}^{\rm pure}$:

$$U_{e\nu'_e} = c_1, \qquad U_{eN'_+} = s_1 c_2, \qquad U_{eN'_-} = -is_1 s_2 \tag{2.51}$$

Since we assume $M_{\nu'_e}$ to be zero only the two heavy mass eigenstates will contribute to the effective mass $m_{\nu_e}^{\rm eff}$. Depending on their masses there are three limiting cases to consider:

(1) $M_{N'_-} \ll p_F$

In this case both eigenstates are light and one would expect from eq.(2.18) a contribution of $m_{\nu_e}^{\rm eff} = s_1^2(M_{N'_+}c_2^2 - M_{N'_-}s_2^2)$ to the effective mass. However, in the model considered here this quantity vanishes, as may be seen from equation (2.50). This is because in a model where all the involved neutrino mass eigenstates m_i are much smaller than p_F the expression for the effective mass as given in eq.(2.18) equals the electron neutrino element of the mass matrix eq.(2.16)[8] : $\sum_i U_{ei}^2 m_i = M_{ee}$. As can be seen from eq.(2.45) this element is zero in our model. However lepton number *is* broken and so there is no fundamental reason why there shouldn't be neutrinoless double beta decay in this case. In fact the expression for $m_{\nu_e}^{\rm eff}$ as given in eq.(2.18)

[8]Notice that this is *not* the case in models where some of the neutrinos are significantly heavier than p_F such as any models in which the light electron mass is generated via the see-saw mechanism.

represents only the leading contribution when approximating the integral (2.20) in this limit. Working to sub-leading order in the sterile neutrino masses we then obtain from eq.(2.21) the following contribution to $m_{\nu_e}^{\rm eff}$ in this model:

$$m_{\nu_e}^{\rm eff} \simeq \frac{\pi s_1^2}{4E_F p_F}\left| M_{N'_+}^3 c_2^2 \left[\frac{1}{2} + \log\left(\frac{2E_F}{M_{N'_+}}\right)\right] - M_{N'_-}^3 s_2^2 \left[\frac{1}{2} + \log\left(\frac{2E_F}{M_{N'_-}}\right)\right]\right| \tag{2.52}$$

(2) $M_{N'_+} \gg p_F$
In this case, which is opposite to the above, both neutrinos are heavy compared to the scale set by the fermi momentum p_F. We then obtain their contribution to $m_{\nu_e}^{\rm eff}$ from eq.(2.23):

$$m_{\nu_e}^{\rm eff} \simeq \frac{s_1^2 p_F^2}{3}\left|\frac{c_2^2}{M_{N'_+}} - \frac{s_2^2}{M_{N'_-}}\right| \tag{2.53}$$

(3) $M_{N'_+} \ll p_F$ and $M_{N'_-} \gg p_F$
In this last case we can still rely on eq.(2.18) for the light neutrino contribution to the effective mass and so obtain:

$$m_{\nu_e}^{\rm eff} \simeq s_1^2\left|M_{N'_+} c_2^2 - \frac{s_2^2 p_F^2}{3M_{N'_-}}\right| \tag{2.54}$$

With these estimates one can determine the masses and couplings of the sterile neutrinos which are consistent with the present non-observation of $\beta\beta_{0\nu}^{\rm pure}$. The constraints that are obtained in this way are plotted in figure 2.4. The solid lines correspond to the cases (for different values of the lepton number breaking parameter ϵ) where $m_{\nu_e}^{\rm eff} \sim 1$ eV and the model produces a $\beta\beta_{0\nu}^{\rm pure}$ rate that is close to present experimental sensitivity. Consequently the area below these lines is allowed by $\beta\beta_{0\nu}$ decay experiments.

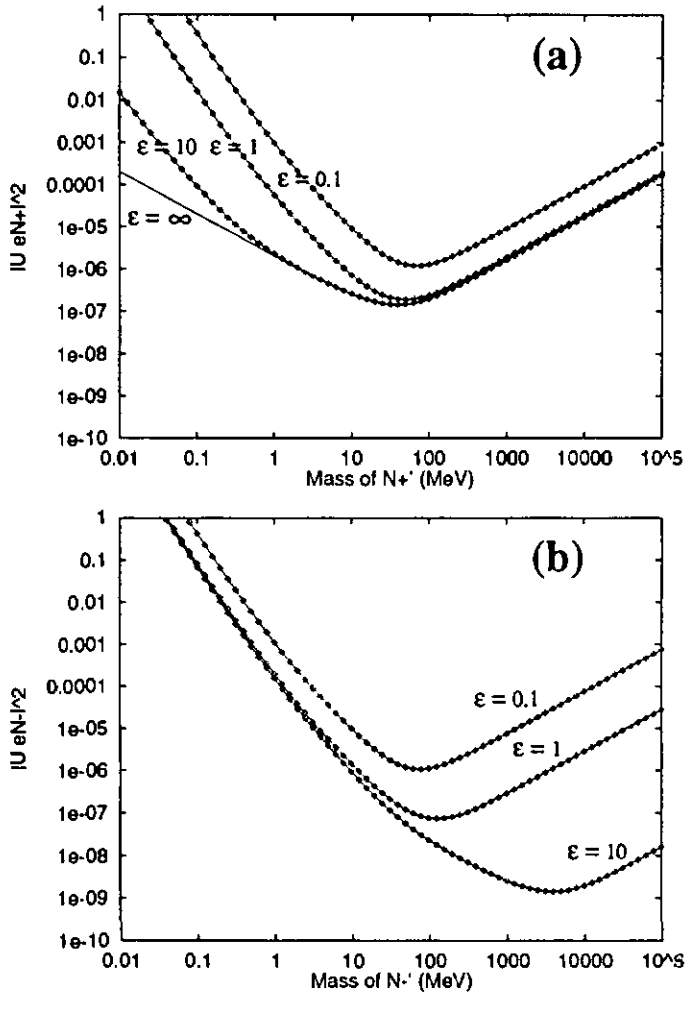

Figure 2.4: This figure plots the region in the $U_{ei}^2 - m_i$ plane (Fig. a, (b) for N'_+, (N'_- respectively)) that is allowed by current $\beta\beta_{0\nu}$ experiments for various different values of the parameter ϵ as defined in eq.(2.49) . The area below the corresponding lines is the allowed region. The limiting case of very large ϵ appears as the solid line labelled "$\epsilon = \infty$", which also corresponds to the contribution of a single sterile neutrino that mixes with ν_e. In the other limit, as ϵ becomes small, the mixing angles required for an observable rate have to be larger - the corresponding lines start to move upwards in the figure - which is due to the two mass eigenstates approaching the lepton number conserving limit of a pseudo Dirac spinor.

By comparing the values of masses and mixing angles that lie close to the solid lines in figure 2.4 with other experimental, astrophysical and cosmological constraints we can then infer the allowed regions of parameter space in which the model presented here yields a $\beta\beta_{0\nu}^{\text{pure}}$ rate close to observability. The relevant phenomenological bounds will be discussed in section 2.6 and have been, for the present case, summarized in figure 2.5. Also included in this figure is the naturalness bound discussed below. Upon comparing the two figures one then extracts the allowed region in the $\epsilon - M_{N'_+}$ plane as shown in figure 2.6.

As can be seen from figure 2.6 one finds that the masses of N'_+ that can be naturally obtained within the model presented here and that are consistent with all phenomenological limits as well as with an $\beta\beta_{0\nu}^{\text{pure}}$ signal close to experimental sensitivity, lie in the range of $2 - 10$ GeV. For these masses, the couplings that are required to produce observable neutrinoless double beta decay are roughly $|U_{ei}^2| \sim 10^{-5}$.

As will be described in section 2.6 such parameters place our model close to the current limits of detection at LEP, where the heavy sterile neutrinos can be searched for through the decay $Z^0 \to N\nu_e$, with the subsequent charged-current decay of the sterile neutrino, N, into quarks and leptons. This shows how LEP results can be used to help distinguish between different models for $\beta\beta_{0\nu}^{\text{pure}}$ should this decay ever be observed, and illustrates the rich interplay that is possible between low- and high-energy experiments.

2.4.3 Naturalness

The one thing that remains to be done is to investigate as to how natural it was to choose parameters $\tilde{\lambda}_e$ and μ_+ to be approximately zero. This choice allowed us to obtain a $\beta\beta_{0\nu}^{\text{pure}}$ decay rate which receives a negligible contribution from the exchange of the very light electron neutrino mass eigenstate ν'_e and requires some justification in parts of the parameter space we consider here.

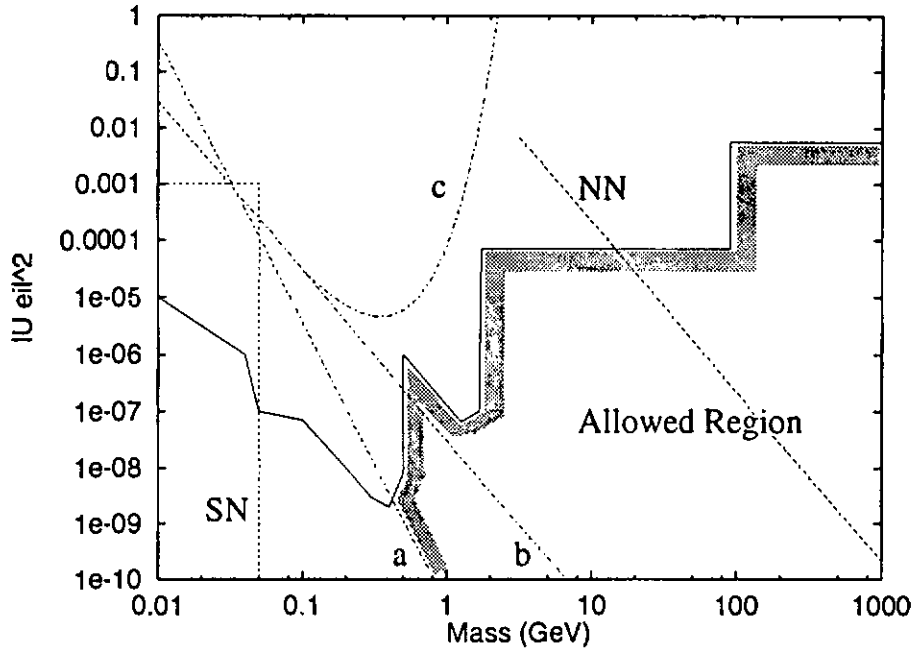

Figure 2.5: This figure summarizes the phenomenological constraints on heavy singlet neutrinos as relevant for section 2.4. The region above the solid line is ruled out by the various laboratory bounds. The region below and to the left of the dashed line labelled SN is excluded by the observations of SN1987a. The dashed line labelled NN depicts the naturalness bound as discussed in the text (eq.(2.55)) for $\epsilon = 0.1$. In the region to the right and above this line fine tuning is required. Finally the dash-dotted curves labelled a, b and c represent the nucleosynthesis bounds. The lifetime of a sterile neutrino is less than 0.1 sec to the right of curve a. A particle decouples after having become non relativistic in the region to the right of line b, but it will nevertheless decouple at or above a temperature of ~ 100 MeV to the right and below line c. Line a thus represents the only relevant nucleosynthesis bound in our case, and the region to the right of line a and below the solid line is allowed.

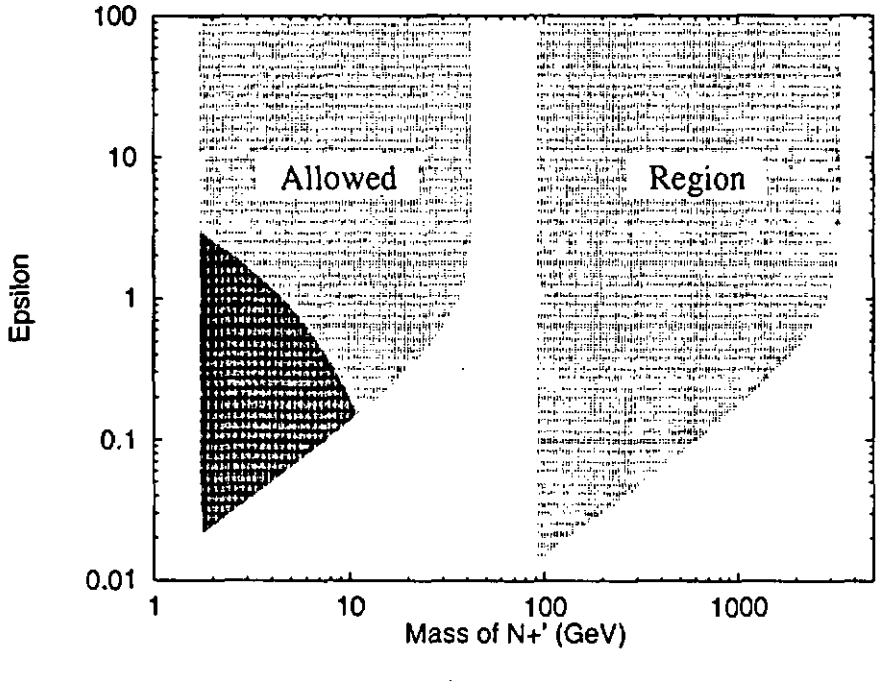

Figure 2.6: We plot here the region of the parameter space in the $\epsilon - M_{N'_+}$ plane which is obtained by requiring masses and mixing angles which yield a $\beta\beta_{0\nu}$ signal close to observability, as depicted by the various lines in fig. 2.4, together with the various phenomenological bounds displayed in fig. 2.5. The allowed area is marked by shading, and extends upwards beyond the region depicted in the figure towards higher values of ϵ without changing the mass range. The darker area represents the part of the parameter space in which the smallness of the ν'_e mass is explained in a way which is technically natural in the sense explain in the text. In the lightly-shaded region a finetuning of $\tilde{\lambda}_e$ and μ_+ is required in order to keep the ν'_e mass below 1 eV. Notice that, since $M_{N'_-} \geq M_{N'_+}$, the analogous figure in the $\epsilon - M_{N'_-}$ plane would be shifted to the right according to eq.(2.50).

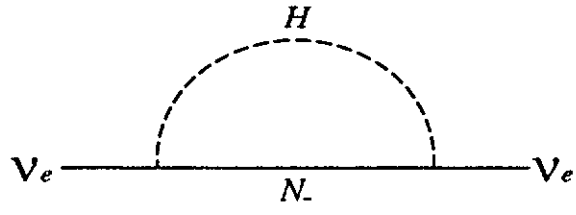

Figure 2.7: The Feynman graph which dominates the renormalization-group mixing of μ_- with $\tilde{\lambda}_e$ and μ_+.

The neglect of the light neutrino contribution to $\beta\beta_{0\nu}$ relies on our decision to choose this mass to be much lighter than 1 eV. At tree level this can always be accomplished by choosing the parameters $\tilde{\lambda}_e$ and μ_+ to be sufficiently small. A naturalness problem can arise, however, if $m_{\nu'_e}$ is chosen to be too small in comparison with the parameter μ_-, which provides the lepton-number violating contribution to the heavy-neutrino masses. This is because a nonzero μ_- generates, through loops, nonzero contributions to $\tilde{\lambda}_e$ and μ_+, and if these loop-induced contributions are large enough, then the ν'_e exchange graph can only be neglected in $\beta\beta_{0\nu}^{\rm pure}$ if the loop-induced mass is cancelled by the tree-level term. A naturalness problem arises if the required cancellation becomes implausibly precise.

More quantitatively, we imagine our model to be an effective theory which is obtained after some unknown physics above some scale Λ has been integrated out. We then use the renormalization group to run the couplings in this effective theory down from the scale Λ to the much lower energies that are relevant for $\beta\beta$ decay. In this way we can compute the contribution to the ν'_e mass which is produced by the mixing between the parameters $\tilde{\lambda}_e$ and μ_+, and μ_- as they are run down from the scale Λ. We regard the theory to be natural if these contributions to the ν'_e mass are not larger than, say, $O(1$ eV), and so do not need to be carefully cancelled by a 'bare' contribution to $m_{\nu'_e}$ at the scale Λ.

The dominant graph to consider is that of figure 2.7, in which a SM Higgs scalar is emitted and absorbed by the light neutrino state. Its contribution

to the light-neutrino mass is, in order of magnitude:

$$\delta M_{\nu_e'}(\mu) \sim \left(\frac{\lambda_e}{4\pi}\right)^2 \mu_- \log\left(\frac{\Lambda^2}{\mu^2}\right). \tag{2.55}$$

For numerical purposes we take the logarithm in this expression to be unity. Requiring the rest of the result to be smaller than $O(1\ \text{eV})$ then produces the bound labelled NN in figure 2.5. Notice that the heavier the sterile neutrinos $N_\pm'$ are, the more precise the tuning has to be, so that the requirement of naturalness can be used to exclude the mass range $10\ \text{GeV} \lesssim M_{N_+'} \lesssim 3\ \text{TeV}$ and a lepton violation parameter ϵ larger than $\epsilon \gtrsim 3$ as can be seen from figure 2.6.

2.5 Models for double Majoron emission

In this section explicit models are provided for the emission of two scalars in neutrinoless double beta decay [3]. Having explicit models rather than generic underlying couplings allows us to subject the new physics associated with these models to phenomenological bounds. This enables us to see how large the $\beta\beta_{\varphi\varphi}$ rate can be expected to get in the corresponding class (IIC,IIE) of models. Also we can in this way get indications on what other experiments could further differentiate the new physics should such an exotic decay mode ever be observed. The relevant phenomenological bounds are summarized in section 2.6. To get a rough estimate of the decay rates we apply the formulas of sections 2.3.6 and 2.3.8.

2.5.1 A fermion based model for class IIC ($n = 3$)

Inspired by the generic scalar-neutrino interaction term given in equation (2.31) on page 60 we supplement the SM model with a scalar ϕ that carries one unit of lepton number, $L_e(\phi) = 1$, as well as with three Majorana fields $\nu_\pm$ an N_0, which have lepton number assignments $L_e(\gamma_L \nu_\pm) = \pm 1$ and

$L_e(N_0) = 0$ respectively. It should be kept in mind that all these particles are taken to be gauge singlets in order to avoid bounds coming from direct detection at LEP. With this particle content the SM lagrangian is supplemented with the following lepton number conserving mass terms and Yukawa couplings[9]:

$$\begin{aligned} \mathcal{L}_{\text{mass}} &= -M(\overline{\nu_+}\gamma_R\nu_-) - \frac{m}{2}(\overline{N_0}\gamma_R N_0) + \text{h.c.} \\ \mathcal{L}_{\text{yuk}} &= -\lambda(\overline{L}\gamma_R\nu_-)H - g_-(\overline{\nu_-}\gamma_R N_0)\phi^* - g_+(\overline{\nu_+}\gamma_R N_0)\phi + \text{h.c.} \end{aligned} \tag{2.56}$$

where the couplings have again been taken to be real. The neutrino mass spectrum is fully determined by $\mathcal{L}_{\text{mass}}$ and by the Yukawa term involving the SM Higgs in $\mathcal{L}_{\text{yuk}}$. One finds one $L_e = 0$ mass eigenstate, N_0 with mass m, one massless state, $\nu'_e = \nu_e c_0 - \nu_+ s_0$, and one massive Dirac spinor ν_s formed by ν_- and the combination orthogonal to ν'_e: $\nu_s = \gamma_L\nu'_+ + \gamma_R\nu_-$, with $\nu'_+ = \nu_+ c_0 + \nu_e s_0$, which has a mass $M_s = \sqrt{M^2 + \lambda^2 v^2}$. Here v denotes as usual the *vev* of the SM Higgs and c_0 and s_0 are the cosine and sine of the mixing angle, θ, which is defined by $\tan\theta = \lambda v/M$.

The Yukawa couplings of these mass eigenstates take the form of eq.(2.31), with

$$A_{\nu'_e N_0} = 0, \qquad A_{\nu_s N_0} = g_-, \qquad B_{\nu'_e N_0} = -g_+ s_0, \qquad B_{\nu_s N_0} = g_+ c_0 \tag{2.57}$$

Applying these values to the general result for the amplitude as given in eqs.(2.32) and (2.33) then yields:

[9]Notice that the scalar ϕ could in principle develop a vacuum expectation value $\langle\phi\rangle = u$ and so break electron number spontaneously. In practice it is however a good approximation to work in the limit $u \approx 0$. This is because the absence of a $\beta\beta^{\text{pure}}_{0\nu}$ signal constrains the combination $g_i u$ to be small, while the couplings g_i themselves cannot be too small if one desires an appreciable $\beta\beta_{\varphi\varphi}$ rate. We therefore take $u = 0$ and lepton number strictly conserved in what follows.

$$\mathcal{A}(\beta\beta^{(n=3)}_{\varphi\varphi}) = -\left(\frac{2}{3\pi^2}\right)^{\frac{1}{2}} M_s^2 s_\theta^2 \int \frac{d^4q}{(2\pi)^4} \frac{(g_-^2 m q^2 + 2g_+ g_- c_\theta M_s q^2 - g_+^2 c_\theta^2 M_s^2 m) W_\mu{}^\mu}{(q^2 - i\epsilon)(q^2 - M_s^2 - i\epsilon)(q^2 - m^2 - i\epsilon)} \tag{2.58}$$

This expression implies that the $\beta\beta_{\varphi\varphi}$ decay rate is maximized for large couplings and mixing angles, and for sterile-neutrino masses in the vicinity of the nuclear-physics scale, $p_F \sim 60$ MeV, which defines the important integration region in eq.(2.58). In order to see how big this rate can get we therefore have to see how close we can get to this optimal range using phenomenologically acceptable values for the various parameters. The relevant constraints are summarized in section 2.6, and they suggest that the amplitude can be made biggest for the following values of masses and mixing angles:

$$M_s \sim 350 \text{ MeV}; \quad m \sim 1 \text{ MeV}; \quad \theta \sim 7.5 \times 10^{-2}; \quad g_+ \sim 0.2 \tag{2.59}$$

or, provided we relax the bound on m coming from nucleosynthesis (as explained in section 2.6)

$$M_s \sim m \sim 350 \text{ MeV}; \quad \theta \sim 7.5 \times 10^{-2}; \quad g_+ \sim 1 \tag{2.60}$$

Interestingly, the coupling constant g_- need not be large. Notice also that the smallness of θ implies $\lambda v \ll M_s \approx M$ and that ν_e' is dominantly the electron neutrino.

Using these values, and recalling that the integration momentum satisfies $q \lesssim p_F \ll M_s$, we find eq.(2.58) to be given approximately by

$$\mathcal{A}(\beta\beta^{(n=3)}_{\varphi\varphi}) = -\left(\frac{2}{3\pi^2}\right)^{\frac{1}{2}} g_+^2 s_\theta^2 c_\theta^2 m \int \frac{d^4q}{(2\pi)^4} \frac{W_\mu{}^\mu}{(q^2 - i\epsilon)(q^2 - m^2 - i\epsilon)} \tag{2.61}$$

To obtain a rough estimate of the sensitivity of the current experiments to the $\beta\beta_{\varphi\varphi}$ signal predicted by this model, we compare the total rate obtained within this model with the Gelmini-Roncadelli rate (see eq.(2.27) on page 58).

This comparison can then be translated into an effective GR coupling $g_{\rm eff}$ (eq.(2.26)) which we find to be[10]

$$g_{\rm eff}(\beta\beta^{(n=3)}_{\varphi\varphi}) \sim (0.008) g_+^2 s_\theta^2 c_\theta^2 \left(\frac{Q}{p_F}\right) \approx 10^{-8}\ (10^{-6}) \qquad (2.62)$$

With eq.(2.59) (respectively (2.60)) in mind we take $g_+ \sim 0.2$ (respectively $g_+ \sim 1$), $s_\theta \sim 0.1$, $Q \sim 2$ MeV, $m \sim 2$ MeV (respectively $m \sim 350$ MeV) and $p_F \sim 60$ MeV in obtaining this number. Given the current experimental sensitivity of $g_{\rm eff} \gtrsim 10^{-4}$ (eq.(2.28)) a coupling of 10^{-8} is probably hopeless to be observed, one at the level of 10^{-6} on the other hand is close enough to observability to warrant a more detailed comparison of this type of model with the data.

2.5.2 A scalar based model for class IIC ($n = 3$)

We now turn to $\beta\beta_{\varphi\varphi}$ decays that are entirely due to an exotic Higgs sector and are independent of neutrino physics altogether. One of the goals we pursue in doing so is to show that the rates obtained in this type of models are generically too small to have any chance of being observed by $\beta\beta_{0\nu}$ experiments. This is because any such models necessarily involves scalars that are not electroweak gauge singlets and which can therefore be pair-produced at LEP as long as their masses are below ~ 45 GeV. Taking them to be heavier than this bound however suppresses the rate by several powers of p_F/M, with M standing for the scalar masses, destroying any hope of getting an observable signal.

We take a simple model of the type presented in section 2.3.8. To obtain the couplings required by eq.(2.38) we have to supplement the SM with: (*i*) a second SM Higgs doublet, χ, which has non-zero lepton number $L = -1$; (*ii*) a singlet Higgs boson field, ϕ, with lepton number $L = +1$, and (*iii*) a

[10] In obtaining this value for $g_{\rm eff}$ we have made use of the approximation (2.13) of the nuclear matrix elements.

weak isotriplet scalar field, Δ, with $L = -2$. With this particle content the interactions of eq.(2.38) can be written in the following form:

$$\mathcal{L}_{\rm tri} = \mu_1 H^\dagger \chi \phi + \frac{\mu_2}{2} \chi^T \Delta^\dagger \chi + \text{h.c.} \tag{2.63}$$

The Δ electron coupling has the same form as in eq.(2.38). To simplify the expression for the amplitude eq.(2.39) that has been obtained for the more general case we apply the approximation of the nuclear matrix elements discussed earlier (see eq.(2.13)) and obtain

$$\mathcal{A}_s(\beta\beta^{(n=3)}_{\varphi\varphi}) \sim \frac{1}{(2\pi)^3} \frac{2}{3} \sqrt{\frac{32}{3\pi^2}} s_\theta^2 h \mu_2 w^0_{GT} \left(\frac{P_f E_F}{M^2_\Delta} \right) \mathcal{F}(p_F, M_\chi) \tag{2.64}$$

where factor of $E_F^2 w_F^0$ has been neglected in comparison with $p_F^2 w^0_{GT}$ in the nominator of eq.(2.39). In this equation $s_\theta \propto \mu_1$ is the mixing angle which controls the strength of the mixing between the light mass eigenstate, φ, and the singlet field, ϕ. $\mathcal{F}(p_F, M_\chi)$ finally is a function obtained by performing the q integration, which takes the values $\mathcal{F} \sim 1$ for $M_\chi \lesssim p_F$ and $\mathcal{F} \sim (p_F/M_\chi)^4$ for $M_\chi \gg p_F$. Comparing the total rate so obtained with the rate of the GR model can, as before, be summarized in the effective GR coupling that so results:

$$g_{\text{eff}_s}(\beta\beta^{(n=3)}_{\varphi\varphi}) \approx (0.02) \frac{|w^0_{GT}|}{|w^0_F - w^0_{GT}|} h s_\theta^2 \left(\frac{\mu_2 Q}{M^2_\Delta} \right) \mathcal{F}(p_F, M_\chi) \tag{2.65}$$

As usual, the rate is largest if all of the exotic scalars have couplings that are as large as possible, and masses that are in the range of $(10 - 100)$ MeV. This is impossible however since the new scalars are subject to the heavy mass bounds from LEP. The effective coupling g_{eff_s} is therefore suppressed by factors of $(Q/M_\Delta)(p_F/M_\chi)^4 \sim 10^{-16}$ and so is far to small to be detectable. This suppression factor is so huge that not even implementing direct new Yukawa couplings to the quarks can solve the problem.

2.5.3 A fermion based model for class IIE ($n = 7$)

To build a model of this type, in which lepton number is unbroken and which contains a Goldstone scalar, φ, that carries lepton number $L_e(\varphi) = 1$, we have to invoke a global nonabelian flavour symmetry. This symmetry should act on leptons and should contain ordinary lepton number as a generator.

The simplest case is to take the lepton-number symmetry group to be $G = SU(2) \times U_{L'}(1)$, with G broken down to the $U_L(1)$ of lepton number, so that the Goldstone bosons of the broken generators can carry the unbroken quantum number similar to the case of the 'would-be' Goldstone bosons in the spontaneously broken electroweak gauge symmetry. This can be done by working with a variation of a model presented in refs. [32, 33] for the case of single Goldstone emission (type IID). We therefore add the following electroweak-singlet, left-handed fermions to the standard model: $N = \binom{N_+}{N_0}$, s_0 and s_-, which transform under the flavour symmetry, G, as: $N \sim \left(\mathbf{2}, \frac{1}{2}\right)$, $s_0 \sim (\mathbf{1}, 0)$ and $s_- \sim (\mathbf{1}, -1)$. If the unbroken lepton number is chosen to be $L_e = T_3 + L'$, where L' is the generator of $U_{L'}(1)$, then the subscripts of N_+, N_0, s_0 and s_- give the corresponding particle's lepton charge. In order to implement the symmetry breaking pattern $G \to U_L(1)$, we also introduce the electroweak-singlet scalar field, $\Phi = \binom{\phi_+}{\phi_0}$, which transforms under G as: $\Phi \sim \left(\mathbf{2}, \frac{1}{2}\right)$.

For this model the most general renormalizable G-invariant mass and Yukawa interactions involving the new fields are

$$\begin{aligned} \mathcal{L}_{\text{mass}} &= -\frac{M}{2}(\overline{s}_0 \gamma_R s_0) + \text{h.c.} \qquad (2.66) \\ \mathcal{L}_{\text{yuk}} &= -\lambda(\overline{L}\gamma_R s_-)H + g_-(\overline{N}\gamma_R s_-)\tilde{\Phi} + g_0\,(\overline{N}\gamma_R s_0)\Phi + \text{h.c.} \end{aligned}$$

If the scalar fields acquire the *vev*'s $\langle H^0 \rangle = v$ and $\langle \phi_0 \rangle = u$ (which we take, for simplicity, to be real), then G breaks to $U_L(1)$ as required. As always, mixings with ν_μ and ν_τ are neglected and the couplings λ, g_- and g_0 are taken to be real.

The following mass spectrum emerges in this model: First, there is one

massless $L_e = +1$ state, $\nu_e' = \nu_e c_0 - N_+ s_0$, where the mixing angle, θ, satisfies: $\tan\theta = \lambda v/g_- u$. Then, there is a massive $L_e = +1$ Dirac state, $\nu_s = \gamma_L N_+' + \gamma_R s_-$, with $N_+' = N_+ c_0 + \nu_e s_0$, and with mass $M_s = \sqrt{\lambda^2 v^2 + g_-^2 u^2}$. There are also two Majorana $L_e = 0$ states, $\nu_\pm$, which respectively have masses $M_\pm = \frac{1}{2}\left[\sqrt{M^2 + 4g_0^2 u^2} \pm M\right]$. These mass eigenstates are related to N_0 and s_0 by:

$$\begin{pmatrix} \nu_- \\ \nu_+ \end{pmatrix} = \begin{pmatrix} ic_\varphi & is_\varphi \\ -s_\varphi & c_\varphi \end{pmatrix} \begin{pmatrix} N_0 \\ s_0 \end{pmatrix} \tag{2.67}$$

with $\tan(2\varphi) = 2g_0 u/M$. The factors of i in this mixing matrix are needed to ensure that both mass eigenvalues, $M_\pm$, are positive.

The connection to the generic interactions given for models of this type in eq.(2.34) is then made by identifying

$$X_{\nu_e'\nu_-} = i\frac{s_0 c_\varphi}{u}, \quad X_{\nu_e'\nu_+} = \frac{s_0 s_\varphi}{u}, \quad X_{\nu_s\nu_-} = -i\frac{c_0 c_\varphi}{u}, \quad X_{\nu_s\nu_+} = -\frac{c_0 s_\varphi}{u}. \tag{2.68}$$

Notice that $Y_{ia} = 0$ in this model so that we can directly obtain the amplitude from eq.(2.35):

$$\mathcal{A}(\beta\beta^{(n=7)}_{\varphi\varphi}) = \frac{2}{\sqrt{105}\pi}\frac{s_0^2 c_0^2 M_s^4}{u^2} \times \int \frac{d^4q}{(2\pi)^4} \frac{W_\mu{}^\mu}{(q^2 - i\epsilon)(q^2 - M_s^2 - i\epsilon)^2} \left[\frac{s_\varphi^2 M_+}{(q^2 - M_+^2 - i\epsilon)} - \frac{c_\varphi^2 M_-}{(q^2 - M_-^2 - i\epsilon)}\right] \tag{2.69}$$

We quantify the size of this rate in a similar way as already done for the models shown above, namely by means of estimating the magnitude of $g_{\rm eff}$. We therefore choose values for masses and mixing angles that are compatible with the phenomenological bounds of section 2.6, but which also yield a maximal rate. Specifically we take

$$M_s \gtrsim 350\text{MeV}; \quad M_+, M_- \sim \text{ a few MeV}; \quad \theta \sim 7.5 \times 10^{-2}; \quad g_- \sim 0.2 \tag{2.70}$$

The amplitude then simplifies to

$$\mathcal{A}(\beta\beta^{(n=7)}_{\varphi\varphi}) = -\frac{2}{\sqrt{105}\pi}\frac{s_\theta^2 c_\theta^2 g_-^2 M_+ M_-}{M_s^2}(s_\varphi^2 M_- - c_\varphi^2 M_+) \times \int \frac{d^4q}{(2\pi)^4}\frac{W_\mu{}^\mu}{(q^2 - i\epsilon)(q^2 - M_+^2 - i\epsilon)(q^2 - M_-^2 - i\epsilon)} \tag{2.71}$$

To see this keep in mind that in the limit of small θ we have $u \sim \frac{M_s}{g_-}$.

After applying the approximation eq. (2.13) for the nuclear matrix elements we can compare the above expression with the amplitude of the GR model. This yields an equivalent g_{eff} of

$$g_{\text{eff}} \sim (0.0006) s_\theta^2 c_\theta^2 g_-^2 \left(\frac{Q^3}{M_s^2 p_F}\right) \sim 10^{-14} \tag{2.72}$$

where the values of eq.(2.70) have been applied and we take the mixing angle to satisfy $\tan(\varphi) \sim 1/\sqrt{2}$ to maximize the rate (*i.e.* equivalently $M_+ \sim 2M_-$). Specifically we take $M_+ \sim E_F \sim Q \sim 2$ MeV, $g_- \sim 0.2$, $s_\theta \sim 0.1$ and $M_s \sim 6p_F \sim 360$ MeV.

In the above we have chosen 0.2 as the maximal value for g_-, as is naively required by kaon decay measurements (see section 2.6). It is probable that values as large as $g_- \simeq 1$ would actually prove to be consistent with these measurements in a more careful treatment, however. This is because the scalar's derivative coupling provides an additional suppression to its contribution to kaon decays. If so, then the upper bound on g_{eff} can be relaxed to around $g_{\text{eff}} \lesssim 10^{-12}$.

It is clear that this rate is far too small to have any chance of being detected, largely due to the suppression by powers of Q that originate with the extremely soft electron spectrum. We consider this model therefore only as an example that such an exotic decay spectrum, with spectral index $n = 7$, can *in principle* exist.

Notice that this type of models, where the energy spectrum of the outgoing electrons is softer than the SM $\beta\beta_{2\nu}$ spectrum, is hard to detect experimentally, not only because it seems to be difficult to create models that

predict appreciably strong decay rates, but also because the background is strongest for small electron energies. In fact the background is so strong that an $n = 7$ decay spectrum could have hidden behind it and so remained undetected up to now.

2.6 Phenomenological constraints

Here we will discuss the various phenomenological constraints the models discussed in the previous sections (2.4 and 2.5) have to satisfy. Since the SM is in these models supplemented by additional sterile neutrinos and scalars we focus primarily on the constraints on these.

2.6.1 Laboratory limits

There is a wide variety of experimental constraints on models involving electroweak singlet neutrinos and scalars. For heavy sterile neutrinos it is essentially their mixing with the (active) electron neutrino that is bounded. The bounds obtained on this coupling can be subdivided into different classes according to whether they stem from high-energy precision electroweak measurements rather than from low-energy data, or according to whether the sterile neutrino decays dominantly via the SM charged current weak process or not. The coupling of gauge singlet scalars to neutrinos on the other hand can be bounded through the non-observation of exotic meson decays. Most of these experimental bounds are explained more in detail in an excellent review by Gilman [52].

Decays of pions and kaons

At low energies we have those experiments which examine the decays of pions [54] and kaons [55] at rest, and search for nonstandard contributions to the decay rate and the outgoing electron spectrum. These experiments constrain

the masses of sterile neutrinos in a model-independent way from a few up to $\sim$ 350 MeV. For example, for neutrinos in the mass range between 1 and 100 MeV, the measured $\Gamma(\pi \to e\nu)/\Gamma(\pi \to \mu\nu)$ rate provides a mass-dependent bound on $|U_{ei}|$. For a 1 MeV neutrino the bound is $|U_{ei}|^2 < 10^{-3}$ at the 90% C.L., whereas the respective bounds for a 10 MeV and a 50 MeV neutrino are 10^{-5} and 5×10^{-7} [54]. Similar searches for a nonstandard component to $K \to e\nu$ [55] extend this limit up to sterile-neutrino masses of 350 MeV. These bounds do not make any assumptions on the decay modes of the sterile neutrino and can thus be applied to all models discussed before. This is not generally the case for sterile lepton masses above 350 MeV however as we will see below.

These same experiments, as well as measurements of the muon lifetime, also provide the only relevant experimental limits on the couplings of light scalars as present in the models for Majoron emission of section 2.5. They do so through the non-observation of weak decays into very light scalars in addition to neutrinos [56]. Specifically these limits come from precision measurements of the Michel parameter, ρ, in muon decay, and from using the measured decay spectra of the outgoing leptons to constrain decays such as $K \to lN\varphi$ or $\pi \to lN\varphi$. The failure to observe such decays can be expressed as an upper bound on a hypothetical dimensionless Yukawa coupling, $\tilde{g}_{\rm eff}$, of an effective $\nu_e - N - \varphi$ interaction. In terms of this coupling, the current bounds are respectively $\tilde{g}_{\rm eff} \lesssim 5.7 \times 10^{-2}$ (Muon decay), $\lesssim 1.6 \times 10^{-2}$ (pion decay) and $\lesssim 1.3 \times 10^{-2}$ (kaon decay) [56][11]. Of course, these bounds assume that the kinematics permit the emission of $N\varphi$ in these decays.

Decay mode dependent limits

The experiments described here do rely crucially on the assumption that the isosinglet leptons decay dominantly via their charged current weak in-

[11] These bounds can be even more stringent if additional model-dependent assumptions for the couplings involved are made.

teractions. They therefore do not apply to the models of Majoron emission discussed in section 2.5 since in these models the relevant sterile neutrinos decay dominantly into the light scalars and neutrinos. They are relevant however for the model of $\beta\beta^{\rm pure}_{0\nu}$ of section 2.4.

The mass threshold of kaons and pions can be circumvented by investigating the decays of charmed mesons such as observed in beam-dump experiments. These can constrain sterile lepton masses up to ~ 2 GeV, with a sensitivity of $|U_{ei}|^2 \lesssim 10^{-7}$. For masses below ~ 0.5 GeV the bound becomes as good as $|U_{ei}|^2 \sim 0.5 \times 10^{-9}$ [57]. (For a detailed discussion of the involved detection mechanisms see *e.g.* [52]).

For neutrinos with masses that are more than a few GeV, measurements at the Z pole provide the strongest limits. For $M_{N^i_\pm} < M_Z$, the best bounds come from the nonobservation of the decay of a Z into a sterile and a standard neutrino, $Z \to N\bar{\nu} \to W^* e\bar{\nu}$, with the subsequent decay of the sterile neutrino through a virtual boson, W^*. The bound obtained in this way is $|U_{ei}|^2 < 7 \times 10^{-5}$ [53, 58, 59].

Universality bounds

The best decay mode independent limits for sterile neutrinos with masses above ~ 350 MeV come from the reduction of the effective charged-current coupling of the electron, which is suppressed by the cosine of the mixing angle between ν_e and the heavy sterile state. This reduction potentially affects electroweak precision experiments by influencing the measured value of Fermi's constant, G_F, that is inferred from muon decay. It also shows up as a failure of lepton universality in low-energy weak decays. This leads to the bound $|U_{ei}| < 7.5 \times 10^{-2}$ (2σ) for masses above ~ 350 MeV [10, 60]. Another bound comes from the reduction of the neutral current coupling of the electron-neutrino, leading to a decreased number of light neutrino species as deduced from Z's invisible width. However this bound is somewhat weaker than the aforementioned universality bound, and applies only to sterile neutrinos that are heavier than about 90 GeV, hence it is of no particular importance in

our case.

Connection to the models presented before

In the case of the model for $\beta\beta^{\rm pure}_{0\nu}$ discussed in section 2.4 all of the bounds mentioned above apply. They have been summarized in figure 2.5 on page 75. The region so constrained in the mass-mixing angle plane is the area below the solid line in this figure.

For the models of Majoron emission in section 2.5 there is only one sterile state, the heavy Dirac neutrino ν_s, that mixes with ν_e and we need only constrain the masses and mixings of this one particle. Since in this case the bounds coming from beam-dump experiments and the search for exotic Z decays do not apply the strongest limit for $M_s \gtrsim 350$ MeV is the universality bound presented above. To maximize the $\beta\beta_{\varphi\varphi}$ rate we prefer a mixing angle, θ, that is as large as possible, and so we choose ν_s to be heavy enough to evade the bounds from pion and kaon decay — $M_s \gtrsim 350$ MeV — and we take θ to saturate the universality bound — $\theta \lesssim 7.5 \times 10^{-2}$.

The bounds on scalar-neutrino couplings applies in these models if the $L_e = 0$ sterile fermions, N_a, are sufficiently light compared to the π, K and/or μ, as is certainly the case for $m_{N_a} \sim 1$ MeV. For m_{N_a} in this mass range, the effective coupling that is then bounded in this analysis turns out to be $\tilde{g}_{\rm eff} \approx s_\theta c_\theta g_\pm$ (g_+ for the '$n = 3$' and g_- for the '$n = 7$' model). As a result, keeping in mind the bound on θ above, the couplings $g_\pm$ must be smaller than 0.18.

It is clear however that provided N_a is too heavy to be produced in these kinds of decays (i.e. $m_{N_a} \gtrsim 350$ MeV) then the bound described above no longer applies, and $g_\pm$ can be of order unity. We are led to consider $m_{N_a} \sim 1$ MeV because of the specific way we choose to avoid conflict with nucleosynthesis (see subsection 2.6.2 below). If another way to evade this bound should be found, or if we simply accept the comparatively large number of effective degrees of freedom contributed at this epoch, then $g_\pm$ can indeed be as large as $g_\pm \sim 1$.

2.6.2 Nucleosynthesis

Standard big-bang cosmology very successfully explains the abundances of light elements produced during the nucleosynthesis (BBN) epoch [61]. In fact, this success leaves little room for the existence of new species of particles at this critical time. Specifically if there were new particles present at a temperature of $\sim 0.1 - 2$ MeV their additional degrees of freedom would increase the expansion rate of the universe leading to an earlier freeze-out of neutron-proton converting interactions and thus to a larger amount of neutrons that eventually would be cooked into ^4He [12]. The bound on the number of additional degrees of freedom is conventionally stated in terms of the maximal number of additional light neutrino species allowed at nucleosynthesis δN_ν [63]:

$$\delta N_\nu \lesssim 0.4 \quad (95\%\text{C.L.}) \tag{2.73}$$

This bound, being based on observed abundances of light elements such as $^4He, ^7Li, ^2H$ and ^3He, has to be interpreted with caution. First it is not straightforward to extrapolate from the observed to the primordial abundances (especially in the case of ^7Li) and second there is currently a controversy going on ([63], [64]). Hata *et.al.* [64] have very recently pointed out that the total number of light neutrino degrees of freedom actually preferred by nucleosynthesis seems to be incompatible with 3 so that the bound (2.73) can only be obtained by imposing the constraint $\delta N_\nu \geq 0$ to the data, and therefore corresponds to a very bad fit. According to them the preferred number of light neutrino species at nucleosynthesis actually is

$$N_\nu = 2.0 \pm 0.3 \qquad (1\sigma) \tag{2.74}$$

which seems to be in conflict with what one would normally expect for the SM of electroweak interactions. As we will see below one of the ways we try to accommodate nucleosynthesis in the models of Majoron emission can

[12] For a well written introduction to BBN see [62].

actually lead to an effective number of light neutrinos that is smaller than 3, well in agreement with equation (2.74).

The basic condition to satisfy the bound (2.73) is to ensure that the energy density at the nucleosynthesis temperature, $T_{BBN} \simeq 1MeV$, due to additional particles is much less than that of an ordinary neutrino species. For sterile particles that are still relativistic during BBN (*i*.e. with masses below $\sim$ 1 MeV) this can be realized by having them decouple before the QCD phase transition at $T_{QCD} \sim 200$ MeV. In this case they become sufficiently diluted compared to ordinary particles due to the reheating of the photon bath during the phase transition (see e.*g*. [62]).

If the particles are heavier than $\sim$ 1 MeV on the other hand the most straightforward way is to not having them being present at all during nucleosynthesis. This can most easily be achieved by letting them decouple and subsequently decay sufficiently early. In fact this is the bound relevant for the model of $\beta\beta_{0\nu}^{\text{pure}}$ of section 2.4, since the heavy sterile neutrinos in this model dominantly decay through charged current weak interactions and thus have much longer lifetimes than the sterile neutrinos of comparable mass in the Majoron models of section 2.5.

Unfortunately these methods are not of any help as soon as there is a light ($m \lesssim 1$ MeV) particle which is still in thermal equilibrium with either the SM neutrinos or the photon bath at BBN and so has an unsuppressed contribution to the energy density. This is *e.g.* the case for the very light scalars of the Majoron models of section 2.5, since these couple through dimensionless couplings to ordinary neutrinos, such as ν_e, and are so kept in thermal equilibrium down to the relevant temperatures. In fact this makes a conflict with nucleosynthesis generic for models which can produce $\beta\beta_{\varphi}$ and $\beta\beta_{\varphi\varphi}$ decays.

Luckily there is a loophole in the above reasoning, provided there are sterile neutrinos with suitable masses and couplings present in the theory, as was first observed in [65] and applied to a case similar to the present one in [44]: Suppose that a heavy neutrino state either decays [65] or annihi-

lates [44] into particles that are in equilibrium with ordinary neutrinos, right after these neutrinos freeze out of chemical equilibrium with the photon bath (*i*.e. $T_\nu \sim 2.3$ MeV.) Provided this happens before the neutron-proton ratio freezes out (at $T_{n/p} \sim 0.7$ MeV), then the abundance of neutrinos will be increased relative to the standard cosmological scenario. This overabundance of neutrinos will act to suppress the neutron abundance at freezeout, and so decreases the predicted production of ^4He. As a result it contributes to nucleosynthesis as a *negative* contribution to δN_ν [65].

Consider, therefore, a single Majorana neutrino with a mass in the critical region (*i*.e. $\sim 1-2$ MeV) which is still in equilibrium with n_S species of real scalars in addition to the $n_F = 3$ species of ordinary neutrinos, when it becomes nonrelativistic. Such a particle will annihilate out right during the critical epoch, thereby heating the neutrino-scalar bath above that of the photon bath. Then the magnitude of δN_ν that results due to the above mechanism turns out to be [65, 44] $\delta N_\nu = -4.6\,\delta n$, where

$$\delta n = \left(\frac{n}{n_o}\right)\left(\frac{E}{E_o}\right)^2 - 1 = \left(\frac{(n_F+1)+\frac{4}{7}n_S}{n_F+\frac{4}{7}n_S}\right)^{5/3} - 1 \qquad (2.75)$$

Here n/n_o and E/E_o denote the ratios of the electron-neutrino number densities and energies after and before annihilation. The second expression is obtained from the first one using entropy conservation.

Connection to the models discussed before

According to the Supernovae bound discussed below the heavy sterile neutrinos $N'_\pm$ of the $\beta\beta^{\text{pure}}_{0\nu}$ model of section 2.4 have to be heavier than ~ 50 MeV. To avoid conflict with nucleosynthesis they therefore have to decay with lifetimes shorter than ~ 0.1 sec. This excludes any values for masses and mixing angles that do not satisfy the following condition:

$$\left(\frac{M_{N'_\pm}}{\text{GeV}}\right)^5 |U_{ei}|^2 \gtrsim 3.6 \times 10^{-11} \qquad (2.76)$$

This limit is depicted by the line labelled (a) in figure 2.5 on page 75. Values that lie to the left and below this curve are excluded. Upon closer inspection one sees however that the sterile neutrinos $N'_{\pm}$ do only decouple after having become nonrelativistic *i.e.* when they lie to the right or above line (b) in the same figure. This is because the region where the neutrinos decay sufficiently fast and decouple while being relativistic, *i.e.* the region between lines (a) and (b), drives one into a regime which is excluded by the laboratory bounds provided one asks for a $\beta\beta^{\text{pure}}_{0\nu}$ rate close to observability at the same time. So for the present case of interest particles $N'_{\pm}$ will decouple while being nonrelativistic, $T_D \lesssim M_{N'_{\pm}}$. In this case their number density is exponentially suppressed by the Boltzmann factor. This dilution makes them decouple earlier than one would otherwise expect without Boltzmann suppression. This is shown by line (c) in figure 2.5: The sterile neutrinos will always decouple at or above a temperature of $\sim$ 100 MeV provided they lie to the right or below this curve. This in turn means that they have again to decay fast enough, eq.(2.76), in order not to contribute excessively to the energy density at nucleosynthesis.

For the models of Majoron emission in section 2.5 the loophole described before has to be applied in order to avoid conflict with nucleosynthesis. Apart from a heavy Dirac state ν_s, that has to be heavier than $\sim$ 350 MeV to avoid the various laboratory limits, these models contain very light complex scalars as well as massive Majorana neutrinos N.

The sterile neutrinos in these models are kept in thermal equilibrium with the photon bath by neutrino scattering via scalar exchange. They remain therefore in equilibrium long after the temperature has dropped below their mass. Provided they are sufficiently heavy they will therefore never contribute to the energy density at BBN. However the scalars do contribute and so we have to require the Majorana neutrinos to have a mass around 1 MeV, since in this case they annihilate right in time to reheat the neutrino sector. For the '$n = 3$' model of section 2.5.1 this means that the Majorana state N_0 should have a mass $m \sim 1$ MeV so that we can employ eq.(2.75)

with $N_F = 3$ and $n_S = 2$ (complex scalar) yielding a shift $\delta n = 0.43$ and so a total number of additional neutrino species $\delta N_\nu = \frac{8}{7} - 4.6 \times 0.43 = -0.86$ which jives actually very well with what is required by BBN [64]. As the mass of N_0 raises above $T_\nu \sim 2.3$ MeV, δN_ν raises to $\frac{8}{7}$ so that a N_0 slightly heavier than T_ν is still allowed. In the '$n = 7$' model of section 2.5.3 the large number of light scalar degrees of freedom necessitates that both Majorana neutrinos $\nu_\pm$ have a mass in the critical vicinity of a few MeV. This then leads in the 'best' case to a $\delta N_\nu = -1$.

2.6.3 Other constraints from astrophysics and cosmology

As we will see shortly there arise only very few constraints relevant for the models considered here from the many potential possibilities there are for such bounds.

Stellar evolution

Sterile particles produced in the core of stars can disrupt our understanding of stellar evolution since they can provide an extremely efficient additional cooling mechanism for a star. The sterile neutrinos in the models considered here are however simply too heavy to be produced in significant numbers inside the core of a star. They are therefore not constrained by stellar evolution. The same conclusion also holds for the light scalars in these models, although for different reasons. In this case the scalars are light enough to be produced, but they only couple appreciably to neutrinos. But since temperatures and densities inside a star are not sufficiently high to produce a thermal or degenerate population of neutrinos, scalars are not produced in significant quantities from the interior of the star. Direct couplings with other particles, such as electrons, can arise due to loop effects, but these are too small to be

significant[13].

Supernovae

Populations of neutrinos *are* maintained, however, within the cores of supernovae, due to the much higher temperatures ($\sim 50-100$ MeV) and densities that are found there. Here the light scalars as well as the MeV Majorana neutrinos N can be produced in significant numbers. However since both of them are also in thermal equilibrium with the ordinary SM neutrinos, they are trapped in the core of the supernova and so do not lead to premature cooling.

The situation is completely different however for the $\beta\beta_{0\nu}^{\rm pure}$ model of section 2.4 since there are no scalars present in this model which keep the sterile neutrinos in thermal equilibrium with the SM neutrinos. Yet the sterile states $N'_{\pm}$ of this model can be produced in significant numbers through their charged current weak interactions. The strength of these interactions depends on the size of the mixing angle with the electron neutrino. The analysis we require is very similar to the case of right-handed neutrinos discussed in ref.[66]. As was shown there one has to consider two cases. First if the mixing is sufficiently strong the sterile neutrinos will again be in thermal equilibrium so that there arises no bound. If the mixing angle is too small on the other hand they will not be produced in large enough numbers to contribute significantly to a premature cooling of the SN core. Such a nonstandard cooling mechanism would then lead to a shortened cooling pulse of SM neutrinos coming from the supernovae and contradict SN 1987A observations. The bounds that so arise are:

$$3\times 10^{-2} \lesssim |U_{ei}|, \text{ or else } |U_{ei}| \lesssim 10^{-5}. \qquad (2.77)$$

they are depicted by the line labelled SN in figure 2.5. Notice that this bound does not apply for sterile neutrinos that are heavier than the core temperature of the supernovae (~ 50 MeV).

[13]This is treated more in detail in [33].

'Present-day' cosmology

Finally one might worry about the influence the light scalars entertained in models of section 2.5 might have on structure formatiou and the energy density of the universe observed today. Since φ would remain in thermal equilibrium with the electron neutrinos (through exchange of virtual Majorana states N) until a temperature in the region of 1 eV if it was light, it inevitably annihilates out to the neutrino sector once it becomes nonrelativistic. It will therefore never dominate the energy density of the universe and hence also not affect structure formation nor the age of the universe in any significant way. This in turn means that φ can have any mass below 1 MeV.

3

Naturally degenerate Neutrinos

As has been pointed out by refs.[67] the solar neutrino problem, the atmospheric neutrino anomaly and the presently required amount of hot dark matter (HDM) can be simultaneously described only by the known three neutrinos, provided they are almost degenerate in mass. This chapter discusses this scenario and presents an explicit model that produces the required mixings and squared-mass splittings in a natural way [4]. The model is set in a see-saw scenario in which the light neutrino masses are primarily generated by a family of heavy singlet neutrinos. It assumes the existence of an approximate family symmetry which mixes the light neutrinos as well as their right-handed partners among themselves. This symmetry is then explicitly broken by the interactions of a heavy sterile neutrino leading to the required departure from complete degeneracy.

3.1 Introduction

The main signature for neutrino mass is, apart from neutrinoless double-beta decay discussed in the previous chapter and 'direct' observation in electron endpoint spectra in single beta decays, the observation of flavor oscillations.

Since massless neutrinos (and massive but strictly degenerate neutrinos for that matter) are necessarily flavor diagonal, they preserve this quantum number during propagation and no oscillations are observed. As soon as neutrinos have a non-degenerate mass pattern however, a nontrivial CKM-type mixing in lepton-flavor space becomes possible, and consequently flavor eigenstates are then linear combinations of different mass eigenstates. These mass eigenstates propagate differently with a time dependence $\exp(-it(p+\frac{m^2}{2E}))$ (ultra-relativistic case) that leads to an evolution of the flavor content as the neutrino propagates through space. The probability that a neutrino flavor 'i' has transformed to another flavor 'j' after it has travelled a distance L through space then depends on the mixing angles θ (*i*.e. the linear combination of mass eigenstates that makes up the neutrino), the mass-squared differences $\Delta m^2_{ab} \equiv m^2_a - m^2_b$ of the mass eigenstates and the neutrino energy and can be written as (2 neutrino case):

$$P(\nu_i \to \nu_j) = \sin^2(2\theta)\sin^2\left(\frac{\Delta m^2}{4E}L\right) \tag{3.1}$$

Such oscillations of one lepton-flavor into another can be observed because charged current interactions are directly sensitive to the flavor content of the neutrino[1]. To summarize, neutrino oscillation phenomena require non-zero mass and lepton-flavor number violation both of which are absent in the minimal standard model.

Out of the various, more or less significant, hints for deviations from the

[1]Even detection mechanisms based on '$\nu - e$' scattering rely on this fact in that the '$\nu_e - e$' scattering cross section is about 7 times bigger that those for '$\nu_{\mu,\tau} - e$' due to the additional charged current S-channel contribution.

SM in the neutrino sector only three have survived up to now[2]. These are the solar neutrino deficit, the atmospheric neutrino anomaly and the possibility that neutrinos may constitute the bulk part of hot dark matter as required by Galaxy formation. They are described in some detail below. For a more thorough review the reader is again referred to ref.[25] as well as a very recent account on the subject by Paul Langacker [69] and references therein.

3.1.1 The solar neutrino problem

Because of their weak couplings neutrinos penetrate matter much more easily than other particles. They provide therefore a natural means of probing the interior of the sun. Carrying to us otherwise unobtainable information about nuclear reactions in the suns core, solar neutrinos give rise to an important additional experimental test of astrophysical solar models.

The value of neutrinos as messengers from suns interior is also underlined by their rich energy spectrum, which contains independent information about different nuclear processes. The five most important of which, with respect to observable neutrino production, are

- The (pp) cycle : $E_\nu \lesssim 0.42$ MeV
- Electron capture by ^{7}Be : $E_\nu \simeq 0.86$ MeV (90%)[3]
- The (pep) reaction : $E_\nu \simeq 1.44$ MeV
- The (CNO) cycle : $E_\nu \lesssim 1.8$ MeV
- Decay of ^{8}B: $E_\nu \lesssim 14$ MeV

[2]Notice that there is a recent, though still very tentative indication for new physics, coming from the possible observation of neutrino oscillations at LSND [68], which is ignored here.

[3]There is another line at 0.38 MeV (10%) which is less important for present day experiments.

where the energy of the neutrinos produced is indicated. The (pp) cycle, the main source of energy in the sun, is a reaction chain that converts 4 protons to $^4\mathrm{He} + 2\mathrm{e}^+ + 2\nu_e$. Among its side products one also finds small amounts of the heavier elements ^{7}Be and ^{8}B. The ^{8}B decay produces a continuous neutrino spectrum whereas the neutrinos produced by electron capture of ^{7}Be have distinct energies. A monochromatic peak is also produced by the (pep) reaction '$2p + e \to d + \nu$'. Finally there is the (CNO) cycle where the fusion of four protons to ^{4}He is catalyzed by a ^{12}C. The decays of the heavier elements F, N and O produced in the intermediate steps of this cycle give rise to a continuous neutrino spectrum.

How is this rich energy spectrum being probed on earth? There are currently four experiments based on three different detection mechanisms running. All these experiments have a lower energy threshold below which they are no longer sensitive to neutrinos and so as this threshold becomes smaller they detect neutrinos stemming from a larger set of nuclear reactions. The different experiments, their used detection mechanism, energy threshold and measured neutrino fluxes are summarized in table 3.1.

Upon inspection of table 3.1 one notices that the measured neutrino fluxes are significantly smaller than what one would expect within the standard solar model (SSM). This is what people originally referred to as the solar neutrino problem.

A second aspect arises when one compares the Homestake with the Kamiokande result. Homestake reports a stronger suppression but is at the same time also sensitive to ^{7}Be neutrinos. This discrepancy can only be resolved if the ^{7}Be neutrino flux is almost completely suppressed compared to its SSM prediction[4].

This experimental situation makes it very hard to explain the solar neu-

[4] Actually the central value of the ^{7}Be flux as obtained from a combined fit of the four experiments turns out to be slightly negative. Upon excluding the unphysical region in the fit one obtains an upper bound of 0.07 (95%CL) in units of the SSM flux (see *e.g.* ref.[69] and references therein).

Experiment(s)	Detection mechanism	Energy threshold and sensitivity	Measured neutrino flux
Homestake	$^{37}Cl + \nu_e \rightarrow ^{37}Ar + e^-$ (Chlorine)	$E_\nu > 0.81$ MeV *pep*, *CNO*, ^{7}Be and ^{8}B	0.32 ± 0.05
SAGE, GALLEX	$^{71}Ga + \nu_e \rightarrow ^{71}Ge + e^-$ (Gallium)	$E_\nu > 0.23$ MeV all of the above including the *pp* cycle	0.59 ± 0.08
Kamiokande	Water Cerenkov detector ($\nu - e$ scattering)	$E_\nu > 7$ MeV sensitive only to ^{8}B neutrinos	0.50 ± 0.10

Table 3.1:

The four solar neutrino experiments. The third column gives the lower energy threshold below which experiments are no longer sensitive to neutrinos. It also indicates the nuclear processes to which the corresponding experiment is sensitive. The last column gives the solar neutrino flux as measured by those experiments (a combined value is given for the two Gallium experiments) in units of the Bahcall and Pinsonneault (BP) standard solar model expectation. The errors indicated are the combined experimental and theoretical errors.

trino problem in terms of astrophysical solutions. Nonstandard solar models[5] can explain for an overall suppression of the ^{7}Be and ^{8}B fluxes because they often lead to a smaller core temperature of the sun and these fluxes depend strongly on this temperature (^{7}Be-flux $\sim T_{\rm core}^8$, ^{8}B-flux $\sim T_{\rm core}^{18}$). However reducing the core temperature should suppress the ^{8}B flux much more than the ^{7}Be flux. In other words since ^{8}B is made from ^{7}Be it seems impossible to get the ^{7}Be flux smaller than the ^{8}B flux by means of astrophysical solutions alone. Also (pp) cycle neutrinos, direct witnesses of the main energy production mechanism inside the sun, are subject to the total solar luminosity constraint and hence vary only weakly with $T_{\rm core}$. Nonstandard solar models are therefore not suited to explain the (pp) neutrino suppression.

What has been said above makes clear that an astrophysical solution of the solar neutrino problem is unlikely, and an explanation in terms of particle physics is asked for[6].

In fact vacuum neutrino oscillations as described before constitute a simple solution to the solar neutrino problem on their own. An electron neutrino produced in the suns core could have converted to another flavor on its journey to earth and be invisible to our detectors, leading to an apparent depletion of the neutrino flux. This 'just-so' solution has a long oscillation length and would require mass-squared differences around $\Delta m^2 \sim 10^{-10}$ eV^2 and large mixing angles $\sin^2 2\theta \gtrsim 0.75$.

Another, very popular and probably also more 'natural', explanation is the so-called Mikheyev-Smirnov-Wolfenstein (MSW) mechanism[70].

This mechanism places neutrino oscillations in the interior of the sun where the matter background, essentially the electron density, affects the flavor oscillation. In fact the mass eigenstates depend on the electron den-

[5]There is a large variety of nonstandard solar models that are obtained by *e.g.* exploiting uncertainties in nuclear cross sections or by departing from the minimal version and including new ingredients such as *e.g.* large magnetic fields in the core.

[6]Of course there is the third possibility that some of the experiments do not give correct results.

sity and evolve to their vacuum values as one leaves the sun. In addition transitions between the different mass eigenstates become possible as soon as off-diagonal elements (of the mass matrix) are introduced by a strongly varying electron density. This mechanism allows for a complex energy dependent suppression of electron neutrinos on earth. It jives very well together with the standard solar model in fits to the data.

The MSW solution requires that the electron neutrino oscillates to another species[7] ($\nu_e - \nu_\mu$ or $\nu_e - \nu_\tau$) with the following squared-mass splittings and mixing angles:

$$\Delta m^2 \simeq 10^{-5}\ \mathrm{eV}^2, \quad \sin^2 2\theta \simeq 10^{-2} \text{ or } \sin^2 2\theta \simeq 0.5 \tag{3.2}$$

i.e. there is a small angle 'non-adiabatic' and a large angle 'vacuum' solution. Furthermore, if $\nu_e - \nu_\tau$ conversion provides the MSW solution and the atmospheric neutrino deficit described below is due to $\nu_e - \nu_\mu$ oscillations then the latter also depletes the solar neutrino flux and the allowed squared-mass difference for the $\nu_e - \nu_\tau$ oscillations is enlarged to include $\Delta m^2_{e\tau} \simeq 10^{-4}\ \mathrm{eV}^2$ [71].

3.1.2 The atmospheric neutrino anomaly

As cosmic rays hit the outer layers of the atmosphere highly energetic mesons and hadrons are produced. They in turn give rise to the so-called atmospheric neutrinos via their subsequent decays. The main production mechanism of these neutrinos is the pion decay chain:

$$\begin{aligned} \pi^+ \rightarrow \quad & \mu^+ + \nu_\mu \\ & \mu^+ \rightarrow e^+ + \overline{\nu_\mu} + \nu_e. \end{aligned} \tag{3.3}$$

Neutrinos produced in such a way have in general much higher energies ($\sim$ GeV) than the solar ones ($\sim$ MeV) and so constitute an entirely different part of the overall neutrino spectrum observed on earth.

[7] The oscillation to a sterile species is also possible ($\nu_e - \nu_s$) but is not considered here.

It is difficult to predict the absolute atmospheric ν_e and ν_μ fluxes on earth however, mainly because of the incomplete knowledge of the cosmic ray spectrum and theoretical estimates typically involve errors as large as 30%. This obstacle can be avoided by considering only the ratio

$$R \equiv \frac{\Phi(\nu_\mu + \overline{\nu_\mu})}{\Phi(\nu_e + \overline{\nu_e})} \tag{3.4}$$

of absolute ν_μ versus ν_e fluxes. Theoretical estimates of R then typically yield errors around 5%.

Naively one would expect $R \simeq 2$ from the main production chain eq.(3.3). However not all of the muons decay before they reach earth and so R is generally larger than 2 and depends on neutrino energies. This effect starts to be important for neutrino energies above ~ 1 GeV [8].

Experiments often state their results in terms of the 'ratio of ratios'

$$r \equiv \frac{R_{\rm exp}}{R_{\rm th}} \tag{3.5}$$

where $R_{\rm th}$ is usually determined by Monte-Carlo simulations taking detector specifications into account.

The atmospheric neutrino anomaly consists of the fact that some experiments observe a value of r which is smaller than one.

The collaborations which do so are the two Cerenkov detectors Kamiokande and IMB as well as the tracking calorimeter Soudan II (they all observe an r value around $r \sim 0.6$) although the latter one has significantly larger errors - as do the two remaining experiments of the same type, NUSEX and Fréjus, both of which report central values of r close to 1 but with very large errors[9]. The exact experimental results as well as references to the various experimental groups can be found in [25].

[8] For sub-GeV neutrinos R is only a few percent larger than 2.

[9] Notice that the anomaly was also observed for multi-GeV events by Kamiokande. This excludes a possible explanation in terms of proton decay, and in fact atmospheric neutrinos constitute a major background for proton decay searches.

If these values of r were to be taken at face value they would represent either a ν_μ deficit and/or a ν_e surplus and could be explained by means of large angle neutrino oscillations $\nu_\mu - \nu_e$ or $\nu_\mu - \nu_\tau$ in vacuum[10]. The required squared-mass splittings and mixing angles are

$$\Delta m^2 \simeq 10^{-2}\ \mathrm{eV}^2, \quad \sin^2 2\theta \simeq 0.5 \tag{3.6}$$

This oscillation solution is also supported by an observed, although statistically not yet completely convincing, dependence of multi-GeV events on the azimuthal angle (Kamiokande).

The atmospheric neutrino anomaly is however much less credible than the solar neutrino deficit. This is mainly due to the fact that the deficit has not been observed by the Fréjus and NUSEX collaborations (although the involved errors are so large that their results are still compatible with a low r value). Also IMB has excluded some parts of the parameter space of $\nu_\mu - \nu_\tau$ oscillations by looking at upward-going muons. Specifically they analyzed the numbers of stopping to through-going muons and compared the upward- with the downward-going muon fluxes (although here the background presents an important problem). More recently the negative results of Fréjus as well as the final results of the Bugey reactor experiment have added their part by excluding a large portion of the available parameter space for the $\nu_\mu - \nu_e$ oscillation solution, leaving only little room for this option.

3.1.3 Hot dark matter

There is now compelling evidence that the bulk of the matter of the universe is invisible, and reasonably persuasive arguments that much or most of this dark matter is not baryons (See e.g. ref.[72]). Furthermore, the observed distribution of matter on the largest scales, together with the recently measured pattern of fluctuations in the cosmic microwave background, appear to indicate that roughly 30% of this particle dark matter should have been

[10] Oscillations to a sterile species $\nu_\mu - \nu_s$ are excluded by nucleosynthesis constraints.

relativistic during the crucial epoch for galaxy formation. If this hot, dark matter (HDM) should consist of the known neutrinos, certainly the most conservative assumption, then their masses should satisfy

$$\sum_i m_{\nu_i} \simeq 7 - 30 \text{ eV}. \tag{3.7}$$

This equation is more commonly known under the form $\Omega_\nu h^2 \approx \frac{\sum_i m_{\nu_i}}{90 \text{ eV}}$ which describes the neutrino contribution to the total energy density Ω (normalized to the critical density) of the universe (see *e.g.* [62]. The large range allowed by eq.(3.7) is due to the uncertainty in the value of the Hubble constant ($0.5 < h < 1$, where h is the Hubble constant in units of 100 Km sec^{-1} Mpc^{-1}).

3.2 Degenerate neutrinos

Several people have recently pointed out a solution to all three problems described above [67]. This solution is particularly simple since it involves only the known three neutrino species.

First it is clear that one needs at least three neutrino flavors to solve the solar and the atmospheric neutrino problem both by means of an oscillation solution. Furthermore the required squared-mass splittings are tiny compared to the mass scale requested by hot dark matter. The only way to solve all three points, without having to refer to a light sterile neutrino that also mixes, is to assume that all three neutrinos are almost degenerate with a mass in the eV range.

Furthermore the so required mass pattern would have to exhibit a hierarchy in the splittings. In other words, pairs of oscillating states will differ in mass by only 10^{-2} eV (and $10^{-4} - 10^{-5}$ eV) out of a total mass which is of order 1 eV. As was remarked in some of refs.[67], such a degenerate pattern is difficult to come by in a natural way in renormalizable gauge theories and,

in particular, at first sight appears not to be what is expected of a 'see-saw' mechanism for generating neutrino masses.

Since the involved neutrino masses are of the Majorana type the overall degenerate mass value is subject to an upper bound coming from L_e violation measurements in neutrinoless double beta decay. Recently this upper bound has been significantly improved to $m_{\nu_e}^{\text{eff}} < 0.68$ eV (90%CL) [46]. Although in the sub-eV range, it can be relaxed a bit once the uncertainty of the involved nuclear matrix elements is taken into account. For the degenerate neutrino scenario this essentially means two things: First, the overall mass of the neutrinos can at best reach the lower value asked for by HDM eq.(3.7) - should the required amount of HDM ever increase (or alternatively should the value of the Hubble constant increase) then degenerate SM neutrinos could only contribute partially to the HDM - and second, going close to the $\beta\beta_{0\nu}$ detection limit means that a non-zero $\beta\beta_{0\nu}$ rate should be observed in the near future when these limits are further lowered. In the absence of such an observation the degenerate neutrinos again could not explain HDM on their own. [11]

The following section investigates the structure the light neutrino mass matrix should have in order to produce the right mass splittings and mixing angles. Section 3.4 then presents a model which generates such a mass pattern in a technically natural way. The model is set in a see-saw scenario and applies an approximate family symmetry among the light neutrinos which is eventually broken by the interactions of a heavy sterile neutrino. The required hierarchy of small mass splittings is then obtained in terms of heavy mass *ratios*, and does not require the introduction of new dimensionless couplings that are much smaller than unity. Sections 3.3 and 3.4 follow very closely publication [4].

[11] As a possible way out there has been recently a mass matrix proposed which is able to accommodate all the three requirements despite the low limit on the electron mass [73]. However there is as yet no model that explains this 'maximally mixing' mass matrix naturally.

To solve the solar as well as the atmospheric neutrino deficit the model of section 3.4 will use either one of the following two mixing scenarios:

$$\begin{array}{rcc} & \text{ATM} & \text{SOLAR} \\ \text{CASE I}: & \nu_\mu - \nu_e & \nu_e - \nu_\tau \\ \text{CASE II}: & \nu_\mu - \nu_\tau & \nu_e - \nu_\mu \end{array} \tag{3.8}$$

furthermore it will apply the small angle (non-adiabatic) solution to the solar neutrino problem. To summarize, it will generate the following mass splittings and mixing angles (*c.f.* eqs.(3.2 and 3.6)) :

$$\begin{array}{rcc} & \Delta m[\text{ eV}] & \sin^2 2\theta \\ \text{ATM} & 10^{-2} & 0.5 \\ \text{SOLAR} & 10^{-5} - 10^{-4} & 10^{-2} \end{array} \tag{3.9}$$

3.3 A mass matrix that works

The main observation for the purposes of model building is that the light-neutrino mass matrix should be a sum of successively smaller contributions:

$$\mathbf{m} = \mathbf{m}_0 + \mathbf{m}_1 + \mathbf{m}_2 \tag{3.10}$$

with $\mathbf{m}_0 = m_0 \mathbf{I}$ proportional to the 3×3 unit matrix, $\mathbf{m}_1$ a rank-one matrix with elements which are $O(10^{-2} m_0)$ in magnitude, and $\mathbf{m}_2$ a generic matrix whose elements are $O(10^{-4} m_0)$.

A representative example of a matrix of this type, which is of the form that is actually generated by the model of the next section, is:

$$\mathbf{m} = m_0 \left[\mathbf{I} + \epsilon\, \mathbf{e}\mathbf{e}^T - \delta\, \left(\mathbf{e}\mathbf{f}^T + \mathbf{f}\mathbf{e}^T\right) + \xi\, \mathbf{f}\mathbf{f}^T\right]. \tag{3.11}$$

In this expression, $m_0 \simeq 1 - 2$ eV sets the scale of the common overall mass, e and f are arbitrary unit vectors in neutrino flavor-space, *i.e.*

$\mathbf{e}^T\mathbf{e} \equiv \sum_{i=1}^{3} e_i^2 = 1$ *etc.* The three quantities ϵ, δ and ξ are all taken to be much smaller than unity.

Upon diagonalization of matrix (3.11) one obtains the following eigenvalues:

$$\begin{aligned} m_3 &= m_0 \\ m_\pm &= m_0 \left\{ \left(1 + \frac{\epsilon+\xi}{2} - \delta c_\alpha \right) \right. \\ &\qquad \left. \pm \frac{1}{2} \left[\epsilon^2 + \xi^2 + 4\delta^2 - 4\delta(\epsilon+\xi)c_\alpha - 2\epsilon\xi(1-2c_\alpha^2) \right]^{1/2} \right\} \end{aligned} \tag{3.12}$$

where $c_\alpha = \mathbf{e} \cdot \mathbf{f}$. c_α denotes thus the cosine of the angle α between the vectors $\mathbf{e}$ and $\mathbf{f}$. The corresponding eigenvectors are:

$$\begin{pmatrix} \mathbf{e}_+ \\ \mathbf{e}_- \end{pmatrix} = \begin{pmatrix} c_\theta & s_\theta \\ -s_\theta & c_\theta \end{pmatrix} \begin{pmatrix} \mathbf{e} \\ \mathbf{e}' \end{pmatrix}, \qquad \text{and} \qquad \mathbf{e}_3 = \mathbf{e} \times \mathbf{e}' \tag{3.13}$$

here the mixing angle θ is given through

$$\tan 2\theta = \frac{2(\xi c_\alpha - \delta)s_\alpha}{\epsilon - 2\delta c_\alpha - \xi(1-2c_\alpha^2)} \tag{3.14}$$

and the vector $\mathbf{e}'$ is defined to be the unit vector which is orthogonal to $\mathbf{e}$ and coplanar with $\mathbf{e}$ and $\mathbf{f}$. It is given explicitly through

$$\mathbf{e}' = \frac{1}{s_\alpha}(f - c_\alpha \mathbf{e}). \tag{3.15}$$

Using the eigenvectors eq.(3.13) we can now readily write down the mixing matrix $\mathbf{V}$ which relates the weak-interaction to the propagation eigenstates:

$$\begin{pmatrix} \nu_e \\ \nu_\mu \\ \nu_\tau \end{pmatrix} = \begin{pmatrix} e_1 c_\theta + \frac{s_\theta}{s_\alpha}(f_1 - e_1 c_\alpha) & -e_1 s_\theta + \frac{c_\theta}{s_\alpha}(f_1 - e_1 c_\alpha) & \frac{1}{s_\alpha}(c_2 f_3 - e_3 f_2) \\ e_2 c_\theta + \frac{s_\theta}{s_\alpha}(f_2 - e_2 c_\alpha) & -e_2 s_\theta + \frac{c_\theta}{s_\alpha}(f_2 - e_2 c_\alpha) & \frac{1}{s_\alpha}(e_3 f_1 - e_1 f_3) \\ e_3 c_\theta + \frac{s_\theta}{s_\alpha}(f_3 - e_3 c_\alpha) & -e_3 s_\theta + \frac{c_\theta}{s_\alpha}(f_3 - e_3 c_\alpha) & \frac{1}{s_\alpha}(e_1 f_2 - e_2 f_1) \end{pmatrix} \begin{pmatrix} \nu_+ \\ \nu_- \\ \nu_3 \end{pmatrix} \tag{3.16}$$

Given this mixing matrix and the mass eigenvalues eq.(3.12) we would now like to see what choices for the various parameters can reproduce equations (3.8) and (3.9). In fact the two cases of eq.(3.8) are reproduced by the following choice for ϵ, δ and ξ:

$$\begin{aligned} \text{CASE I} &: \epsilon \sim \varepsilon^2 \gg \delta \sim \varepsilon^3 \gg \xi \sim \varepsilon^4 \\ \text{CASE II} &: \xi \sim \varepsilon^2 \gg \delta \sim \varepsilon^3 \gg \epsilon \sim \varepsilon^4 \end{aligned} \tag{3.17}$$

where ε is a smallish parameter of the theory and is about $\varepsilon \sim 0.1$ for the case of interest. As we will see in the following section, these values for ϵ, δ and ξ can be naturally obtained within the specific model presented there. Using relations (3.17) the mass eigenvalues of eq.(3.12) simplify to (CASE I):

$$\begin{aligned} m_+ &= m_0 \left[1 + \epsilon - 2c_\alpha \delta + c_\alpha^2 \xi + \frac{\delta^2 s_\alpha^2}{\epsilon} + O(\varepsilon^5) \right] \\ m_- &= m_0 \left[1 + s_\alpha^2 \xi - \frac{\delta^2 s_\alpha^2}{\epsilon} + O(\varepsilon^5) \right] \end{aligned} \tag{3.18}$$

These expressions imply the mass splittings: $\Delta m^2_{+-} \sim \Delta m^2_{3+} \sim O(\varepsilon^2)$ and $\Delta m^2_{3-} \sim O(\varepsilon^4)$. Notice that the smaller splitting here is $O(\varepsilon^4)$ even though the parameter δ is itself of order ε^3. Given that eq.(3.12) is symmetric under the exchange $\epsilon \leftrightarrow \xi$ one obtains similar mass splittings as in eq.(3.18) also for the CASE II where the hierarchy of ϵ and ξ is reversed.

The expression for the mixing angle θ also simplifies to become:

$$\begin{aligned} \text{CASE I} \qquad \tan 2\theta &\approx \frac{-2\delta s_\alpha}{\epsilon} \sim O(\varepsilon) \\ \text{CASE II} \qquad \tan 2\theta &\approx \frac{-2c_\alpha s_\alpha}{1 - 2c_\alpha^2} = \tan 2\alpha \sim O(1) \end{aligned} \tag{3.19}$$

The mixing matrix V of eq.(3.16) can now be further simplified by making the following choices:

$$\begin{aligned} \text{CASE I} &: \mathrm{e} = (s_\beta, c_\beta, 0) \; ; \; \mathrm{f} = (0, 0, 1) \\ \text{CASE II} &: \mathrm{e} = (s_\beta, c_\beta, 0) \; ; \; \mathrm{f} = (c_\alpha s_\beta, c_\alpha c_\beta, s_\alpha) \end{aligned} \tag{3.20}$$

where s_β and c_β denote the sine and cosine of an up-to-now arbitrary angle β. The choice of **e** and **f** in CASE I implies that $c_\alpha = 0$ so that both cases lead to the following simplified mixing matrix:

$$\mathbf{V} = \begin{pmatrix} s_\beta c_\theta & -s_\beta s_\theta & c_\beta \\ c_\beta c_\theta & -c_\beta s_\theta & -s_\beta \\ s_\theta & c_\theta & 0 \end{pmatrix}. \tag{3.21}$$

The conditions of equations (3.8) and (3.9) can now be satisfied in the following way:

For CASE I eq.(3.19) implies that $\sin^2 2\theta \approx 10^{-2}$ so that we can solve the solar neutrino problem through '$\nu_e - \nu_\tau$' oscillations. By choosing then β to be large so that $\sin^2 2\beta \approx 0.5$ the atmospheric neutrino oscillations are governed by '$\nu_e - \nu_\mu$' oscillations.

In CASE II on the other hand $\theta \approx \alpha$ need not be small so that by choosing $\sin^2 2\theta \approx 0.5$ we satisfy the atmospheric neutrino observations through '$\nu_\mu - \nu_\tau$' conversion. The MSW '$\nu_e - \nu_\mu$' solution can then be obtained by taking $\sin^2 2\beta \approx 10^{-2}$.

3.4 A model of naturally degenerate neutrinos

3.4.1 Masses and Yukawa couplings

We now would like to build a model which naturally produces a mass matrix of the type of eq.(3.11). In order to do so we must ensure, as a first approximation, a degenerate set of eV neutrinos. We can easily do so by demanding an approximate symmetry under which the light neutrinos rotate into one another in a real representation. We therefore require an approximate $O(3)$ symmetry under which the usual standard-model (SM) neutrinos, ν_i, transform according to $\nu_i \to \mathcal{O}_{ij}\, \nu_j$, with $\mathcal{O}_{ij}$ a real, 3×3, orthogonal matrix. An

eV-size mass for these neutrinos is then obtained via the see-saw mechanism [26] through introducing three electroweak-singlet neutrinos, s_i, which also transform as triplets under the approximate $O(3)$ symmetry.

With this particle content the most general renormalizable lagrangian beyond the SM that respects this $O(3)$ symmetry is

$$\mathcal{L}_{\rm inv} = -\frac{M}{2}\,(s_i\,s_i) - \lambda\,(L_i\,s_i)\,H + \text{h.c.} \tag{3.22}$$

here $H = \binom{\phi^+}{\phi^0}$ and $L_i = \binom{\nu_i}{e_i}$ denote respectively the SM Higgs and lepton doublets. As long as $M \gg \lambda v$, where $v \simeq 174$ GeV is the SM Higgs *vev*, the see-saw mechanism applies and the light neutrinos receive a mass $m_0 = \lambda^2 v^2/M$ upon diagonalization of lagrangian (3.22). Choosing $m_0 \simeq 2$ eV then requires $M/\lambda^2 \simeq 2 \times 10^{13}$ GeV.

It is clear that the $O(3)$ symmetry is not an exact symmetry at this level since it is explicitly broken in the SM by the charged lepton masses. Radiative corrections then introduce small $O(3)$ violating terms into the light neutrino mass matrix. At one loop the induced splittings are proportional to the corresponding charged lepton masses, although this needs not be so at higher loops [74]. These radiative corrections are unfortunately not large enough to cause the wanted splittings between mass eigenstates and so we are led to introduce a further source of $O(3)$ breaking.

In order to produce the desired mass matrix of eq.(3.11), we require $O(3)$-breaking order parameters, e_i and f_i, which transform as triplets. We therefore supplement the model with one more singlet neutrino, N, which is also neutral under $O(3)$. We permit the couplings of N to the other fields to explicitly break the $O(3)$ symmetry. The most general renormalizable couplings for the N field are then

$$\mathcal{L}_N = -\frac{m}{2}\,(N\,N) - \mu_i\,(s_i\,N) - g_i\,(L_i\,N)\,H + \text{h.c.} \tag{3.23}$$

The mass matrix that is induced at tree level by lagrangians (3.22) and

(3.23) then has the following form in a basis of flavor eigenstates:

$$\mathbf{M} = \begin{array}{c} \\ \vec{\nu} \\ \vec{h} \end{array} \begin{array}{c} \begin{array}{cc} \vec{\nu}^T & \vec{h}^T \end{array} \\ \begin{pmatrix} \mathbf{0} & \mathbf{B} \\ \mathbf{B}^T & \mathbf{C} \end{pmatrix} \end{array} \qquad \text{with} \quad \mathbf{B} = \begin{array}{c} \\ \nu_e \\ \nu_\mu \\ \nu_\tau \end{array} \begin{array}{c} \begin{array}{cccc} s_1 & s_2 & s_3 & N \end{array} \\ \begin{pmatrix} \lambda v & & & g_e v \\ & \lambda v & & g_\mu v \\ & & \lambda v & g_\tau v \end{pmatrix} \end{array}$$

$$\text{and} \quad \mathbf{C} = \begin{array}{c} \\ s_1 \\ s_2 \\ s_3 \\ N \end{array} \begin{array}{c} \begin{array}{cccc} s_1 & s_2 & s_3 & N \end{array} \\ \begin{pmatrix} M & & & \mu_1 \\ & M & & \mu_2 \\ & & M & \mu_3 \\ \mu_1 & \mu_2 & \mu_3 & m \end{pmatrix} \end{array} \tag{3.24}$$

where $\mathbf{0}$ is a 3×3 zero matrix and the vectors $\vec{\nu}$ and $\vec{h}$ are given by $\vec{\nu}^T = (\nu_e, \nu_\mu, \nu_\tau)$ and $\vec{h}^T = (s_1, s_2, s_3, N)$ respectively.

3.4.2 A desired set of model parameters

Provided that $\lambda v, g_i v \ll M, m, \mu_i$ we can now partially diagonalize matrix $\mathbf{M}$ above. This is essentially similar to diagonalizing a 2×2 see-saw matrix. After the rotation, which leaves the light neutrino flavor basis ($\vec{\nu}$) undisturbed, the off diagonal submatrices (what was $\mathbf{B}$ in eq.(3.24)) will be zero with the diagonal submatrices having themselves nonzero entries that exhibit the typical see-saw hierarchy. In other words the light neutrino mass matrix $\mathbf{m}$ will be nondiagonal with eV size entries. It is given explicitly through

$$\mathbf{m} = -\mathbf{B}\,\mathbf{C}^{-1}\,\mathbf{B}^T \tag{3.25}$$

$\mathbf{m}$ as obtained by this equation is actually exactly of the form of equation (3.11) with the vectors $\mathbf{e}$ and $\mathbf{f}$ being the vectors $\vec{\mu}$ and $\vec{g}$ respectively normalized to unity. In components one finds:

$$m_0 = \frac{\lambda^2 v^2}{M}, \quad \epsilon = \frac{\mu^2}{mM}, \quad \delta = \frac{\mu g}{m\lambda}, \quad \xi = \frac{g^2 M}{\lambda^2 m}, \quad e_i = \frac{\mu_i}{\mu}, \quad f_i = \frac{g_i}{g} \tag{3.26}$$

where g and μ are the absolute length of vectors $\vec{g}$ and $\vec{\mu}$.

Given the connection eq.(3.26) between the model parameters and the quantities we used earlier it is now straightforward to find representative sets of values for μ_i, M, m, g_i and λ that reproduce the solutions of eqs.(3.8,3.9). Three possibilities for each of the two cases are:

$$\begin{array}{lllll} \text{(Ia)} & \mu \sim \varepsilon M & \sim \varepsilon m & ; & g \sim \varepsilon^2 \lambda \\ \text{(Ib)} & \mu \sim M & \sim \varepsilon^2 m & ; & g \sim \varepsilon \lambda \\ \text{(Ic)} & \mu \sim M/\varepsilon & \sim \varepsilon^3 m & ; & g \sim \lambda \\ \text{(IIa)} & \mu \sim \varepsilon M & \sim \varepsilon^3 m & ; & g \sim \lambda \\ \text{(IIb)} & \mu \sim \varepsilon^2 M & \sim \varepsilon^2 m & ; & g \sim \varepsilon \lambda \\ \text{(IIc)} & \mu \sim M & \sim \varepsilon^4 m & ; & g \sim \lambda/\varepsilon \end{array} \tag{3.27}$$

3.4.3 Naturalness

There are two issues that have to be considered:

First we are interested to see how the demanded hierarchy in the squared-mass differences $(10^{-2}, 10^{-5})$ (3.11) is realized in this model. In fact the required small splittings amongst the light-neutrino masses are ultimately due to the relative size of the symmetry breaking terms, μ_i and g_i, in comparison with the $O(3)$-invariant couplings, M, m and λ. However, as can be seen from eq.(3.27), the ratios of these couplings need not always be small. In fact one can choose model parameters such that any ratios are not smaller than 10^{-2} (*c.f.* examples (Ia),(Ib) and (IIb) above) and still the wanted mass hierarchy is reproduced.

The second issue concerns loop corrections. How do $O(3)$ violating radiative corrections affect the mass pattern that has arisen at tree level in the above model? SM electroweak interactions, as has already been mentioned before, do not give rise to sizeable contributions that could compete with the tree level inferred ones above. But how is it about the $O(3)$ violating terms of eq.(3.23)? Is it consistent to choose the $O(3)$-breaking interactions

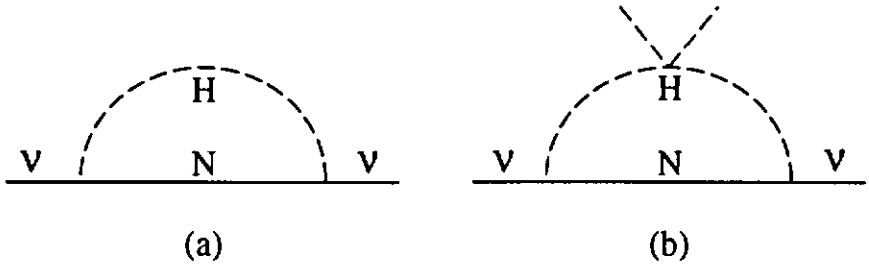

Figure 3.1: Examples of radiative corrections that give rise to $O(3)$ violating operators. Graph (a) shows a contribution to a neutrino kinetic term. Diagram (b) yields a large-logarithm enhanced contribution to the $(L_iL_j)HH$ operator.

as large as we have and yet *not* to include any N-independent $O(3)$-breaking terms, such as $(s_i\, s_j)$, $(L_i\, s_j)H$ or $(L_iL_j)HH$? The answer to this question is 'yes' although it gives rise to some additional constraints for the values of the involved couplings.

It is clear that loops involving the symmetry-breaking N-interactions must inevitably induce all possible $O(3)$-breaking couplings amongst the other neutrinos. But the point is that unless g_i, λ and g_i/λ should be larger than ~ 0.1, these induced terms only perturb the above mass eigenvalues by amounts that are smaller than a part in $10^4 - 10^5$, and so they are negligible in comparison to the effects which we have considered.

This is particularly clear for the induced contributions to symmetry-breaking operators like $(s_i\, s_j)$, since the one-loop contributions to these are strongly suppressed by small mass insertions or loop factors. (These suppressions arise because any symmetry-breaking loop must necessarily involve a virtual N field, and this only becomes possible, given only two external s_i lines, at two loops and beyond, or at one loop with a number of mass insertions.)

Notice that the constraint $g_i/\lambda \lesssim 0.1$ - quoted above and explained below - rules out the examples (Ic), (IIa) and (IIc) of equation (3.27) leaving us only with those cases that were anyhow favoured by the hierarchy considerations above.

Loop-induced corrections to the remaining symmetry breaking operators $(L_i s_j)H$ and $(L_i L_j)HH$ can arise at 1-loop however - two examples are shown in figure 3.1 - they are for example generated by flavor changing contributions to the various neutrino kinetic terms (see graph (a) in fig. 3.1).

Their generic size is respectively of order $\lambda g_i g_j/(16\pi^2)$ and $g_i g_j/(16\pi^2)$, which is innocuous provided that g_i and λ are smaller than $O(0.1)$. One of the most dangerous contributions comes from corrections that are enhanced by large logarithms. An example is the second graph of figure 3.1. It contributes to the operator $(L_i L_j)HH$ and is induced by the Higgs self-coupling $\zeta\,(H^\dagger H)^2$. This graph contributes an amount to ξ which is ζ-dependent, but of order $\zeta(g/4\pi\lambda)^2 \ln(m_H^2/M^2)$. For a small Higgs mass $m_H \sim 80$ GeV and a large Higgs self interaction $\zeta \sim 0.1$ this can be numerically as large as $\sim 0.03(g/\lambda)^2$. Such an enhancement can strengthen the bound on g/λ by factors of 5 or so.

To close this chapter it should be said that the model presented above represents an existence proof for the degenerate neutrino solution to the atmospheric and the solar neutrino problem as well as HDM. The same problem has also been approached - at about the same time - by several other authors from the point of view of $SO(10)$ grand unified theories [75].

References

[1] P. Bamert and C.P. Burgess, *Negative S and Light New Physics*, *Zeit. Phys.* C66 (1995) 495.

[2] P. Bamert, C.P. Burgess and R.N. Mohapatra, *Heavy Sterile Neutrinos and Neutrinoless Double-Beta Decay*, *Nucl. Phys.* **B438** (1995) 3.

[3] P. Bamert, C.P. Burgess and R.N. Mohapatra, *Multi-Majoron Modes for Neutrinoless Double-Beta Decay*, *Nucl. Phys.* **B** in press (hep-ph/9412365) (1995).

[4] P. Bamert and C.P. Burgess, *Naturally Degenerate Neutrinos*, *Phys. Lett.* **329B** (1994) 289.

[5] D. Schaile, CERN-PPE-94-162, 27th International Conference on High Energy Physics (ICHEP), Glasgow, Scotland, 20-27 Jul 1994;
The LEP Electroweak Working Group, *A Combination of Preliminary LEP Electroweak Results for the 1995 Winter Conferences*, preprint LEPEWWG/95-01, ALEPH 95-038, DELPHI 95-37, L3 Note 1736, OPAL Note TN284.

[6] SLD Collaboration (Michael J. Fero, for the collaboration), SLAC-PUB-6679, 27th International Conference on High Energy Physics (ICHEP), Glasgow, Scotland, 20-27 Jul 1994.

[7] B. Lynn, M. Peskin, R. Stuart, in *Physics at LEP* vol. 1, CERN Report 86-02, pp. 90 – 152.

[8] M.E. Peskin and T. Takeuchi, *Phys. Rev. Lett.* **65** (1990) 964; *Phys. Rev.* **D46** (1992) 381;
W.J. Marciano and J.L. Rosner, *Phys. Rev. Lett.* **65** (1990) 2963;
D.C. Kennedy and P. Langacker, *Phys. Rev. Lett.* **65** (1990) 2967.

[9] C.P. Burgess, Preprint McGill-94/50 (hep-ph/9411257) (1994).

[10] C.P. Burgess, S. Godfrey, H. König, D. London and I. Maksymyk, *Phys. Rev.* **D49** (1994) 6115.

[11] I. Maksymyk, C.P. Burgess and D. London, *Phys. Rev.* **D50** (1994) 529.

[12] I. Maksymyk and S. Fleming, Preprint UTTG-04-95 (hep-ph/9504272) (1995).

[13] C.P. Burgess, S. Godfrey, H. König, D. London and I. Maksymyk, *Phys. Lett.* **326B** (1994) 276.

[14] G. Altarelli and R. Barbieri, *Phys. Lett.* **253B** (1991) 161;
G. Altarelli, R. Barbieri and S. Jadach, *Nucl. Phys.* **B369** (1992) 3, (erratum) *ibid.***B376** (1992) 444;
G. Altarelli, R. Barbieri and F. Caravaglios, *Nucl. Phys.* **B405** (1993) 3.

[15] N. Evans, Preprint Swansea SWAT/40 (hep-ph/9408308) (1994).

[16] H. Georgi, *Nucl. Phys.* **B363** (1991) 301;
E. Gates and J. Terning, *Phys. Rev. Lett.* **67** (1991) 1840;
E. Ma and P. Roy, *Phys. Rev. Lett.* **68** (1992) 2879;
M. Luty and R. Sundrum, *Phys. Rev. Lett.* **70** (1993) 529;
L. Lavoura, L.-F. Li, *Phys. Rev.* **D48** (1993) 234;
M.J. Dugan and L. Randall, *Phys. Lett.* **264B** (1991) 154.

[17] N. Evans, *Phys. Rev.* **D49** (1994) 4785; *Phys. Lett.* **340B** (1994) 81.

[18] L. Lavoura and L.F. Li, *Phys. Rev.* **D49** (1994) 1409;
N. Evans, *Phys. Rev.* **D49** (1994) 4785.

[19] A. Zee, *Phys. Lett.* **161B** (1985) 141.

[20] The CDF Collaboration, F. Abe *et al.*, *Phys. Rev. Lett.* **69** (1992) 3439.

[21] H. Georgi and M. Machacek, *Nucl. Phys.* **B262** (1985) 463;
M.S. Chanowitz and M. Golden, *Phys. Lett.* **165B** (1985) 105;
J.F. Gunion, R. Vega and J.Wudka, *Phys. Rev.* **D42** (1990) 1673, *Phys. Rev.* **D43** (1991) 2322;
P. Bamert and Z. Kunszt, *Phys. Lett.* **306B** (1993) 335.

[22] The CDF Collaboration, F. Abe *et al.*, *Phys. Rev.* **D48** (1993) 3939.

[23] The H1 Collaboration, I. Abt *et al.*, *Nucl. Phys.* **B396** (1993) 3;
The ZEUS Collaboration, M. Derrick *et al.*, *Phys. Lett.* **306B** (1993) 173.

[24] G. Bhattacharyya, S. Banerjee and P. Roy, *Phys. Rev.* **D45** (1992) R729.

[25] G. Gelmini and E. Roulet, Preprint UCLA-94-TEP-36 (hep-ph/9412278) (1994).

[26] M. Gell-Mann, P. Ramond and R. Slansky, in *Supergravity*, ed. by F. van Nieuwenhuizen and D. Freedman (Amsterdam, North Holland, 1979) 315;
T. Yanagida, in the Proceedings of the Workshop on *Unified Theory and Baryon Number in the Universe*, ed. by O. Sawada and A. Sugamoto (KEK, Tsukuba, 1979) 95;
R.N. Mohapatra and G. Senjanović, *Phys. Rev. Lett.* **44** (1980) 912.

[27] G.B. Gelmini and M. Roncadelli, *Phys. Lett.* **99B** (1981) 411.

[28] H.M. Georgi, S.L. Glashow and S. Nussinov, *Nucl. Phys.* **B193** (1981)) 297.

[29] M. Moe, *Int. J. Mod. Phys.* **E2** (1993) 507.

[30] M. Moe and P. Vogel, *Ann. Rev. Nucl. Part. Sci.* **44**, (1994) 247.

[31] C.P. Burgess and J.M. Cline, in the proceedings of *The 1st International Conference on Nonaccelerator Physics*, Bangalore, January 1994, (World Scientific, Singapore), (hep-ph/9401334).

[32] C.P. Burgess and J.M. Cline, *Phys. Lett.* **298B** (1993) 141.

[33] C.P. Burgess and J.M. Cline, *Phys. Rev.* **D49** (1994) 5925.

[34] R. Mohapatra and E. Takasugi,*Phys. Lett.* **211B** (1988) 192.

[35] Z.G. Berezhiani, A.Yu. Smirnov and J.W.F. Valle, *Phys. Lett.* **291B** (1992) 99.

[36] C.D. Carone, *Phys. Lett.* **308B** (1993) 85.

[37] F.T. Avignone III *et.al.*, in *Neutrino Masses and Neutrino Astrophysics,* proceedings of the lV Telemark Conference, Ashland, Wisconsin, 1987, edited by V. Barger, F. Halzen, M. Marshak and K. Olive (World Scientific, Sinagpore, 1987), p. 248;
M. Moe, M. Nelson, M. Vient and S. Elliott, *Nucl. Phys.* (Proc. Suppl.) **B31** (1993).

[38] Y. Chikashige, R.N. Mohapatra and R.D. Peccei, *Phys. Rev. Lett.* **45** (1980) 1926.

[39] H. Primakoff and S.P. Rosen, *Rep. Prog. Phys.***22** (1959) 121.

[40] A. Halprin, P. Minkowski, H. Primakoff and P. Rosen, *Phys. Rev.* **D13** (1976) 2567.

[41] W. Haxton and G. Stephenson, *Prog. in Particle and Nucl. Physics* **12** (1984) 409;
J. Vergados, *Phys. Rep.* **133** (1986) 1;
M. Doi, T. Kotani, H. Nishiura and E. Takasugi, *Prog. Theor. Phys., Prog. Theor. Phys. Suppl.* **83** (1985) 1.

[42] A. Staudt, K. Muto and H.V. Klapdor-Kleingrothaus, *Europhys. Lett.* **13** (1990) 31;
T. Tomoda *et.al.*, *Rep. Prog. Phys.* **54** (1991) 53;
H.V. Klapdor-Kleingrothhaus, *Prog. Part. Nucl. Phys.* **32** (1994) 261, for a review.

[43] J. Engel, P. Vogel and M.R. Zirnbauer, *Phys. Rev.* **C37** (1988) 731.

[44] C.P. Burgess and O. Hernández, *Phys. Rev.* **D48** (1993) 4326.

[45] J.-L. Vuilleumier, Preprint NEIP-95-006 (1995);
J.-C. Vuilleumier *et.al.*, *Phys. Rev.* **D48** (1993) 1009.

[46] A. Balysh *et.al.*(presented by K. Zuber), 27th International Conference on High Energy Physics (ICHEP), Glasgow, Scotland, 20-27 Jul 1994, (hep-ex/9502007).

[47] L. Wolfenstein, *Phys. Lett.* **107B** (1981) 77.

[48] The CALTECH-PSI-NEUCHATEL collaboration, G. Gervasio, Talk presented at the 1995 Trento workshop on neutrinoless double beta decay.

[49] B. Kayser, F. Gibra-Debu and F. Perrier, *Physics of Massive Neutrinos*, (World Scientific, 1989).

[50] R. N. Mohapatra, *Phys. Rev.* **D34** (1986) 3457;
R. N. Mohapatra and J. D. Vergados, *Phys. Rev. Lett.* **47** (1981) 1713;
J. Schecter and J. W. F. Valle, *Phys. Rev.* **D25** (1982) 2951.

[51] C.N. Leung and S.T. Petcov, *Phys. Lett.* **145B** (1984) 416.

[52] F.J. Gilman, *Comments Nucl. Part. Phys.* **16** (1986) 231.

[53] M.C. Gonzalez-Garcia, A. Santamaria and J.W.F. Valle, *Nucl. Phys.* **B342** (1990) 108;
M. Dittmar, M.C. Gonzalez-Garcia, A. Santamaria and J.W.F. Valle, *Nucl. Phys.* **B332** (1990) 1.

[54] D.I. Britton *et.al.*, *Phys. Rev.* **D46** (1992) R885; *Phys. Rev. Lett.* **68** (1992) 3000.

[55] R. Shrock, *Phys. Lett.* **96B** (1980) 159;
T. Yamazaki *et.al.*, in Proc. XIth Intern. Conf. on Neutrino Physics and Astrophysics, K. Kleinknecht and E.A. Paschos (World Scientific, Singapore, 1984) p. 183.

[56] V. Barger, W. Y. Keung and S. Pakvasa, *Phys. Rev.* **D25** (1982) 907;
T. Goldman, E. Kolb and G. Stephenson, *Phys. Rev.* **D26** (1982) 2503;
A. Santamaria, J. Bernabeu and A. Pich, *Phys. Rev.* **D36** (1987) 1408;
C. E. Picciotto *et.al.*, *Phys. Rev.* **D37** (1988) 1131.

[57] G. Bernardi *et.al.*, *Phys. Lett.* **203B** (1988) 332;
J. Dorenbosch *et.al.*, *Phys. Lett.* **166B** (1986) 473;
R.C. Ball *et.al.*, preprint UM HE 85-09, (1985) unpublished;
A.M. Cooper-Sarkar *et.al.*, *Phys. Lett.* **160B** (1985) 207.

[58] L.N. Chang, D. Ng and J. Ng, *Phys. Rev.* **D50** (1994) 4589.

[59] The L3 Collaboration, *Phys. Lett.* **316B** (1993) 427.

[60] W. Marciano and A. Sirlin, *Phys. Rev. Lett.* **71** (1993) 3629.

[61] T. Walker *et.al.*, *Ap. J.* **376**, 51(1991).

[62] E. Kolb and M. Turner, *The early universe*, Frontiers in physics vol. 69, Addison-Wesley Publishing Company (1990).

[63] C. Copi, D. Schramm and M. Turner, preprint FERMILAB-Pub-95/140-A, (astro-ph/9506094), (1995);
K. Olive and S. Scully, preprint UMN-TH-1341/95, (astro-ph/9506131), (1995).

[64] N. Hata *et.al.*, preprint OSU-TA-6-95, (hep-ph/9505319), (1995).

[65] K. Enqvist, K. Kainulainen and M. Thomson, *Phys. Rev. Lett.* **68** (1992) 744; *Nucl. Phys.* **B373** (1992) 498.

[66] R. Barbieri and R.N. Mohapatra, *Phys. Rev.* **D39** (1989) 1229;
G. Raffelt and D. Seckel, *Phys. Rev. Lett.* **60** (1989) 1793;
K. Kainulainen, J. Maalampi and J.T. Peltoniemi, *Nucl. Phys.* **B358** (1991) 435.

[67] D. Caldwell and R. Mohapatra, *Phys. Rev.* **D48** (1993) 3259;
S.T. Petcov and A.Yu. Smirnov, *Phys. Lett.* **322B** (1994) 109;
A. Joshipura, Ahmedabad preprint.

[68] The LSND Collaboration (C. Athanassopoulos, *et.al.*, Preprint LA-UR-95-1238 (nucl-ex/9504002), (1995).

[69] P. Langacker, Preprint UPR-0652-T (hep-ph/9503327), Talk given at 4th International Conference on Physics Beyond the Standard Model, Lake Tahoe, CA, 13-18 Dec 1994.

[70] L. Wolfenstein, *Phys. Rev.* **D17** (1978) 2369;
S.P. Mikheyev and A.Yu. Smirnov, *Yad. Fiz.* **42** (1985) 1441 [*Sov. J. Nucl. Phys.* **42** (1986) 913].

[71] A.S. Joshipura and P.I. Krastev, *Phys. Rev.* **D50** (1994) 3484.

[72] The contributions of P.J.E. Peebles, J.L. Tonry and K. Griest, in *Relativistic Astrophysics and Particle Cosmology*, ed. by C.W. Akerlof and M.A. Srednicki, Annals of the New York Academy of Sciences, Vol 688, (New York, 1993).

[73] R.N. Mohapatra and S. Nussinov, preprint UMD-PP-95-61 (hep-ph/9411274) (1994).

[74] D. Choudhury, R. Ghandhi, J. Gracey and B. Mukhopadhyaya, *Phys. Rev.* **D50** (1994) 3468.

[75] D. Caldwell and R. Mohapatra, *Phys. Rev.* **D50** (1994) 3477
A. Ioannissyan and J.W.F. Valle, *Phys. Lett.* **332B** (1994) 93;
D. Lee and R. Mohapatra, *Phys. Lett.* **329B** (1994) 463;
A. Joshipura, *Zeit. Phys.* **C64** (1994) 31.

Acknowledgements

I am finally confronted with the task of acknowledging the support and help I have received from many people during the years I have worked on this thesis. This is not an easy task since any approach appears to be incomplete and things that should have been said remain unmentioned or not adequately displayed. I nonetheless hope that these acknowledgements are as complete as they can be and that any omissions will be readily forgiven since they surely were not intended.

On the professional level I would like to thank first of all my official thesis adviser Jean-Pierre Derendinger who, apart from having provided all the support one could ask for, has also shown a lot of confidence in me, especially when it turned out that I would do most of the work related to my thesis not with him and not entirely in his domain of research. He was also always available when I had a problem and needed some advice, on physics as well as on other important things such as my future 'career' plans.

Then I would like to express my deep gratitude to Cliff Burgess. It was him who has made me experience the 'joys' of physics. In fact the whole thesis as presented here is based on a fruitful and productive collaboration with him, a collaboration that even continues as I write, and so he was in any practical sense my 'real' thesis adviser. During these years I have learned a lot from him, not only on the physics level, but also on a general professional and personal level.

It is also a pleasure to acknowledge the other people I have collaborated

with during the last years. These are: Rabi Mohapatra whom I started to work with, without having met him in person (although we got to know each other eventually), Ivan Maksymyk and last but bot least Zoltan Kunszt who was my adviser when I did my diploma at ETH - which eventually resulted in my first publication. Zoltan will also attend the defense of this thesis as will Cliff Burgess, Jean-Pierre Derendinger and Jean-Luc Vuilleumier.

I have enjoyed the time in Neuchâtel and at the 'Institut de Physique' and would like to mention all the friends who have made my stay here worthwhile. Starting with my *vis-a-vis* Philippe Page these are Armelle Barelli, Philippe Jacquod, Fernando Quevedo, Jaques Farine, Matteo Mombelli, Pierre Beran and all the others - the list would be long. Philippe Page will also come to McGill University in Montréal where we'll both venture into our first post-doc position.

Then I owe a lot of thanks to my parents. When I was a child they always tried to reinforce whatever talents or interests I might have shown. Later on they supported me during my studies of physics at ETH and so have facilitated a large part of my education in the first place. This success is therefore also to their credit.

Last but not least there is the one person who had to suffer most during the past few weeks. This is my girlfriend Ursula Christ. She has shown a lot of patience and has helped me wherever she could. Well, I'll thank her in person for this.